Bibliography

Ackermann, J. M., Pegg, A. E., and McCloskey, D. E. (2003) Drugs affecting the cell cycle via actions on the polyamine metabolic pathway. *Prog Cell Cycle Res*, **5**, 461–8. 4

Ahn, H. J., Kim, K. H., Lee, J., Ha, J. Y., Lee, H. H., Kim, D., Yoon, H. J., Kwon, A. R., and Suh, S. W. (2004) Crystal structure of agmatinase reveals structural conservation and inhibition mechanism of the ureohydrolase superfamily. *J Biol Chem*, **279** (48), 50505–13. 24

Albeck, S., Dym, O., Unger, T., Snapir, Z., Bercovich, Z., and Kahana, C. (2008) Crystallographic and biochemical studies revealing the structural basis for antizyme inhibitor function. *Protein Sci*, **17** (5), 793–802. 76

Almrud, J. J., Oliveira, M. A., Kern, A. D., Grishin, N. V., Phillips, M. A., and Hackert, M. L. (2000) Crystal structure of human ornithine decarboxylase at 2.1 a resolution: structural insights to antizyme binding. *J Mol Biol*, **295** (1), 7–16. 74, 86

Amarantos, I. and Kalpaxis, D. L. (2000) Photoaffinity polyamines: interactions with AcPhe-tRNA free in solution or bound at the p-site of *Escherichia coli* ribosomes. *Nucleic Acids Res*, **28** (19), 3733–3742. 3

Amarantos, I., Zarkadis, I. K., and Kalpaxis, D. L. (2002) The identification of spermine binding sites in 16S rRNA allows interpretation of the spermine effect on ribosomal 30S subunit functions. *Nucleic Acids Res*, **30** (13), 2832–2843. 3

Andrews, K. T., Tran, T. N., Lucke, A. J., Kahnberg, P., Le, G. T., Boyle, G. M., Gardiner, D. L., Skinner-Adams, T. S., and Fairlie, D. P. (2008) Potent antimalarial activity of histone deacetylase inhibitor analogues. *Antimicrob Agents Chemother*, **52** (4), 1454–1461. 21

Aravind, L., Iyer, L. M., Wellems, T. E., and Miller, L. H. (2003) *Plasmodium* biology: genomic gleanings. *Cell*, **115** (7), 771–85. 38, 39

Assaraf, Y. G., Golenser, J., Spira, D. T., Messer, G., and Bachrach, U. (1987) Cytostatic effect of DL-α-difluoromethylornithine against *Plasmodium falciparum* and its reversal by diamines and spermidine. *Parasitol Res*, **73** (4), 313–318. 7

Bach, R., Canepa, C., and Glukhovtsev, M. (1999) Influence of electrostatic effects on activation barriers in enzymatic reactions: Pyridoxal 5́-phosphate-dependent decarboxylation of α-amino acids. *J Am Chem Soc*, **121** (28), 6542–6555. 75

Bachrach, U. (2005) Naturally occurring polyamines: interaction with macromolecules. *Curr Protein Pept Sci*, **6** (6), 559–566. 2

Baggio, R., Cox, J. D., Harper, S. L., Speicher, D. W., and Christianson, D. W. (1999) A new chromophoric assay for arginase activity. *Anal Biochem*, **276** (2), 251–253. 71

Bahl, A., Brunk, B., Crabtree, J., Fraunholz, M. J., Gajria, B., Grant, G. R., Ginsburg, H., Gupta, D., Kissinger, J. C., Labo, P., Li, L., Mailman, M. D., Milgram, A. J., Pearson, D. S., Roos, D. S., Schug, J., Stoeckert, Jr, C. J., and Whetzel, P. (2003) PlasmoDB: the *Plasmodium* genome resource. A database integrating experimental and computational data. *Nucleic Acids Res*, **31** (1), 212–5. 38, 85

Bailey, T. L. and Elkan, C. (1994) Fitting a mixture model by expectation maximization to discover motifs in biopolymers. *Proc Int Conf Intell Syst Mol Biol*, **2**, 28–36. 19

Bale, S., Brooks, W., Hanes, J. W., Mahesan, A. M., Guida, W. C., and Ealick, S. E. (2009) Role of the sulfonium center in determining the ligand specificity of human *S*-adenosylmethionine decarboxylase. *Biochemistry*, **48** (27), 6423–6430. 80

Bale, S., Lopez, M. M., Makhatadze, G. I., Fang, Q., Pegg, A. E., and Ealick, S. E. (2008) Structural basis for putrescine activation of human *S*-adenosylmethionine decarboxylase. *Biochemistry*, **47** (50), 13404–13417. 81

Bastien, O., Aude, J.-C., Roy, S., and Maréchal, E. (2004a) Fundamentals of massive automatic pairwise alignments of protein sequences: theoretical significance of z-value statistics. *Bioinformatics*, **20** (4), 534–537. 20

Bastien, O., Lespinats, S., Roy, S., Métayer, K., Fertil, B., Codani, J.-J., and Maréchal, E. (2004b) Analysis of the compositional biases in *Plasmodium falciparum* genome and proteome using *Arabidopsis thaliana* as a reference. *Gene*, **336** (2), 163–173. 19

Bastien, O., Roy, S., and Maréchal, E. (2005) Construction of non-symmetric substitution matrices derived from proteomes with biased amino acid distributions. *C R Biol*, **328** (5), 445–453. 20

Bechet, J. and Wiame, J. M. (1965) Indication of a specific regulatory binding protein for ornithinetranscarbamylase in *Saccharomyces cerevisiae*. *Biochem Biophys Res Commun*, **21** (3), 226–234. 28

Bennett, E. M., Ekstrom, J. L., Pegg, A. E., and Ealick, S. E. (2002) Monomeric *S*-adenosylmethionine decarboxylase from plants provides an alternative to putrescine stimulation. *Biochemistry*, **41** (49), 14509–17. 78, 81, 82, 83, 85

Beswick, T. C., Willert, E. K., and Phillips, M. A. (2006) Mechanisms of allosteric regulation of *Trypanosoma cruzi S*-adenosylmethionine decarboxylase. *Biochemistry*, **45** (25), 7797–7807. 82

Bewley, M. C., Jeffrey, P. D., Patchett, M. L., Kanyo, Z. F., and Baker, E. N. (1999) Crystal structures of *Bacillus caldovelox* arginase in complex with substrate and inhibitors reveal new insights into activation, inhibition and catalysis in the arginase superfamily. *Structure*, **7** (4), 435–48. 25, 28, 31, 40

Bewley, M. C., Lott, J. S., Baker, E. N., and Patchett, M. L. (1996) The cloning, expression and crystallisation of a thermostable arginase. *FEBS Lett*, **386** (2-3), 215–8. 25

Birkholtz, L., Joubert, F., Neitz, A. W., and Louw, A. I. (2003) Comparative properties of a three-dimensional model of *Plasmodium falciparum* ornithine decarboxylase. *Proteins*, **50** (3), 464–73. 4, 83, 85, 87, 88

Birkholtz, L. M., Wrenger, C., Joubert, F., Wells, G. A., Walter, R. D., and Louw, A. I. (2004) Parasite-specific inserts in the bifunctional *S*-adenosylmethionine decarboxylase/ornithine decarboxylase of *Plasmodium falciparum* modulate catalytic activities and domain interactions. *Biochem J*, **377** (Pt 2), 439–48. 4, 19, 39, 83, 85, 103, 105, 123, 124

Bitonti, A. J., Dumont, J. A., Bush, T. L., Edwards, M. L., Stemerick, D. M., McCann, P. P., and Sjoerdsma, A. (1989) Bis(benzyl)polyamine analogs inhibit the growth of chloroquine-resistant human malaria parasites (*Plasmodium falciparum*) *in vitro* and in combination with α-difluoromethylornithine cure murine malaria. *Proc Natl Acad Sci U S A*, **86** (2), 651–655. 8

Bitonti, A. J., McCann, P. P., and Sjoerdsma, A. (1987) *Plasmodium falciparum* and *Plasmodium berghei*: effects of ornithine decarboxylase inhibitors on erythrocytic schizogony. *Exp Parasitol*, **64** (2), 237–243. 7

Bjelic, S. and Aqvist, J. (2004) Computational prediction of structure, substrate binding mode, mechanism, and rate for a malaria protease with a novel type of active site. *Biochemistry*, **43** (46), 14521–14528. 21

Bogan, A. A. and Thorn, K. S. (1998) Anatomy of hot spots in protein interfaces. *J Mol Biol*, **280** (1), 1–9. 124, 125

Böhm, M., rzebecher, J. S., and Klebe, G. (1999) Three-dimensional quantitative structure-activity relationship analyses using comparative molecular field analysis and comparative molecular similarity indices analysis to elucidate selectivity differences of inhibitors binding to trypsin, thrombin, and factor Xa. *J Med Chem*, **42** (3), 458–477. 9

Borkovich, K. A. and Weiss, R. L. (1987) Relationship between two major immunoreactive forms of arginase in *Neurospora crassa*. *J Bacteriol*, **169** (12), 5510–7. 30

Bourne, P. and Weissig, H., editors (2003) In *Structural Bioinformatics*. Wiley. 11, 14

Callebaut, I., Prat, K., Meurice, E., Mornon, J.-P., and Tomavo, S. (2005) Prediction of the general transcription factors associated with rna polymerase ii in *Plasmodium falciparum*: conserved features and differences relative to other eukaryotes. *BMC Genomics*, **6**, 100. 19

Cama, E., Colleluori, D. M., Emig, F. A., Shin, H., Kim, S. W., Kim, N. N., Traish, A. M., Ash, D. E., and Christianson, D. W. (2003a) Human arginase II: crystal structure and physiological role in male and female sexual arousal. *Biochemistry*, **42** (28), 8445–51. 25, 27, 30, 31, 40

Cama, E., Emig, F. A., Ash, D. E., and Christianson, D. W. (2003b) Structural and functional importance of first-shell metal ligands in the binuclear manganese cluster of arginase I. *Biochemistry*, **42** (25), 7748–58. 26, 28

Cama, E., Pethe, S., Boucher, J. L., Han, S., Emig, F. A., Ash, D. E., Viola, R. E., Mansuy, D., and Christianson, D. W. (2004) Inhibitor coordination interactions in the binuclear manganese cluster of arginase. *Biochemistry*, **43** (28), 8987–99. 27

Cama, E., Shin, H., and Christianson, D. W. (2003c) Design of amino acid sulfonamides as transition-state analogue inhibitors of arginase. *J Am Chem Soc*, **125** (43), 13052–7. 27

Canutescu, A. A., Shelenkov, A. A., and Dunbrack, Jr, R. L. (2003) A graph-theory algorithm for rapid protein side-chain prediction. *Protein Sci*, **12** (9), 2001–14. 37

Carvajal, N., Martínez, J., de Oca, F. M., Rodríguez, J., and Fernández, M. (1978) Subunit interactions and immobilised dimers of human liver arginase. *Biochim Biophys Acta*, **527** (1), 1–7. 28

Carvajal, N., Martínez, J., and Fernández, M. (1977) Immobilised monomers of human liver arginase. *Biochim Biophys Acta*, **481** (1), 177–183. 28, 71

Carvajal, N., Olate, J., Salas, M., Uribe, E., Lopez, V., Herrera, P., and Cerpa, J. (1999a) Chemical modification and site-directed mutagenesis of human liver arginase: evidence that the imidazole group of histidine-141 is not involved in substrate binding. *Arch Biochem Biophys*, **371** (2), 202–206. 27

Carvajal, N., Rodríguez, J. P., and Fernández, M. (1982) Hybrid, immobilised dimers of human liver arginase. *Biochim Biophys Acta*, **701** (3), 405–407. 28

Carvajal, N., Salas, M., López, V., Uribe, E., Herrera, P., Cerpa, J., and Fuentes, M. (1999b) Manganese-dependent inhibition of human liver arginase by borate. *J Inorg Biochem*, **77** (3-4), 163–167. 27

Carvajal, N., Venegas, A., Oestreicher, G., and Plaza, M. (1971) Effect of manganese on the quaternary structure of human liver arginase. *Biochim Biophys Acta*, **250** (2), 437–442. 27, 28, 71

Cavalli, R. C., Burke, C. J., Kawamoto, S., Soprano, D. R., and Ash, D. E. (1994) Mutagenesis of rat liver arginase expressed in *Escherichia coli*: role of conserved histidines. *Biochemistry*, **33** (35), 10652–7. 26, 27, 28, 71

Childs, A. C., Mehta, D. J., and Gerner, E. W. (2003) Polyamine-dependent gene expression. *Cell Mol Life Sci*, **60** (7), 1394–406. 2, 3

Christopherson, R. I., Cinquin, O., Shojaei, M., Kuehn, D., and Menz, R. I. (2004) Cloning and expression of malarial pyrimidine enzymes. *Nucleosides Nucleotides Nucleic Acids*, **23** (8-9), 1459–1465. 18

Clare, J. J., Belcourt, M., and Farabaugh, P. J. (1988) Efficient translational frameshifting occurs within a conserved sequence of the overlap between the two genes of a yeast ty1 transposon. *Proc Natl Acad Sci U S A*, **85** (18), 6816–6820. 3

Clyne, T., Kinch, L. N., and Phillips, M. A. (2002) Putrescine activation of *Trypanosoma cruzi S*-adenosylmethionine decarboxylase. *Biochemistry*, **41** (44), 13207–13216. 81, 82

Coffino, P. (2001) Antizyme, a mediator of ubiquitin-independent proteasomal degradation. *Biochimie*, **83** (3-4), 319–323. 76

Cohen, S. (1998) In *A Guide to the Polyamines*. Oxford University Press. 1

Coleman, C. S., Stanley, B. A., Viswanath, R., and Pegg, A. E. (1994) Rapid exchange of subunits of mammalian ornithine decarboxylase. *J Biol Chem*, **269** (5), 3155–3158. 76

Cox, J. D., Cama, E., Colleluori, D. M., Pethe, S., Boucher, J. L., Mansuy, D., Ash, D. E., and Christianson, D. W. (2001) Mechanistic and metabolic inferences from the binding of substrate analogues and products to arginase. *Biochemistry*, **40** (9), 2689–701. 27, 30

Da'Dara, A. A., Henkle-Dührsen, K., and Walter, R. D. (1996) A novel trans-spliced mrna from *Onchocerca volvulus* encodes a functional *S*-adenosylmethionine decarboxylase. *Biochem J*, **320 (Pt 2)**, 519–530. 81

Da'dara, A. A. and Walter, R. D. (1998) Molecular and biochemical characterization of *S*-adenosylmethionine decarboxylase from the free-living nematode *Caenorhabditis elegans*. *Biochem J*, **336 (Pt 3)**, 545–550. 81

D'Agostino, L., di Pietro, M., and Luccia, A. D. (2005) Nuclear aggregates of polyamines are supramolecular structures that play a crucial role in genomic dna protection and conformation. *FEBS J*, **272** (15), 3777–3787. 2

D'Agostino, L. and Luccia, A. D. (2002) Polyamines interact with dna as molecular aggregates. *Eur J Biochem*, **269** (17), 4317–4325. 2

Darwin, C. (1859) In *The Origin of Species by Means of Natural Selection: The Preservation of Favored Races in the Struggle for Life (Penguin Classics)*. Penguin Classics. 6

de Beer, T. A., Louw, A. I., and Joubert, F. (2006) Elucidation of sulfadoxine resistance with structural models of the bifunctional *Plasmodium falciparum* dihydropterin pyrophosphokinase-dihydropteroate synthase. *Bioorg Med Chem*, **14** (13), 4433–43. 19

de Beer, T. A. P., Wells, G. A., Burger, P. B., Joubert, F., Marechal, E., Birkholtz, L., and Louw, A. I. (2009) Antimalarial drug discovery: *in silico* structural biology and rational drug design. *Infect Disord Drug Targets*, **9** (3), 304–318. 19

de Terán, H. G., Nervall, M., Dunn, B. M., Clemente, J. C., and Aqvist, J. (2006a) Computational analysis of plasmepsin iv bound to an allophenylnorstatine inhibitor. *FEBS Lett*, **580** (25), 5910–5916. 21

de Terán, H. G., Nervall, M., Ersmark, K., Liu, P., Janka, L. K., Dunn, B., Hallberg, A., and Aqvist, J. (2006b) Inhibitor binding to the plasmepsin IV aspartic protease from *Plasmodium falciparum*. *Biochemistry*, **45** (35), 10529–10541. 21

Delano, W. (2002) The PyMOL Molecular Graphics System on World Wide Web http://www.pymol.org. 37

Delfino, R. T., Santos-Filho, O. A., and Figueroa-Villar, J. D. (2002) Molecular modeling of wild-type and antifolate resistant mutant *Plasmodium falciparum* DHFR. *Biophys Chem*, **98** (3), 287–300. 21

Desai, P. V., Patny, A., Gut, J., Rosenthal, P. J., Tekwani, B., Srivastava, A., and Avery, M. (2006) Identification of novel parasitic cysteine protease inhibitors by use of virtual screening. 2. The available chemical directory. *J Med Chem*, **49** (5), 1576–1584. 21

Desai, P. V., Patny, A., Sabnis, Y., Tekwani, B., Gut, J., Rosenthal, P., Srivastava, A., and Avery, M. (2004) Identification of novel parasitic cysteine protease inhibitors using virtual screening. 1. The ChemBridge database. *J Med Chem*, **47** (26), 6609–6615. 21

Di Costanzo, L., Moulin, M., Haertlein, M., Meilleur, F., and Christianson, D. W. (2007a) Expression, purification, assay, and crystal structure of perdeuterated human arginase I. *Arch Biochem Biophys*, **465** (1), 82–9. 27

Di Costanzo, L., Pique, M. E., and Christianson, D. W. (2007b) Crystal structure of human arginase I complexed with thiosemicarbazide reveals an unusual thiocarbonyl μ-sulfide ligand in the binuclear manganese cluster. *J Am Chem Soc*, **129** (20), 6388–9. 71

Di Costanzo, L., Sabio, G., Mora, A., Rodriguez, P. C., Ochoa, A. C., Centeno, F., and Christianson, D. W. (2005) Crystal structure of human arginase I at 1.29-A resolution and exploration of inhibition in the immune response. *Proc Natl Acad Sci U S A*, **102** (37), 13058–63. 25, 26, 27, 35, 71

DiMasi, J. A., Hansen, R. W., and Grabowski, H. G. (2003) The price of innovation: new estimates of drug development costs. *J Health Econ*, **22** (2), 151–185. 9

Dondorp, A. M., Nosten, F., Yi, P., Das, D., Phyo, A. P., Tarning, J., Lwin, K. M., Ariey, F., Hanpithakpong, W., Lee, S. J., Ringwald, P., Silamut, K., Imwong, M., Chotivanich, K., Lim, P., Herdman, T., An, S. S., Yeung, S., Singhasivanon, P., Day, N. P. J., Lindegardh, N., Socheat, D., and White, N. J. (2009) Artemisinin resistance in *Plasmodium falciparum* malaria. *N Engl J Med*, **361** (5), 455–467. 5

Dowling, D., Costanzo, L., Gennadios, H., and Christianson, D. (2008) Evolution of the arginase fold and functional diversity. *Cell Mol Life Sci*. 24

Dror, R. O., Jensen, M. O., and Shaw, D. E. (2009) Elucidating membrane protein function through long-timescale molecular dynamics simulation. *Conf Proc IEEE Eng Med Biol Soc*, **1**, 2340–2342. 14, 130

Dunathan, H. C. (1966) Conformation and reaction specificity in pyridoxal phosphate enzymes. *Proc Natl Acad Sci U S A*, **55** (4), 712–716. 75

Ekstrom, J. L., Mathews, I. I., Stanley, B. A., Pegg, A. E., and Ealick, S. E. (1999) The crystal structure of human *S*-adenosylmethionine decarboxylase at 2.25 a resolution reveals a novel fold. *Structure*, **7** (5), 583–595. 78, 81

Ekstrom, J. L., Tolbert, W. D., Xiong, H., Pegg, A. E., and Ealick, S. E. (2001) Structure of a human *S*-adenosylmethionine decarboxylase self-processing ester intermediate and mechanism of putrescine stimulation of processing as revealed by the H243A mutant. *Biochemistry*, **40** (32), 9495–504. 79

Ferrara, P., Gohlke, H., Price, D. J., Klebe, G., and Brooks, C. L. (2004) Assessing scoring functions for protein-ligand interactions. *J Med Chem*, **47** (12), 3032–3047. 9

Fields, S. and Song, O. (1989) A novel genetic system to detect protein-protein interactions. *Nature*, **340** (6230), 245–246. 15

Fletcher, S., Cummings, C. G., Rivas, K., Katt, W. P., Hornéy, C., Buckner, F. S., Chakrabarti, D., Sebti, S. M., Gelb, M. H., Voorhis, W. C. V., and Hamilton, A. D. (2008) Potent, *Plasmodium*-selective farnesyltransferase inhibitors that arrest the growth of malaria parasites: structure-activity relationships of ethylenediamine-analogue scaffolds and homology model validation. *J Med Chem*, **51** (17), 5176–5197. 22

Fletcher, S. and Hamilton, A. D. (2006) Targeting protein-protein interactions by rational design: mimicry of protein surfaces. *J R Soc Interface*, **3** (7), 215–33. 70

Flick, K., Ahuja, S., Chene, A., Bejarano, M. T., and Chen, Q. (2004) Optimized expression of *Plasmodium falciparum* erythrocyte membrane protein 1 domains in *Escherichia coli*. *Malar J*, **3**, 50. 18

Fry, D. C. (2006) Protein-protein interactions as targets for small molecule drug discovery. *Biopolymers*, **84** (6), 535–52. 70

Fukumoto, G. H. and Byus, C. V. (1996) A kinetic characterization of putrescine and spermidine uptake and export in human erythrocytes. *Biochim Biophys Acta*, **1282** (1), 48–56. 8

Fuller, J. C., Burgoyne, N. J., and Jackson, R. M. (2009) Predicting druggable binding sites at the protein-protein interface. *Drug Discov Today*, **14** (3-4), 155–161. 18

Gabb, H. A., Jackson, R. M., and Sternberg, M. J. (1997) Modelling protein docking using shape complementarity, electrostatics and biochemical information. *J Mol Biol*, **272** (1), 106–120. 17

Gardner, M. J., Hall, N., Fung, E., White, O., Berriman, M., Hyman, R. W., Carlton, J. M., Pain, A., Nelson, K. E., Bowman, S., Paulsen, I. T., James, K., Eisen, J. A., Rutherford, K., Salzberg, S. L., Craig, A., Kyes, S., Chan, M.-S., Nene, V., Shallom, S. J., Suh, B., Peterson, J., Angiuoli, S., Pertea, M., Allen, J., Selengut, J., Haft, D., Mather, M. W., Vaidya, A. B., Martin, D. M. A., Fairlamb, A. H., Fraunholz, M. J., Roos, D. S., Ralph, S. A., McFadden, G. I., Cummings, L. M., Subramanian, G. M., Mungall, C., Venter, J. C., Carucci, D. J., Hoffman, S. L., Newbold, C., Davis, R. W., Fraser, C. M., and Barrell, B. (2002) Genome sequence of the human malaria parasite *Plasmodium falciparum*. *Nature*, **419** (6906), 498–511. 6, 83

Gardner, M. J., Tettelin, H., Carucci, D. J., Cummings, L. M., Aravind, L., Koonin, E. V., Shallom, S., Mason, T., Yu, K., Fujii, C., Pederson, J., Shen, K., Jing, J., Aston, C., Lai, Z., Schwartz, D. C., Pertea, M., Salzberg, S., Zhou, L., Sutton, G. G., Clayton, R., White, O., Smith, H. O., Fraser, C. M., Adams, M. D., Venter, J. C., and Hoffman, S. L. (1998) Chromosome 2 sequence of the human malaria parasite *Plasmodium falciparum*. *Science*, **282** (5391), 1126–1132. 83

Giles, T. N. and Graham, D. E. (2008) Crenarchaeal arginine decarboxylase evolved from an *S*-adenosylmethionine decarboxylase enzyme. *J Biol Chem*, **283** (38), 25829–25838. 77

Gillet, J. M., Charlier, J., Boné, G., and Mulamba, P. L. (1983) *Plasmodium berghei*: inhibition of the sporogonous cycle by α-difluoromethylornithine. *Exp Parasitol*, **56** (2), 190–193. 7

Glenn, M. P., Chang, S.-Y., Hornéy, C., Rivas, K., Yokoyama, K., Pusateri, E. E., Fletcher, S., Cummings, C. G., Buckner, F. S., Pendyala, P. R., Chakrabarti, D., Sebti, S. M., Gelb, M., Voorhis, W. C. V., and Hamilton, A. D. (2006) Structurally simple, potent, *Plasmodium* selective farnesyltransferase inhibitors that arrest the growth of malaria parasites. *J Med Chem*, **49** (19), 5710–5727. 22

Glenn, M. P., Chang, S.-Y., Hucke, O., Verlinde, C. L. M. J., Rivas, K., Hornéy, C., Yokoyama, K., Buckner, F. S., Pendyala, P. R., Chakrabarti, D., Gelb, M., Voorhis, W. C. V., Sebti, S. M., and Hamilton, A. D. (2005) Structurally simple farnesyltransferase inhibitors arrest the growth of malaria parasites. *Angew Chem Int Ed Engl*, **44** (31), 4903–4906. 22

Goodsell, D. S., Morris, G. M., and Olson, A. J. (1996) Automated docking of flexible ligands: applications of AutoDock. *J Mol Recognit*, **9** (1), 1–5. 10

Gotoh, T., Sonoki, T., Nagasaki, A., Terada, K., Takiguchi, M., and Mori, M. (1996) Molecular cloning of cDNA for nonhepatic mitochondrial arginase (arginase II) and comparison of its induction with nitric oxide synthase in a murine macrophage-like cell line. *FEBS Lett*, **395** (2-3), 119–22. 30

Green, S. M., Eisenstein, E., McPhie, P., and Hensley, P. (1990) The purification and characterization of arginase from *Saccharomyces cerevisiae*. *J Biol Chem*, **265** (3), 1601–7. 28

Green, S. M., Ginsburg, A., Lewis, M. S., and Hensley, P. (1991) Roles of metal ions in the maintenance of the tertiary and quaternary structure of arginase from *Saccharomyces cerevisiae*. *J Biol Chem*, **266** (32), 21474–81. 28

Greenwood, B. M., Fidock, D. A., Kyle, D. E., Kappe, S. H., Alonso, P. L., Collins, F. H., and Duffy, P. E. (2008) Malaria: progress, perils, and prospects for eradication. *The Journal of clinical investigation*, **118** (4), 1266–1276. 4, 5, 6, 7

Grishin, N. V., Osterman, A. L., Brooks, H. B., Phillips, M. A., and Goldsmith, E. J. (1999) X-ray structure of ornithine decarboxylase from *Trypanosoma brucei*: the native structure and the structure in complex with α-difluoromethylornithine. *Biochemistry*, **38** (46), 15174–15184. 74, 75, 76

Grishin, N. V., Phillips, M. A., and Goldsmith, E. J. (1995) Modeling of the spatial structure of eukaryotic ornithine decarboxylases. *Protein Sci*, **4** (7), 1291–1304. 73

Grody, W. W., Dizikes, G. J., and Cederbaum, S. D. (1987) Human arginase isozymes. *Isozymes Curr Top Biol Med Res*, **13**, 181–214. 30

Gupta, R. D., Krause-Ihle, T., Bergmann, B., Müller, I. B., Khomutov, A. R., Müller, S., Walter, R. D., and Lüersen, K. (2005) 3-aminooxy-1-aminopropane and derivatives have an antiproliferative effect on cultured *Plasmodium falciparum* by decreasing intracellular polyamine concentrations. *Antimicrob Agents Chemother*, **49** (7), 2857–2864. 7, 8

Haider, N., Eschbach, M. L., Dias Sde, S., Gilberger, T. W., Walter, R. D., and Lüersen, K. (2005) The spermidine synthase of the malaria parasite *Plasmodium falciparum*: molecular and biochemical characterisation of the polyamine synthesis enzyme. *Mol Biochem Parasitol*, **142** (2), 224–36. 4

Hardman, J. G. and Limbird, L. E. (2001) In *Goodman and Gilman's the Pharmacological Basis of Therapeutics (McGraw-Hill International Editions)*. McGraw-Hill Publishing Co., 10th edition. 5

Hay, S. I., Guerra, C. A., Gething, P. W., Patil, A. P., Tatem, A. J., Noor, A. M., Kabaria, C. W., Manh, B. H., Elyazar, I. R., Brooker, S., Smith, D. L., Moyeed, R. A., and Snow, R. W. (2009) A world malaria map: *Plasmodium falciparum* endemicity in 2007. *PLoS medicine*, **6** (3). 4, 5

Heby, O., Persson, L., and Rentala, M. (2007) Targeting the polyamine biosynthetic enzymes: a promising approach to therapy of african sleeping sickness, Chagas´ disease, and leishmaniasis. *Amino Acids*, **33** (2), 359–366. 3, 4

Hecker, M., Nematollahi, H., Hey, C., Busse, R., and Racké, K. (1995) Inhibition of arginase by NG-hydroxy-L-arginine in alveolar macrophages: implications for the utilization of l-arginine for nitric oxide synthesis. *FEBS Lett*, **359** (2-3), 251–254. 30

Hoyt, M. A., Williams-Abbott, L. J., Pitkin, J. W., and Davis, R. H. (2000) Cloning and expression of the *S*-adenosylmethionine decarboxylase gene of *Neurospora crassa* and processing of its product. *Mol Gen Genet*, **263** (4), 664–673. 81

Humphrey, W., Dalke, A., and Schulten, K. (1996) VMD: visual molecular dynamics. *J Mol Graph*, **14** (1), 33–8, 27–8. 37

Hyde, J. E. (2007) Drug-resistant malaria - an insight. *FEBS J*, **274** (18), 4688–4698. 4, 5

Ivanov, I. and Klein, M. L. (2004) First principles computational study of the active site of arginase. *Proteins*, **54** (1), 1–7. 26

Jackson, K. L., Baldwin, J., Akella, R., Goldsmith, E. J., and Phillips, M. A. (2004) Multiple active site conformations revealed by distant site mutation in ornithine decarboxylase. *Biochemistry*, **43** (41), 12990–12999. 74, 76

Jackson, L. K., Brooks, H. B., Myers, D. P., and Phillips, M. A. (2003a) Ornithine decarboxylase promotes catalysis by binding the carboxylate in a buried pocket containing phenylalanine 397. *Biochemistry*, **42** (10), 2933–2940. 75

Jackson, L. K., Brooks, H. B., Osterman, A. L., Goldsmith, E. J., and Phillips, M. A. (2000) Altering the reaction specificity of eukaryotic ornithine decarboxylase. *Biochemistry*, **39** (37), 11247–11257. 75, 86

Jackson, L. K., Goldsmith, E. J., and Phillips, M. A. (2003b) X-ray structure determination of *Trypanosoma brucei* ornithine decarboxylase bound to D-ornithine and to G418: insights into substrate binding and ODC conformational flexibility. *J Biol Chem*, **278** (24), 22037–22043. 76

Jackson, R. M., Gabb, H. A., and Sternberg, M. J. (1998) Rapid refinement of protein interfaces incorporating solvation: application to the docking problem. *J Mol Biol*, **276** (1), 265–285. 89

Janne, J., Alhonen, L., Pietila, M., and Keinanen, T. A. (2004) Genetic approaches to the cellular functions of polyamines in mammals. *Eur J Biochem*, **271** (5), 877–94. 2

Jean, L., Withers-Martinez, C., Hackett, F., and Blackman, M. J. (2005) Unique insertions within *Plasmodium falciparum* subtilisin-like protease-1 are crucial for enzyme maturation and activity. *Mol Biochem Parasitol*, **144** (2), 187–97. 39

Jenkinson, C. P., Grody, W. W., and Cederbaum, S. D. (1996) Comparative properties of arginases. *Comp Biochem Physiol B Biochem Mol Biol*, **114** (1), 107–32. 27

Kameji, T. and Pegg, A. E. (1987) Effect of putrescine on the synthesis of *S*-adenosylmethionine decarboxylase. *Biochem J*, **243** (1), 285–288. 81

Kanyo, Z. F., Scolnick, L. R., Ash, D. E., and Christianson, D. W. (1996) Structure of a unique binuclear manganese cluster in arginase. *Nature*, **383** (6600), 554–7. Enter text here. 25, 28, 31, 40

Kasam, V., Salzemann, J., Botha, M., Dacosta, A., Degliesposti, G., Isea, R., Kim, D., Maass, A., Kenyon, C., Rastelli, G., Hofmann-Apitius, M., and Breton, V. (2009) WISDOM-II: screening against multiple targets implicated in malaria using computational grid infrastructures. *Malar J*, **8**, 88. 10

Kern, A. D., Oliveira, M. A., Coffino, P., and Hackert, M. L. (1999) Structure of mammalian ornithine decarboxylase at 1.6 a resolution: stereochemical implications of PLP-dependent amino acid decarboxylases. *Structure*, **7** (5), 567–581. 73, 75, 76, 125

Keskin, O., Gursoy, A., Ma, B., and Nussinov, R. (2007) Towards drugs targeting multiple proteins in a systems biology approach. *Curr Top Med Chem*, **7** (10), 943–51. 70

Kihara, D. and Skolnick, J. (2003) The PDB is a covering set of small protein structures. *J Mol Biol*, **334** (4), 793–802. 19

Kim, A. D., Graham, D. E., Seeholzer, S. H., and Markham, G. D. (2000) *S*-Adenosylmethionine decarboxylase from the archaeon *Methanococcus jannaschii*: identification of a novel family of pyruvoyl enzymes. *J Bacteriol*, **182** (23), 6667–6672. 81

Kim, N. N., Cox, J. D., Baggio, R. F., Emig, F. A., Mistry, S. K., Harper, S. L., Speicher, D. W., Morris, Jr, S. M., Ash, D. E., Traish, A., and Christianson, D. W. (2001) Probing erectile function: *S*-(2-boronoethyl)-L-cysteine binds to arginase as a transition state analogue and enhances smooth muscle relaxation in human penile corpus cavernosum. *Biochemistry*, **40** (9), 2678–88. 71

Kinch, L. N. and Phillips, M. A. (2000) Single-turnover kinetic analysis of *Trypanosoma cruzi S*-adenosylmethionine decarboxylase. *Biochemistry*, **39** (12), 3336–3343. 81

Klebe, G. (2006) Virtual ligand screening: strategies, perspectives and limitations. *Drug Discov Today*, **11** (13-14), 580–594. 9

Klepeis, J. L., Lindorff-Larsen, K., Dror, R. O., and Shaw, D. E. (2009) Long-timescale molecular dynamics simulations of protein structure and function. *Curr Opin Struct Biol*, **19** (2), 120–127. 14, 130

Korsinczky, M., Fischer, K., Chen, N., Baker, J., Rieckmann, K., and Cheng, Q. (2004) Sulfadoxine resistance in *Plasmodium vivax* is associated with a specific amino acid in dihydropteroate synthase at the putative sulfadoxine-binding site. *Antimicrob Agents Chemother*, **48** (6), 2214–2222. 21

Kozbial, P. Z. and Mushegian, A. R. (2005) Natural history of *S*-adenosylmethionine-binding proteins. *BMC Struct Biol*, **5**, 19. 77

Krause, T., Luersen, K., Wrenger, C., Gilberger, T. W., Muller, S., and Walter, R. D. (2000) The ornithine decarboxylase domain of the bifunctional ornithine decarboxylase/*S*-adenosylmethionine decarboxylase of *Plasmodium falciparum*: recombinant expression and catalytic properties of two different constructs. *Biochem J*, **352 Pt 2**, 287–92. 4, 83

Lavulo, L. T., Sossong, Jr, T. M., Brigham-Burke, M. R., Doyle, M. L., Cox, J. D., Christianson, D. W., and Ash, D. E. (2001) Subunit-subunit interactions in trimeric arginase. Generation of active monomers by mutation of a single amino acid. *J Biol Chem*, **276** (17), 14242–8. 28, 58, 59, 71

Leach, A. (2001) In *Molecular Modelling: Principles and Applications (2nd Edition)*. Prentice Hall, 2nd edition. 11, 12

Lee, J., Michael, A. J., Martynowski, D., Goldsmith, E. J., and Phillips, M. A. (2007) Phylogenetic diversity and the structural basis of substrate specificity in the β/α-barrel fold basic amino acid decarboxylases. *J Biol Chem*, **282** (37), 27115–27125. 73, 74

Lemcke, T., Christensen, I. T., and Jørgensen, F. S. (1999) Towards an understanding of drug resistance in malaria: three-dimensional structure of *Plasmodium falciparum* dihydrofolate reductase by homology building. *Bioorg Med Chem*, **7** (6), 1003–1011. 21

Lensink, M. F., Méndez, R., and Wodak, S. J. (2007) Docking and scoring protein complexes: CAPRI 3rd edition. *Proteins*, **69** (4), 704–718. 15, 16, 18

Li, H., Meininger, C. J., Hawker, Jr, J. R., Haynes, T. E., Kepka-Lenhart, D., Mistry, S. K., Morris, Jr, S. M., and Wu, G. (2001) Regulatory role of arginase I and II in nitric oxide, polyamine, and proline syntheses in endothelial cells. *Am J Physiol Endocrinol Metab*, **280** (1), E75–82. 30

Li, R., Chen, X., Gong, B., Selzer, P. M., Li, Z., Davidson, E., Kurzban, G., Miller, R. E., Nuzum, E. O., McKerrow, J. H., Fletterick, R. J., Gillmor, S. A., Craik, C. S., Kuntz, I. D., Cohen, F. E., and Kenyon, G. L. (1996) Structure-based design of parasitic protease inhibitors. *Bioorg Med Chem*, **4** (9), 1421–1427. 21

Lijnzaad, P., Berendsen, H. J., and Argos, P. (1996) Hydrophobic patches on the surfaces of protein structures. *Proteins*, **25** (3), 389–397. 123

Lipinski, C. A., Lombardo, F., Dominy, B. W., and Feeney, P. J. (2001) Experimental and computational approaches to estimate solubility and permeability in drug discovery and development settings. *Adv Drug Deliv Rev*, **46** (1-3), 3–26. 9, 10

Liu, H., Elstner, M., Kaxiras, E., Frauenheim, T., Hermans, J., and Yang, W. (2001) Quantum mechanics simulation of protein dynamics on long timescale. *Proteins*, **44** (4), 484–489. 11

Livingstone (2000) The characterization of chemical structures using molecular properties. a survey. *J Chem Inf Comput Sci*, **40** (2), 195–209. 9

Lowa, P. M., Gillet, J., Boné, G., and Schechter, P. J. (1986) α-Difluoromethylornithine inhibits the first part of exoerythrocytic schizogony of *Plasmodium berghei* in rodents. *Ann Soc Belg Med Trop*, **66** (4), 301–308. 7

Luccia, A. D., Picariello, G., Iacomino, G., Formisano, A., Paduano, L., and D'Agostino, L. (2009) The *in vitro* nuclear aggregates of polyamines. *FEBS J*, **276** (8), 2324–2335. 2

Luksch, T., Chan, N.-S., Brass, S., Sotriffer, C. A., Klebe, G., and Diederich, W. E. (2008) Computer-aided design and synthesis of nonpeptidic plasmepsin II and IV inhibitors. *ChemMedChem*, **3** (9), 1323–1336. 21

Marathe, S., Yu, Y. G., Turner, G. E., Palmier, C., and Weiss, R. L. (1998) Multiple forms of arginase are differentially expressed from a single locus in *Neurospora crassa*. *J Biol Chem*, **273** (45), 29776–29785. 30

Mardis, K. L., Sutton, H. M., Zuo, X., Lindsey, J. S., and Tiede, D. M. (2009) Solution-state conformational ensemble of a hexameric porphyrin array characterized using molecular dynamics and X-ray scattering. *J Phys Chem A*, **113** (11), 2516–2523. 11, 128

Markham, G. D., Tabor, C. W., and Tabor, H. (1982) *S*-adenosylmethionine decarboxylase of *Escherichia coli*. studies on the covalently linked pyruvate required for activity. *J Biol Chem*, **257** (20), 12063–12068. 81, 82

Marton, L. J. and Pegg, A. E. (1995) Polyamines as targets for therapeutic intervention. *Annu Rev Pharmacol Toxicol*, **35**, 55–91. 7

McKie, J. H., Douglas, K. T., Chan, C., Roser, S. A., Yates, R., Read, M., Hyde, J. E., Dascombe, M. J., Yuthavong, Y., and Sirawaraporn, W. (1998) Rational drug design approach for overcoming drug resistance: application to pyrimethamine resistance in malaria. *J Med Chem*, **41** (9), 1367–1370. 21

Mehlin, C., Boni, E., Buckner, F. S., Engel, L., Feist, T., Gelb, M. H., Haji, L., Kim, D., Liu, C., Mueller, N., Myler, P. J., Reddy, J. T., Sampson, J. N., Subramanian, E., Voorhis, W. C. V., Worthey, E., Zucker, F., and Hol, W. G. J. (2006) Heterologous expression of proteins from *Plasmodium falciparum*: results from 1000 genes. *Mol Biochem Parasitol*, **148** (2), 144–160. 18

Melby, T. and Westby, M. (2009) Inhibitors of viral entry. *Handb Exp Pharmacol*, (189), 177–202. 18

Méndez, R., Leplae, R., Lensink, M. F., and Wodak, S. J. (2005) Assessment of CAPRI predictions in rounds 3-5 shows progress in docking procedures. *Proteins*, **60** (2), 150–169. 16, 18

Méndez, R., Leplae, R., Maria, L. D., and Wodak, S. J. (2003) Assessment of blind predictions of protein-protein interactions: current status of docking methods. *Proteins*, **52** (1), 51–67. 16, 18

Messenguy, F. and Wiame, J. (1969) The control of ornithinetranscarbamylase activity by arginase in *Saccharomyces cerevisiae*. *FEBS Lett*, **3** (1), 47–49. 28

Mora, A., del Ara Rangel, M., Fuentes, J. M., Soler, G., and Centeno, F. (2000) Implications of the *S*-shaped domain in the quaternary structure of human arginase. *Biochim Biophys Acta*, **1476** (2), 181–90. 28, 40

Moreira, I. S., Fernandes, P. A., and Ramos, M. J. (2007) Hot spots–a review of the protein-protein interface determinant amino-acid residues. *Proteins*, **68** (4), 803–812. 124

Morris, A. L., MacArthur, M. W., Hutchinson, E. G., and Thornton, J. M. (1992) Stereochemical quality of protein structure coordinates. *Proteins*, **12** (4), 345–364. 88

Morris, S. M. (2002) Regulation of enzymes of the urea cycle and arginine metabolism. *Annu Rev Nutr*, **22**, 87–105. 30

Müller, I. B., Gupta, R. D., Lüersen, K., Wrenger, C., and Walter, R. D. (2008) Assessing the polyamine metabolism of *Plasmodium falciparum* as chemotherapeutic target. *Mol Biochem Parasitol*, **160** (1), 1–7. 7, 8

Müller, I. B., Walter, R. D., and Wrenger, C. (2005) Structural metal dependency of the arginase from the human malaria parasite *Plasmodium falciparum*. *Biol Chem*, **386** (2), 117–26. 4, 29, 30, 37, 38, 48, 57, 59, 66, 67

Müller, S., Da'dara, A., Lüersen, K., Wrenger, C., Gupta, R. D., Madhubala, R., and Walter, R. D. (2000) In the human malaria parasite *Plasmodium falciparum*, polyamines are synthesized by a bifunctional ornithine decarboxylase, *S*-adenosylmethionine decarboxylase. *J Biol Chem*, **275** (11), 8097–8102. 4, 82

Müller, S., Liebau, E., Walter, R. D., and Krauth-Siegel, R. L. (2003) Thiol-based redox metabolism of protozoan parasites. *Trends Parasitol*, **19** (7), 320–8. 3, 4

Munder, M., Eichmann, K., Morán, J. M., Centeno, F., Soler, G., and Modolell, M. (1999) Th1/Th2-regulated expression of arginase isoforms in murine macrophages and dendritic cells. *J Immunol*, **163** (7), 3771–3777. 30

Myers, D. P., Jackson, L. K., Ipe, V. G., Murphy, G. E., and Phillips, M. A. (2001) Long-range interactions in the dimer interface of ornithine decarboxylase are important for enzyme function. *Biochemistry*, **40** (44), 13230–13236. 76

Olszewski, K. L., Morrisey, J. M., Wilinski, D., Burns, J. M., Vaidya, A. B., Rabinowitz, J. D., and Llinás, M. (2009) Host-parasite interactions revealed by *Plasmodium falciparum* metabolomics. *Cell Host Microbe*, **5** (2), 191–199. 71

Orry, A. J. W., Abagyan, R. A., and Cavasotto, C. N. (2006) Structure-based development of target-specific compound libraries. *Drug Discov Today*, **11** (5-6), 261–266. 9

Osterman, A., Grishin, N. V., Kinch, L. N., and Phillips, M. A. (1994) Formation of functional cross-species heterodimers of ornithine decarboxylase. *Biochemistry*, **33** (46), 13662–13667. 76

Osterman, A. L., Brooks, H. B., Jackson, L., Abbott, J. J., and Phillips, M. A. (1999) Lysine-69 plays a key role in catalysis by ornithine decarboxylase through acceleration of the schiff base formation, decarboxylation, and product release steps. *Biochemistry*, **38** (36), 11814–11826. 74

Ouzounis, C. A., Kunin, V., Darzentas, N., and Goldovsky, L. (2006) A minimal estimate for the gene content of the last universal common ancestor–exobiology from a terrestrial perspective. *Res Microbiol*, **157** (1), 57–68. 24

Ouzounis, C. A. and Kyrpides, N. C. (1994) On the evolution of arginases and related enzymes. *J Mol Evol*, **39** (1), 101–4. 24

Pankaskie, M. and Abdel-Monem, M. M. (1980) Inhibitors of polyamine biosynthesis. 8. irreversible inhibition of mammalian *S*-adenosyl-L-methionine decarboxylase by substrate analogues. *J Med Chem*, **23** (2), 121–127. 80

Park, M. H., Cooper, H. L., and Folk, J. E. (1981) Identification of hypusine, an unusual amino acid, in a protein from human lymphocytes and of spermidine as its biosynthetic precursor. *Proc Natl Acad Sci U S A*, **78** (5), 2869–2873. 3

Park, M. H., Cooper, H. L., and Folk, J. E. (1982) The biosynthesis of protein-bound hypusine (N_ϵ-(4-amino-2-hydroxybutyl)lysine). lysine as the amino acid precursor and the intermediate role of deoxyhypusine (n epsilon -(4-aminobutyl)lysine). *J Biol Chem*, **257** (12), 7217–7222. 3

Park, M. H., Wolff, E. C., and Folk, J. E. (1993) Is hypusine essential for eukaryotic cell proliferation? *Trends Biochem Sci*, **18** (12), 475–9. 3

Pegg, A. E. and Jacobs, G. (1983) Comparison of inhibitors of *S*-adenosylmethionine decarboxylase from different species. *Biochem J*, **213** (2), 495–502. 80

Phillips, J. C., Braun, R., Wang, W., Gumbart, J., Tajkhorshid, E., Villa, E., Chipot, C., Skeel, R. D., Kale, L., and Schulten, K. (2005) Scalable molecular dynamics with NAMD. *J Comput Chem*, **26** (16), 1781–802. 47

Pizzi, E. and Frontali, C. (2000) Divergence of noncoding sequences and of insertions encoding nonglobular domains at a genomic region well conserved in plasmodia. *J Mol Evol*, **50** (5), 474–480. 83

Pizzi, E. and Frontali, C. (2001) Low-complexity regions in *Plasmodium falciparum* proteins. *Genome Res*, **11** (2), 218–29. 39, 83

Punta, M. and Rost, B. (2005) PROFcon: novel prediction of long-range contacts. *Bioinformatics*, **21** (13), 2960–2968. 116

R Development Core Team (2009) In *R: A Language and Environment for Statistical Computing*. R Foundation for Statistical Computing, Vienna, Austria. ISBN 3-900051-07-0. 102

Rarey, M., Kramer, B., Lengauer, T., and Klebe, G. (1996) A fast flexible docking method using an incremental construction algorithm. *J Mol Biol*, **261** (3), 470–489. 10

Rastelli, G., Sirawaraporn, W., Sompornpisut, P., Vilaivan, T., Kamchonwongpaisan, S., Quarrell, R., Lowe, G., Thebtaranonth, Y., and Yuthavong, Y. (2000) Interaction of pyrimethamine, cycloguanil, WR99210 and their analogues with *Plasmodium falciparum* dihydrofolate reductase: structural basis of antifolate resistance. *Bioorg Med Chem*, **8** (5), 1117–1128. 21, 22

Rattanachuen, W., Jönsson, M., Swedberg, G., and Sirawaraporn, W. (2009) Probing the roles of non-homologous insertions in the n-terminal domain of *Plasmodium falciparum* hydroxymethylpterin pyrophosphokinase-dihydropteroate synthase. *Mol Biochem Parasitol*, **168** (2), 135–142. 39

Recsei, P. A. and Snell, E. E. (1984) Pyruvoyl enzymes. *Annu Rev Biochem*, **53**, 357–387. 79

Rom, E. and Kahana, C. (1994) Polyamines regulate the expression of ornithine decarboxylase antizyme *in vitro* by inducing ribosomal frame-shifting. *Proc Natl Acad Sci U S A*, **91** (9), 3959–3963. 3

Rowe, A. K., Rowe, S. Y., Snow, R. W., Korenromp, E. L., Schellenberg, J. R. A. R., Stein, C., Nahlen, B. L., Bryce, J., Black, R. E., and Steketee, R. W. (2006) The burden of malaria mortality among african children in the year 2000. *International journal of epidemiology*, **35** (3), 691–704. 4

Sabio, G., Mora, A., Rangel, M. A., Quesada, A., Marcos, C. F., Alonso, J. C., Soler, G., and Centeno, F. (2001) Glu-256 is a main structural determinant for oligomerisation of human arginase I. *FEBS Lett*, **501** (2-3), 161–165. 28, 39, 71

Sandmeier, E., Hale, T. I., and Christen, P. (1994) Multiple evolutionary origin of pyridoxal-5'-phosphate-dependent amino acid decarboxylases. *Eur J Biochem*, **221** (3), 997–1002. 73

Santos-Filho, O. A., de Alencastro, R. B., and Figueroa-Villar, J. D. (2001) Homology modeling of wild type and pyrimethamine/cycloguanil-cross resistant mutant type *Plasmodium falciparum* dihydrofolate reductase. A model for antimalarial chemotherapy resistance. *Biophys Chem*, **91** (3), 305–317. 21

Schafer, B., Hauber, I., Bunk, A., Heukeshoven, J., Dusedau, A., Bevec, D., and Hauber, J. (2006) Inhibition of multidrug-resistant HIV-1 by interference with cellular *S*-adenosylmethionine decarboxylase activity. *J Infect Dis*, **194** (6), 740–50. 4

Schlick, T. (2002) In *Molecular Modeling and Simulation*. Springer, 1st edition. 11, 12, 14

Scolnick, L. R., Kanyo, Z. F., Cavalli, R. C., Ash, D. E., and Christianson, D. W. (1997) Altering the binuclear manganese cluster of arginase diminishes thermostability and catalytic function. *Biochemistry*, **36** (34), 10558–65. 25, 26, 28

Seiler, N. (2003a) Thirty years of polyamine-related approaches to cancer therapy. Retrospect and prospect. Part 1. Selective enzyme inhibitors. *Curr Drug Targets*, **4** (7), 537–564. 7

Seiler, N. (2003b) Thirty years of polyamine-related approaches to cancer therapy. Retrospect and prospect. Part 2. Structural analogues and derivatives. *Curr Drug Targets*, **4** (7), 565–585. 7

Sekowska, A., Coppée, J. Y., Caer, J. P. L., Martin-Verstraete, I., and Danchin, A. (2000) *S*-adenosylmethionine decarboxylase of *Bacillus subtilis* is closely related to archaebacterial counterparts. *Mol Microbiol*, **36** (5), 1135–1147. 24, 81

Shi, J., Blundell, T. L., and Mizuguchi, K. (2001) FUGUE: sequence-structure homology recognition using environment-specific substitution tables and structure-dependent gap penalties. *J Mol Biol*, **310** (1), 243–57. 31

Shoemaker, B. A. and Panchenko, A. R. (2007) Deciphering protein-protein interactions. Part I. Experimental techniques and databases. *PLoS Comput Biol*, **3** (3), e42. 15

Singh, B., Sung, L. K., Matusop, A., Radhakrishnan, A., Shamsul, S. S. G., Cox-Singh, J., Thomas, A., and Conway, D. J. (2004) A large focus of naturally acquired *Plasmodium knowlesi* infections in human beings. *Lancet*, **363** (9414), 1017–1024. 4, 21

Snow, R. W., Guerra, C. A., Noor, A. M., Myint, H. Y., and Hay, S. I. (2005) The global distribution of clinical episodes of *Plasmodium falciparum* malaria. *Nature*, **434** (7030), 214–7. 4

Snowden, M. and Green, D. V. (2008) The impact of diversity-based, high-throughput screening on drug discovery: "chance favours the prepared mind". *Curr Opin Drug Discov Devel*, **11** (4), 553–558. 9

Spector, E. B., Rice, S. C., Kern, R. M., Hendrickson, R., and Cederbaum, S. D. (1985) Comparison of arginase activity in red blood cells of lower mammals, primates, and man: evolution to high activity in primates. *Am J Hum Genet*, **37** (6), 1138–45. 30

Spector, E. B., Rice, S. C., Moedjono, S., Bernard, B., and Cederbaum, S. D. (1982) Biochemical properties of arginase in human adult and fetal tissues. *Biochem Med*, **28** (2), 165–75. 30

Stanley, B. A. and Pegg, A. E. (1991) Amino acid residues necessary for putrescine stimulation of human *S*-adenosylmethionine decarboxylase proenzyme processing and catalytic activity. *J Biol Chem*, **266** (28), 18502–18506. 79

Stanley, B. A., Shantz, L. M., and Pegg, A. E. (1994) Expression of mammalian *S*-adenosylmethionine decarboxylase in *Escherichia coli*. determination of sites for putrescine activation of activity and processing. *J Biol Chem*, **269** (11), 7901–7907. 81

Stelzl, U., Worm, U., Lalowski, M., Haenig, C., Brembeck, F. H., Goehler, H., Stroedicke, M., Zenkner, M., Schoenherr, A., Koeppen, S., Timm, J., Mintzlaff, S., Abraham, C., Bock, N., Kietzmann, S., Goedde, A., Toksöz, E., Droege, A., Krobitsch, S., Korn, B., Birchmeier, W., Lehrach, H., and Wanker, E. E. (2005) A human protein-protein interaction network: a resource for annotating the proteome. *Cell*, **122** (6), 957–968. 15

Stemmler, T. L., Sossong, T. M., Goldstein, J. I., Ash, D. E., Elgren, T. E., Kurtz, D. M., and Penner-Hahn, J. E. (1997) Exafs comparison of the dimanganese core structures of manganese catalase, arginase, and manganese-substituted ribonucleotide reductase and hemerythrin. *Biochemistry*, **36** (32), 9847–9858. 25

Sugiyama, T., Suzue, K., Okamoto, M., Inselburg, J., Tai, K., and Horii, T. (1996) Production of recombinant sera proteins of *Plasmodium falciparum* in *Escherichia coli* by using synthetic genes. *Vaccine*, **14** (11), 1069–1076. 18

Tabor, C. W. and Tabor, H. (1984) Polyamines. *Annu Rev Biochem*, **53**, 749–790. 1, 3

Tabor, C. W. and Tabor, H. (1985) Polyamines in microorganisms. *Microbiol Rev*, **49** (1), 81–99. 1

Takatsuka, Y., Yamaguchi, Y., Ono, M., and Kamio, Y. (2000) Gene cloning and molecular characterization of lysine decarboxylase from *Selenomonas ruminantium* delineate its evolutionary relationship to ornithine decarboxylases from eukaryotes. *J Bacteriol*, **182** (23), 6732–6741. 73

Theobald, D. L. and Wuttke, D. S. (2006a) Empirical bayes hierarchical models for regularizing maximum likelihood estimation in the matrix gaussian procrustes problem. *Proc Natl Acad Sci U S A*, **103** (49), 18521–18527. 89

Theobald, D. L. and Wuttke, D. S. (2006b) Theseus: maximum likelihood superpositioning and analysis of macromolecular structures. *Bioinformatics*, **22** (17), 2171–2172. 89

Thompson, J. D., Gibson, T. J., Plewniak, F., Jeanmougin, F., and Higgins, D. G. (1997) The CLUSTAL_X windows interface: flexible strategies for multiple sequence alignment aided by quality analysis tools.q. *Nucleic Acids Res*, **25** (24), 4876–4882. 32, 87

Thorn, K. S. and Bogan, A. A. (2001) ASEdb: a database of alanine mutations and their effects on the free energy of binding in protein interactions. *Bioinformatics*, **17** (3), 284–285. 124

Tiede, D., Mardis, K., and Zuo, X. (2009) X-ray scattering combined with coordinate-based analyses for applications in natural and artificial photosynthesis. *Photosynth Res*. 11, 128

Tolbert, W. D., Ekstrom, J. L., Mathews, I. I., Secrist, 3rd, J. A., Kapoor, P., Pegg, A. E., and Ealick, S. E. (2001) The structural basis for substrate specificity and inhibition of human *S*-adenosylmethionine decarboxylase. *Biochemistry*, **40** (32), 9484–94. 80, 81, 85

Tolbert, W. D., Zhang, Y., Cottet, S. E., Bennett, E. M., Ekstrom, J. L., Pegg, A. E., and Ealick, S. E. (2003) Mechanism of human *S*-adenosylmethionine decarboxylase proenzyme processing as revealed by the structure of the S68A mutant. *Biochemistry*, **42** (8), 2386–95. 79, 80

Toms, A. V., Kinsland, C., McCloskey, D. E., Pegg, A. E., and Ealick, S. E. (2004) Evolutionary links as revealed by the structure of *Thermotoga maritima S*-adenosylmethionine decarboxylase. *J Biol Chem*, **279** (32), 33837–33846. 78

Toney, M. D. (2001) Computational studies on nonenzymatic and enzymatic pyridoxal phosphate catalyzed decarboxylations of 2-aminoisobutyrate. *Biochemistry*, **40** (5), 1378–1384. 75

Toney, M. D. (2005) Reaction specificity in pyridoxal phosphate enzymes. *Arch Biochem Biophys*, **433** (1), 279–287. 74

Toyoda, T., Brobey, R. K., Sano, G., Horii, T., Tomioka, N., and Itai, A. (1997) Lead discovery of inhibitors of the dihydrofolate reductase domain of *Plasmodium falciparum* dihydrofolate reductase-thymidylate synthase. *Biochem Biophys Res Commun*, **235** (3), 515–519. 21

Turner, G. E. and Weiss, R. L. (2006) Developmental expression of two forms of arginase in *Neurospora crassa*. *Biochim Biophys Acta*, **1760** (6), 848–857. 30

van Brummelen, A. C., Olszewski, K. L., Wilinski, D., Llinás, M., Louw, A. I., and Birkholtz, L.-M. (2009) Co-inhibition of *Plasmodium falciparum S*-adenosylmethionine decarboxylase/ornithine decarboxylase reveals perturbation-specific compensatory mechanisms by transcriptome, proteome, and metabolome analyses. *J Biol Chem*, **284** (7), 4635–4646. 7

van Poelje, P. D. and Snell, E. E. (1990) Pyruvoyl-dependent enzymes. *Annu Rev Biochem*, **59**, 29–59. 79

Vasilescu, J. and Figeys, D. (2006) Mapping protein-protein interactions by mass spectrometry. *Curr Opin Biotechnol*, **17** (4), 394–399. 15

Vedadi, M., Lew, J., Artz, J., Amani, M., Zhao, Y., Dong, A., Wasney, G. A., Gao, M., Hills, T., Brokx, S., Qiu, W., Sharma, S., Diassiti, A., Alam, Z., Melone, M., Mulichak, A., Wernimont, A., Bray, J., Loppnau, P., Plotnikova, O., Newberry, K., Sundararajan, E., Houston, S., Walker, J., Tempel, W., Bochkarev, A., Kozieradzki, I., Edwards, A., Arrowsmith, C., Roos, D., Kain, K., and Hui, R. (2007) Genome-scale protein expression and structural biology of *Plasmodium falciparum* and related Apicomplexan organisms. *Mol Biochem Parasitol*, **151** (1), 100–110. 19

Vernon, J. A., Golec, J. H., and Dimasi, J. A. (2009) Drug development costs when financial risk is measured using the fama-french three-factor model. *Health Econ*. 9

Vriend, G. (1990) WHAT IF: a molecular modeling and drug design program. *J Mol Graph*, **8** (1), 52–6, 29. 88

Wallace, H. M. (2007) Targeting polyamine metabolism: a viable therapeutic/preventative solution for cancer? *Expert Opin Pharmacother*, **8** (13), 2109–16. 4

Wallace, H. M., Fraser, A. V., and Hughes, A. (2003) A perspective of polyamine metabolism. *Biochem J*, **376** (Pt 1), 1–14. 2, 4

Wang, C. C. (1995) Molecular mechanisms and therapeutic approaches to the treatment of African trypanosomiasis. *Annu Rev Pharmacol Toxicol*, **35**, 93–127. 7

Weinberg, J. B., Lopansri, B. K., Mwaikambo, E., and Granger, D. L. (2008) Arginine, nitric oxide, carbon monoxide, and endothelial function in severe malaria. *Curr Opin Infect Dis*, **21** (5), 468–475. 71

Wells, G. A., Birkholtz, L. M., Joubert, F., Walter, R. D., and Louw, A. I. (2006) Novel properties of malarial *S*-adenosylmethionine decarboxylase as revealed by structural modelling. *J Mol Graph Model*, **24** (4), 307–18. 19, 83, 85, 86

Wells, G. A., Müller, I. B., Wrenger, C., and Louw, A. I. (2009) The activity of *Plasmodium falciparum* arginase is mediated by a novel inter-monomer salt-bridge between Glu295-Arg404. *FEBS J*, **276** (13), 3517–3530. 23

Willert, E. K., Fitzpatrick, R., and Phillips, M. A. (2007) Allosteric regulation of an essential trypanosome polyamine biosynthetic enzyme by a catalytically dead homolog. *Proc Natl Acad Sci U S A*, **104** (20), 8275–8280. 82

Willert, E. K. and Phillips, M. A. (2009) Cross-species activation of trypanosome *S*-adenosylmethionine decarboxylase by the regulatory subunit prozyme. *Mol Biochem Parasitol*, **168** (1), 1–6. 82

Withers-Martinez, C., Carpenter, E. P., Hackett, F., Ely, B., Sajid, M., Grainger, M., and Blackman, M. J. (1999) PCR-based gene synthesis as an efficient approach for expression of the A+T-rich malaria genome. *Protein Eng*, **12** (12), 1113–1120. 18

Wrenger, C., Lüersen, K., Krause, T., Muller, S., and Walter, R. D. (2001) The *Plasmodium falciparum* bifunctional ornithine decarboxylase, *S*-adenosyl-L-methionine decarboxylase, enables a well balanced polyamine synthesis without domain-domain interaction. *J Biol Chem*, **276** (32), 29651–6. 4, 83

Wright, P. S., Byers, T. L., Cross-Doersen, D. E., McCann, P. P., and Bitonti, A. J. (1991) Irreversible inhibition of *S*-adenosylmethionine decarboxylase in *Plasmodium falciparum*-infected erythrocytes: growth inhibition *in vitro*. *Biochem Pharmacol*, **41** (11), 1713–1718. 7

Xiong, H. and Pegg, A. E. (1999) Mechanistic studies of the processing of human *S*-adenosylmethionine decarboxylase proenzyme. isolation of an ester intermediate. *J Biol Chem*, **274** (49), 35059–35066. 79

Xiong, H., Stanley, B. A., Tekwani, B. L., and Pegg, A. E. (1997) Processing of mammalian and plant *S*-adenosylmethionine decarboxylase proenzymes. *J Biol Chem*, **272** (45), 28342–28348. 81

Xu, D., Tsai, C. J., and Nussinov, R. (1997) Hydrogen bonds and salt bridges across protein-protein interfaces. *Protein Eng*, **10** (9), 999–1012. 125

Xue, H. Y. and Forsdyke, D. R. (2003) Low-complexity segments in *Plasmodium falciparum* proteins are primarily nucleic acid level adaptations. *Mol Biochem Parasitol*, **128** (1), 21–32. 39

Yadava, A. and Ockenhouse, C. F. (2003) Effect of codon optimization on expression levels of a functionally folded malaria vaccine candidate in prokaryotic and eukaryotic expression systems. *Infect Immun*, **71** (9), 4961–4969. 18

Yan, C., Wu, F., Jernigan, R. L., Dobbs, D., and Honavar, V. (2008) Characterization of protein-protein interfaces. *Protein J*, **27** (1), 59–70. 95

Young, L., Jernigan, R. L., and Covell, D. G. (1994) A role for surface hydrophobicity in protein-protein recognition. *Protein Sci*, **3** (5), 717–729. 123

Yuvaniyama, J., Chitnumsub, P., Kamchonwongpaisan, S., Vanichtanankul, J., Sirawaraporn, W., Taylor, P., Walkinshaw, M. D., and Yuthavong, Y. (2003) Insights into antifolate resistance from malarial DHFR-TS structures. *Nat Struct Biol*, **10** (5), 357–65. 21, 39

Zaheer-ul, H., Uddin, R., Yuan, H., Petukhov, P. A., Choudhary, M. I., and Madura, J. D. (2008) Receptor-based modeling and 3D-QSAR for a quantitative production of the butyrylcholinesterase inhibitors based on genetic algorithm. *J Chem Inf Model*, **48** (5), 1092–1103. 10

Appendix A

Supplementary data for Chapter 2

A.1 Inter-monomer interactions in arginase

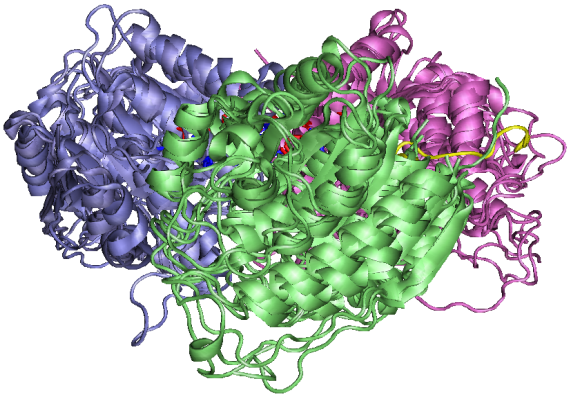

Figure A.1: A summary of inter-monomer interactions in arginase. Click on the image to active 3D. Sub-structures relevant to this work are highlighted in the model tree.

A.2 Co-ordination geometry of Mg^{2+}

A.2.1 Glu 295 Ala

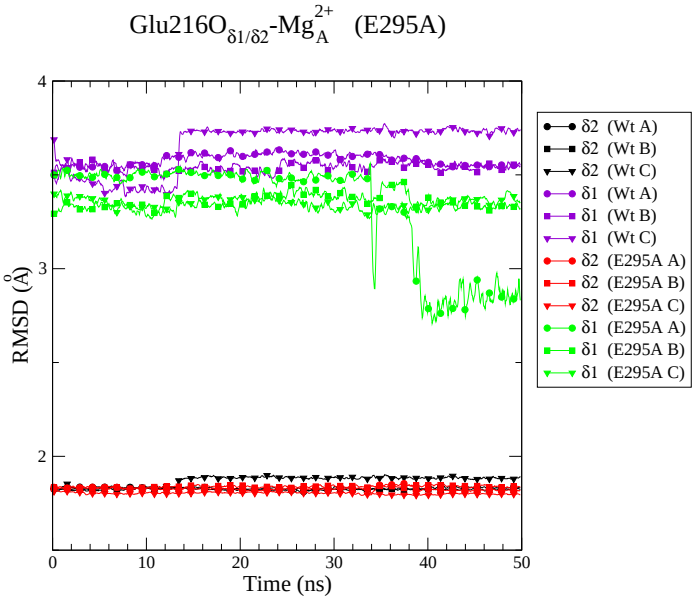

Figure A.2: Interaction between Asp 216 O and Mg_A^{2+} in *pf* Arg Glu 295 Ala compared to wild type. Both carboxyl oxygens ($\delta1/\delta2$) are included. Pairs of carboxyl O are indicated for chains A ($\circ$), B ($\square$) and C ($\triangledown$).

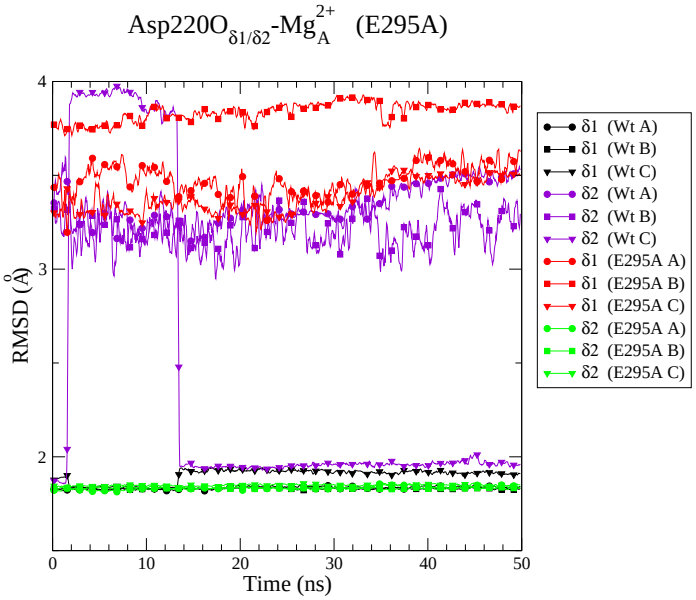

Figure A.3: Interaction between Asp 220 O and Mg_A^{2+} in *pf* Arg Glu 295 Ala compared to wild type. Both carboxyl oxygens ($\delta1/\delta2$) are included. Pairs of carboxyl O are indicated for chains A ($\circ$), B ($\square$) and C ($\triangledown$).

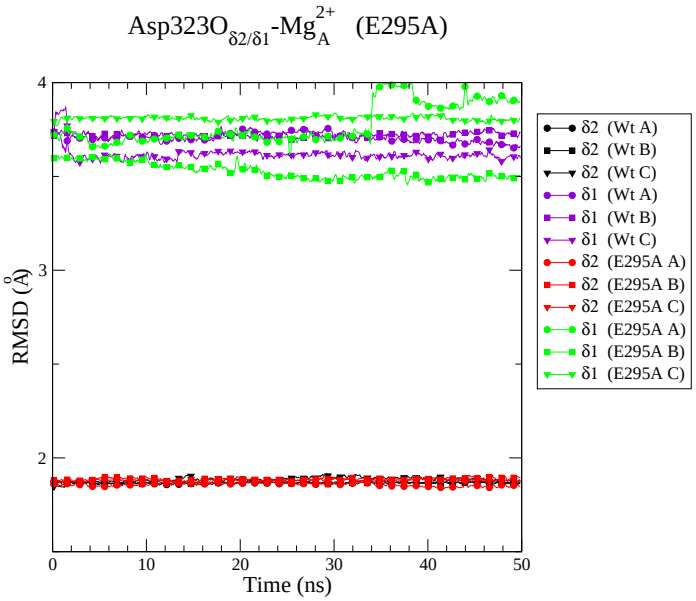

Figure A.4: Interaction between Asp 323 O and Mg^{2+}_{A} in *pf* Arg Glu 295 Ala compared to wild type. Both carboxyl oxygens ($\delta1/\delta2$) are included. Pairs of carboxyl O are indicated for chains A ($\circ$), B ($\square$) and C ($\triangledown$).

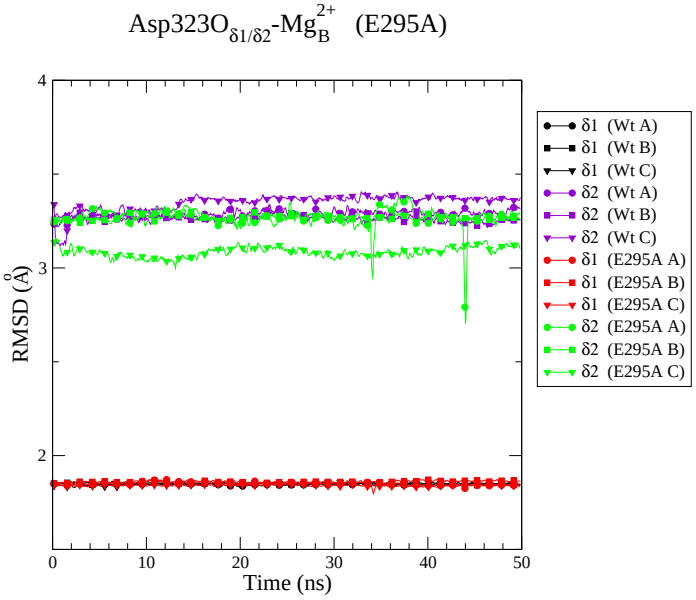

Figure A.5: Interaction between Asp 323 O and Mg^{2+}_{B} in *pf* Arg Glu 295 Ala compared to wild type. Both carboxyl oxygens ($\delta1/\delta2$) are included. Pairs of carboxyl O are indicated for chains A ($\circ$), B ($\square$) and C ($\triangledown$).

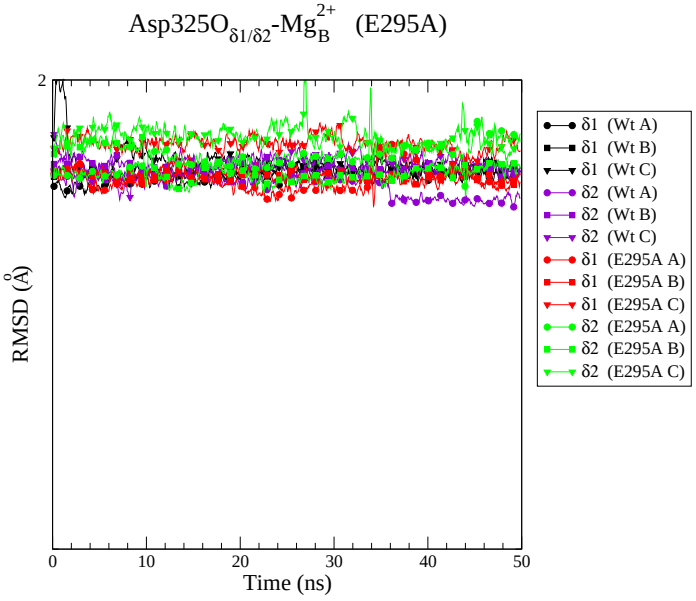

Figure A.6: Interaction between Asp 325 O and Mg^{2+}_{B} in *pf* Arg Glu 295 Ala compared to wild type. Both carboxyl oxygens ($\delta1/\delta2$) are included. Pairs of carboxyl O are indicated for chains A ($\circ$), B ($\square$) and C ($\triangledown$).

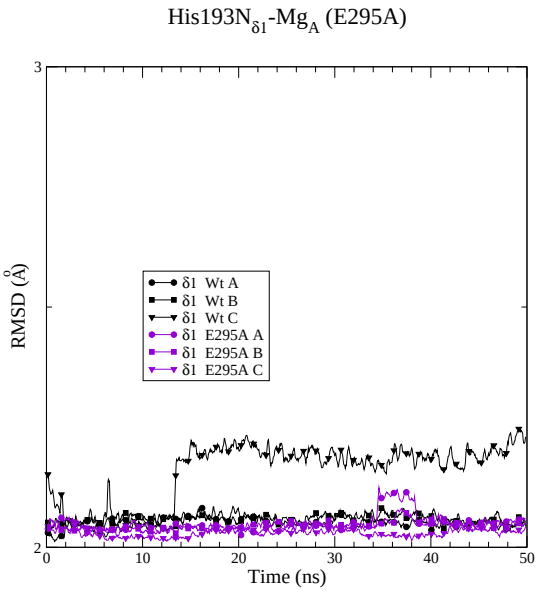

Figure A.7: Interaction between His 193 $N_{\delta1}$ and Mg_A^{2+} in *pf* Arg Glu 295 Ala compared to wild type. Both carboxyl oxygens ($\delta1/\delta2$) are included. Pairs of carboxyl O are indicated for chains A ($\circ$), B ($\square$) and C ($\triangledown$).

A.2.2 Glu 295 Ala/Arg 404 Ala

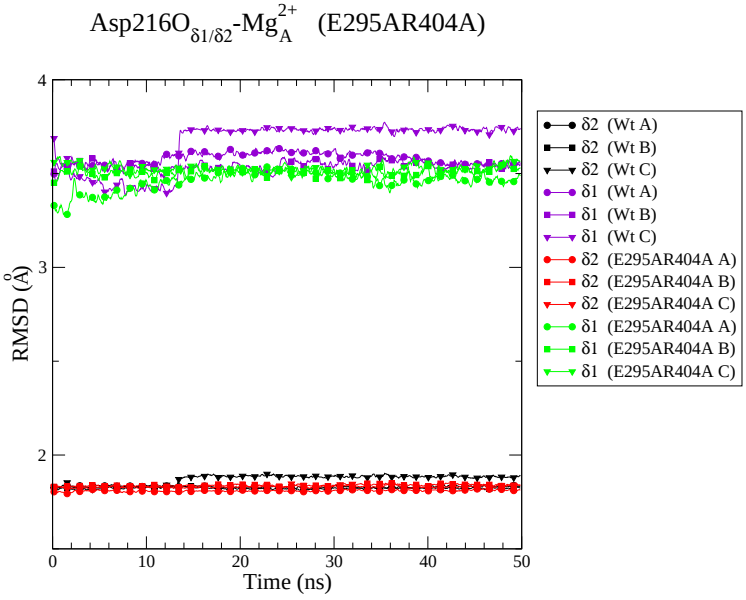

Figure A.8: Interaction between Asp 216 O and Mg_A^{2+} in *pf* Arg Glu 295 Ala/Arg 404 Ala compared to wild type. Both carboxyl oxygens ($\delta1/\delta2$) are included. Pairs of carboxyl O are indicated for chains A ($\circ$), B ($\square$) and C ($\triangledown$).

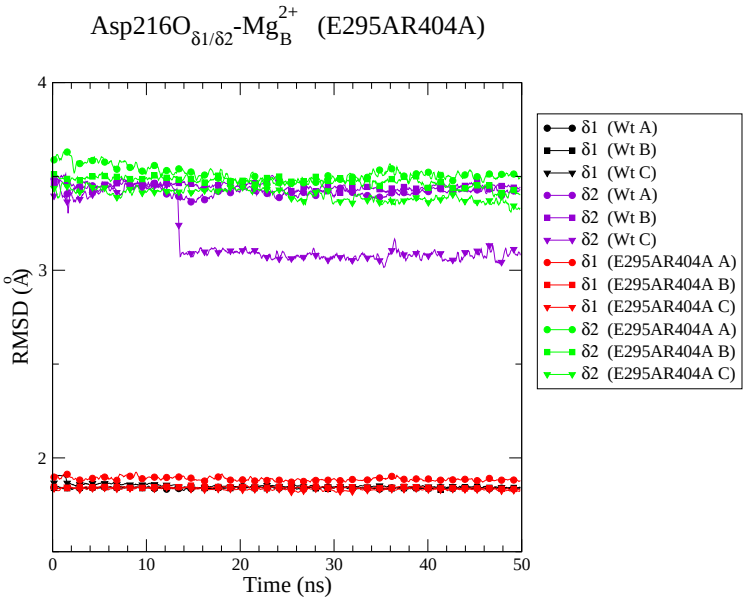

Figure A.9: Interaction between Asp 216 O and Mg^{2+}_{B} in *pf* Arg Glu 295 Ala/Arg 404 Ala compared to wild type. Both carboxyl oxygens ($\delta1/\delta2$) are included. Pairs of carboxyl O are indicated for chains A ($\circ$), B ($\square$) and C ($\triangledown$).

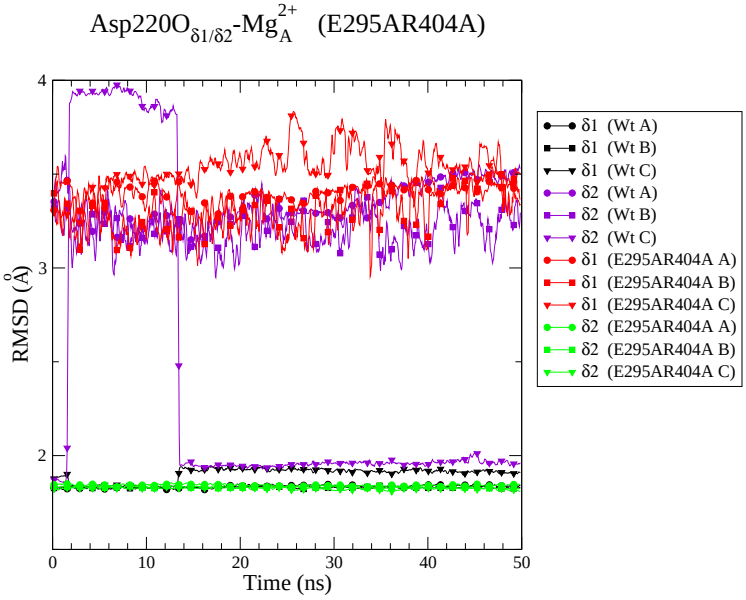

Figure A.10: Interaction between Asp 220 O and Mg^{2+}_{A} in *pf* Arg Glu 295 Ala/Arg 404 Ala compared to wild type. Both carboxyl oxygens ($\delta1/\delta2$) are included. Pairs of carboxyl O are indicated for chains A ($\circ$), B ($\square$) and C ($\triangledown$).

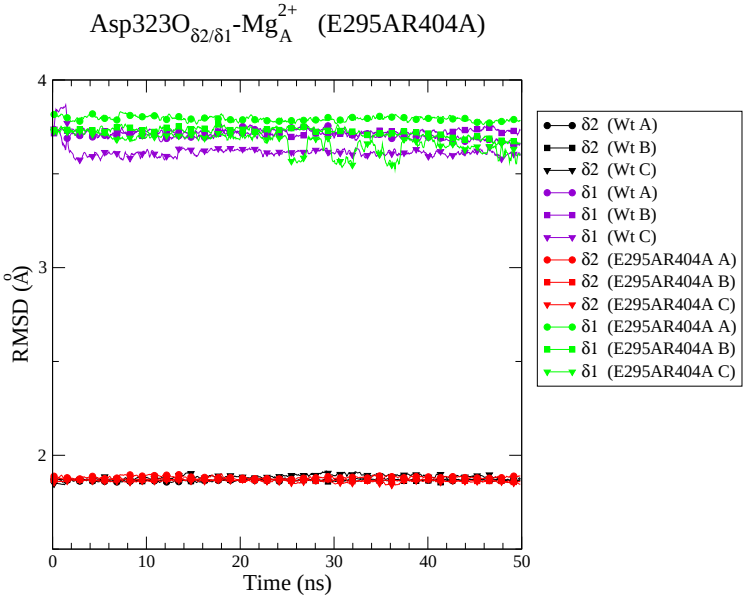

Figure A.11: Interaction between Asp 323 O and Mg^{2+}_{A} in *pf* Arg Glu 295 Ala/Arg 404 Ala compared to wild type. Both carboxyl oxygens ($\delta1/\delta2$) are included. Pairs of carboxyl O are indicated for chains A ($\circ$), B ($\square$) and C ($\triangledown$).

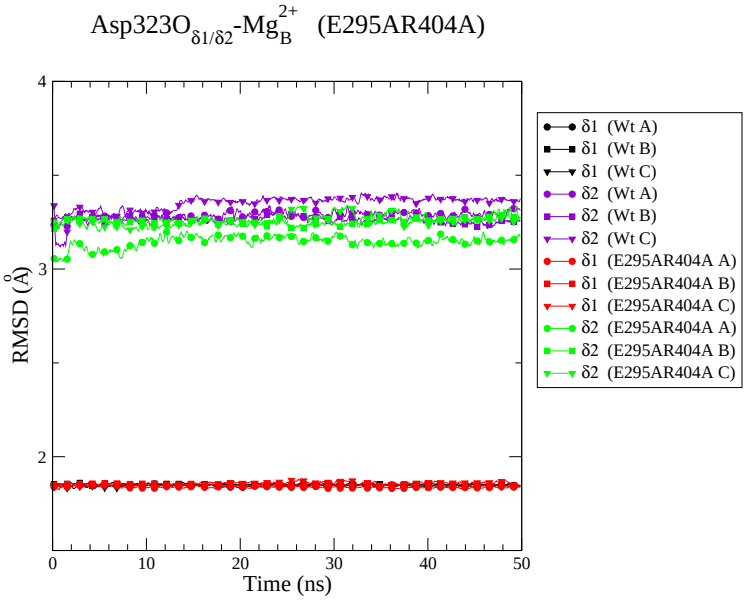

Figure A.12: Interaction between Asp 323 O and Mg_B^{2+} in *pf* Arg Glu 295 Ala/Arg 404 Ala compared to wild type. Both carboxyl oxygens ($\delta1/\delta2$) are included. Pairs of carboxyl O are indicated for chains A ($\circ$), B ($\square$) and C ($\triangledown$).

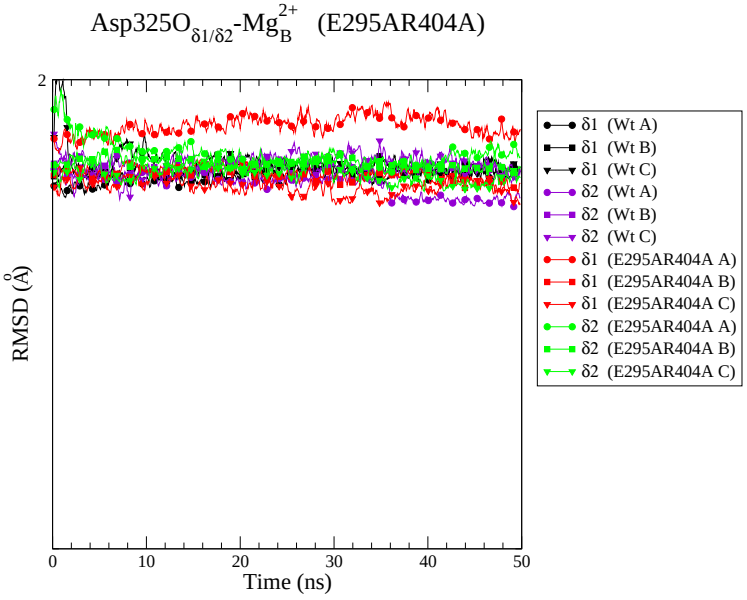

Figure A.13: Interaction between Asp 325 O and Mg_B^{2+} in *pf* Arg Glu 295 Ala/Arg 404 Ala compared to wild type. Both carboxyl oxygens ($\delta1/\delta2$) are included. Pairs of carboxyl O are indicated for chains A ($\circ$), B ($\square$) and C ($\triangledown$).

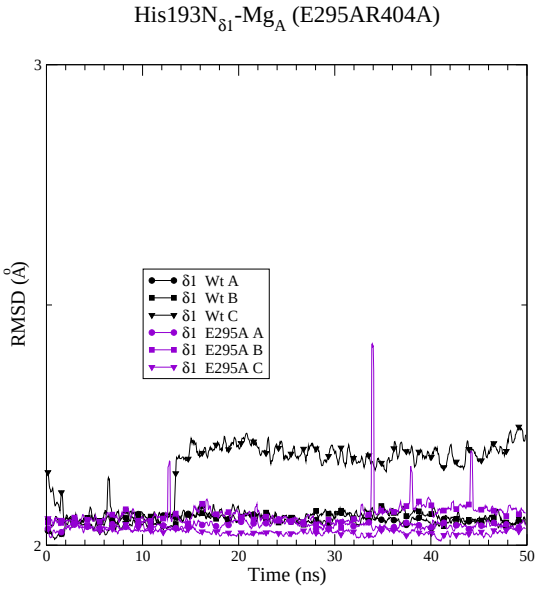

Figure A.14: Interaction between His 193 $N_{\delta1}$ and Mg_A^{2+} in *pf* Arg Glu 295 Ala/Arg 404 Ala compared to wild type. Both carboxyl oxygens ($\delta1/\delta2$) are included. Pairs of carboxyl O are indicated for chains A ($\circ$), B ($\square$) and C ($\triangledown$).

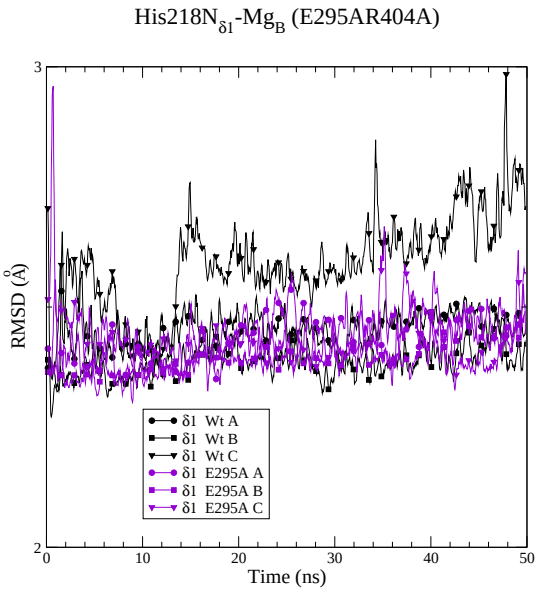

Figure A.15: Interaction between His 218 $N_{\delta 1}$ and Mg_B^{2+} in *pf* Arg Glu 295 Ala/Arg 404 Ala compared to wild type. Both carboxyl oxygens ($\delta 1/\delta 2$) are included. Pairs of carboxyl O are indicated for chains A ($\circ$), B ($\square$) and C ($\triangledown$).

A.2.3 Glu 295 Arg

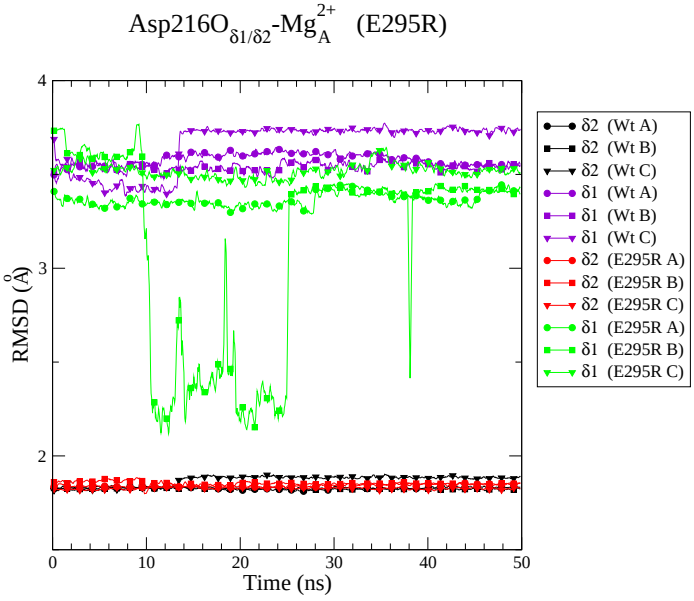

Figure A.16: Interaction between Asp 216 O and Mg_A^{2+} in *pf* Arg Glu 295 Arg compared to wild type. Both carboxyl oxygens ($\delta 1/\delta 2$) are included. Pairs of carboxyl O are indicated for chains A ($\circ$), B ($\square$) and C ($\triangledown$).

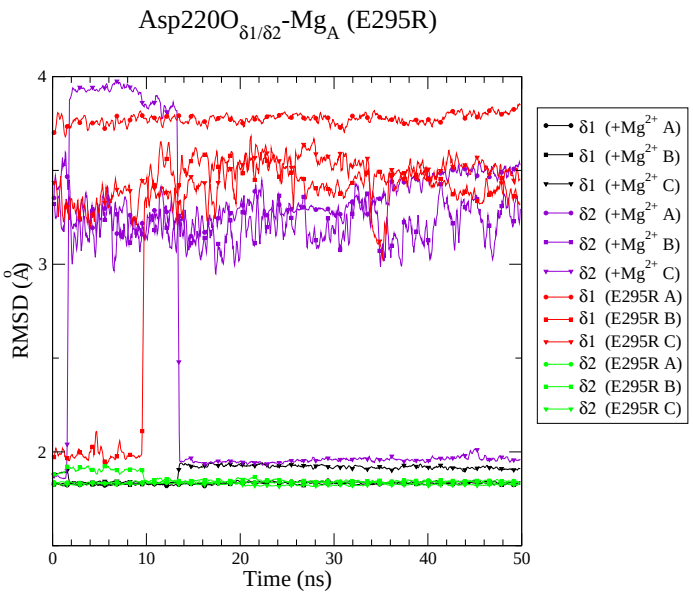

Figure A.17: Interaction between Asp 220 O and Mg_A^{2+} in *pf* Arg Glu 295 Arg compared to wild type. Both carboxyl oxygens ($\delta1/\delta2$) are included. Pairs of carboxyl O are indicated for chains A ($\circ$), B ($\square$) and C ($\triangledown$).

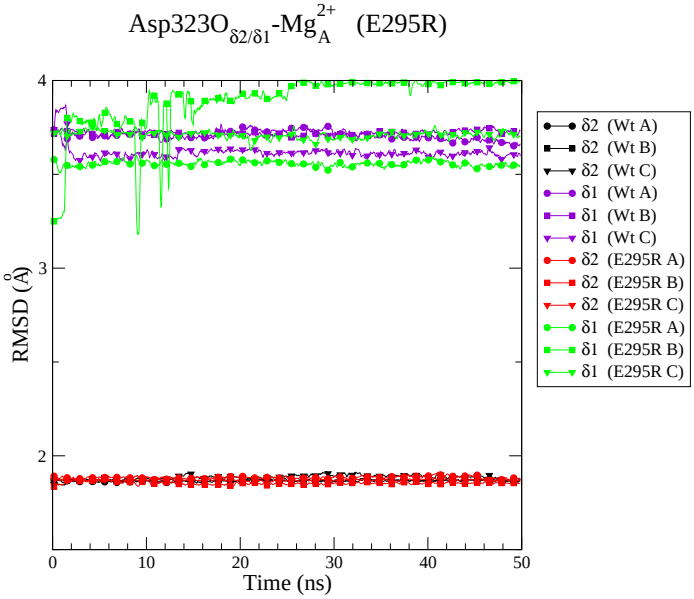

Figure A.18: Interaction between Asp 323 O and Mg_A^{2+} in *pf* Arg Glu 295 Arg compared to wild type. Both carboxyl oxygens ($\delta1/\delta2$) are included. Pairs of carboxyl O are indicated for chains A ($\circ$), B ($\square$) and C ($\triangledown$).

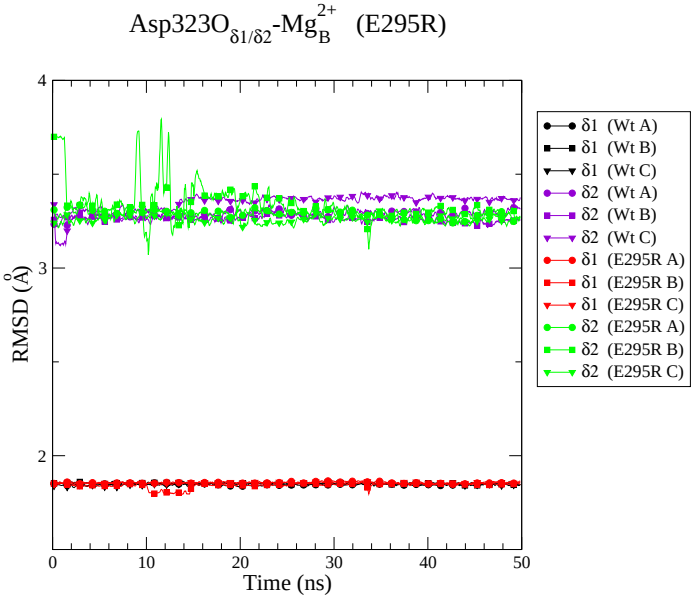

Figure A.19: Interaction between Asp 323 O and Mg_B^{2+} in *pf* Arg Glu 295 Arg compared to wild type. Both carboxyl oxygens ($\delta1/\delta2$) are included. Pairs of carboxyl O are indicated for chains A ($\circ$), B ($\square$) and C ($\triangledown$).

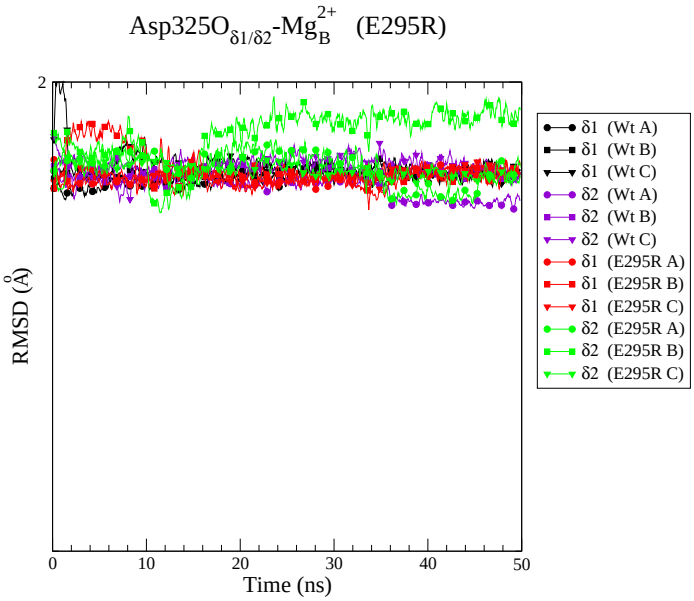

Figure A.20: Interaction between Asp 325 O and Mg_B^{2+} in *pf* Arg Glu 295 Arg compared to wild type. Both carboxyl oxygens ($\delta1/\delta2$) are included. Pairs of carboxyl O are indicated for chains A ($\circ$), B ($\square$) and C ($\triangledown$).

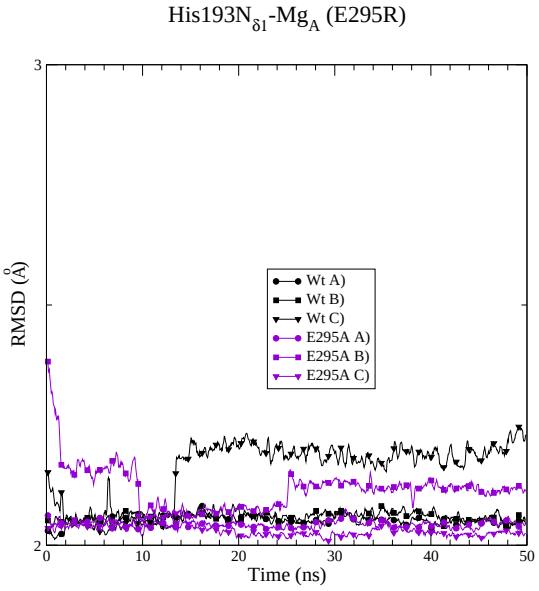

Figure A.21: Interaction between His 193 $N_{\delta1}$ and Mg_A^{2+} in *pf* Arg Glu 295 Arg compared to wild type. Both carboxyl oxygens ($\delta1/\delta2$) are included. Pairs of carboxyl O are indicated for chains A ($\circ$), B ($\square$) and C ($\triangledown$).

A.2.4 Glu 347 Gln

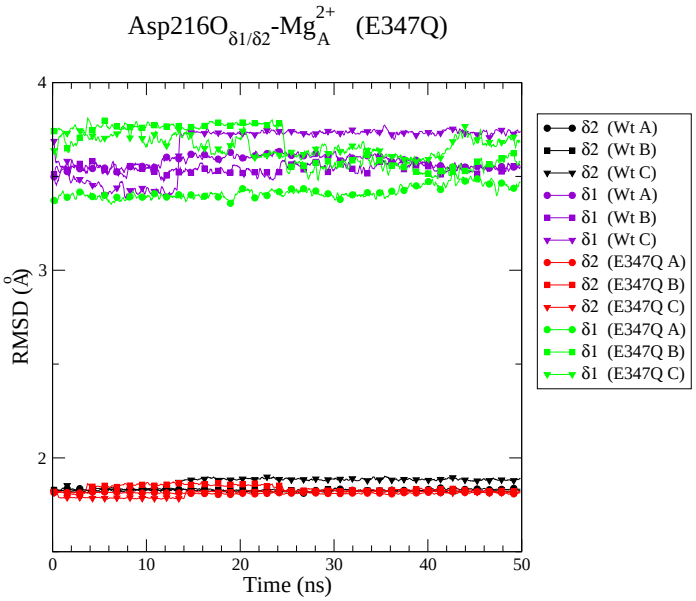

Figure A.22: Interaction between Asp 216 O and Mg^{2+}_{A} in *pf* Arg Glu 347 Gln compared to wild type. Both carboxyl oxygens ($\delta1/\delta2$) are included. Pairs of carboxyl O are indicated for chains A ($\circ$), B ($\square$) and C ($\triangledown$).

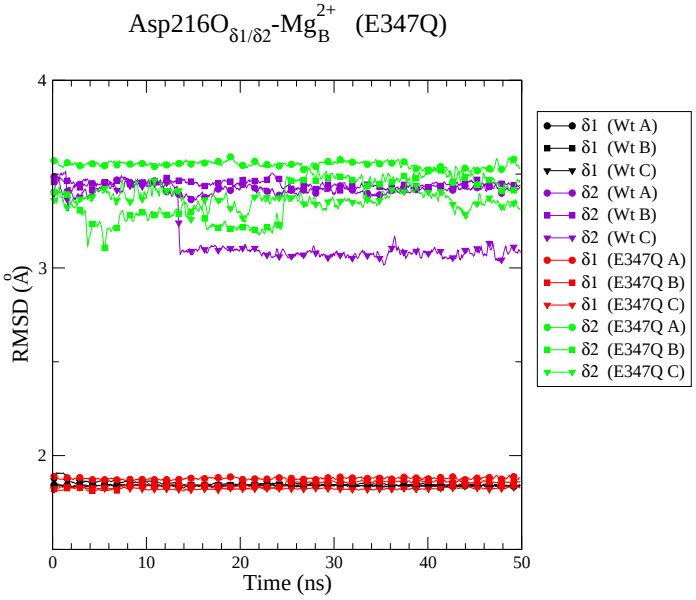

Figure A.23: Interaction between Asp 216 O and Mg^{2+}_{B} in *pf* Arg Glu 347 Gln compared to wild type. Both carboxyl oxygens ($\delta1/\delta2$) are included. Pairs of carboxyl O are indicated for chains A ($\circ$), B ($\square$) and C ($\triangledown$).

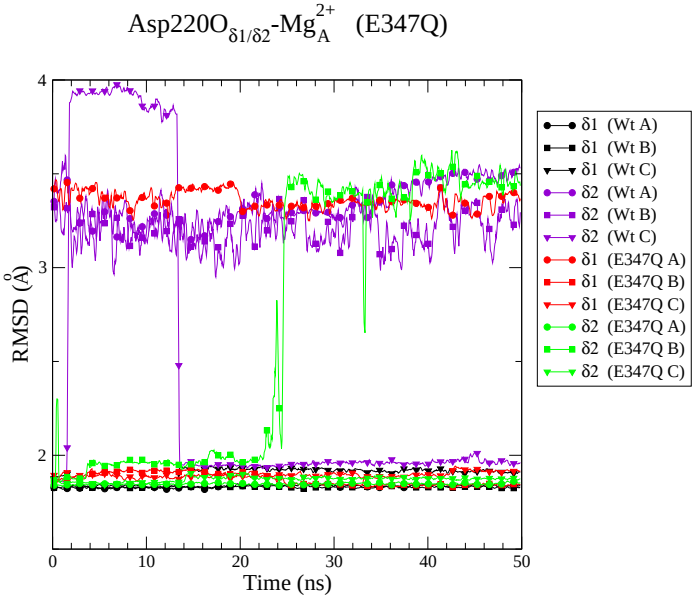

Figure A.24: Interaction between Asp 220 O and Mg^{2+}_{A} in *pf* Arg Glu 347 Gln compared to wild type. Both carboxyl oxygens ($\delta1/\delta2$) are included. Pairs of carboxyl O are indicated for chains A ($\circ$), B ($\square$) and C ($\triangledown$).

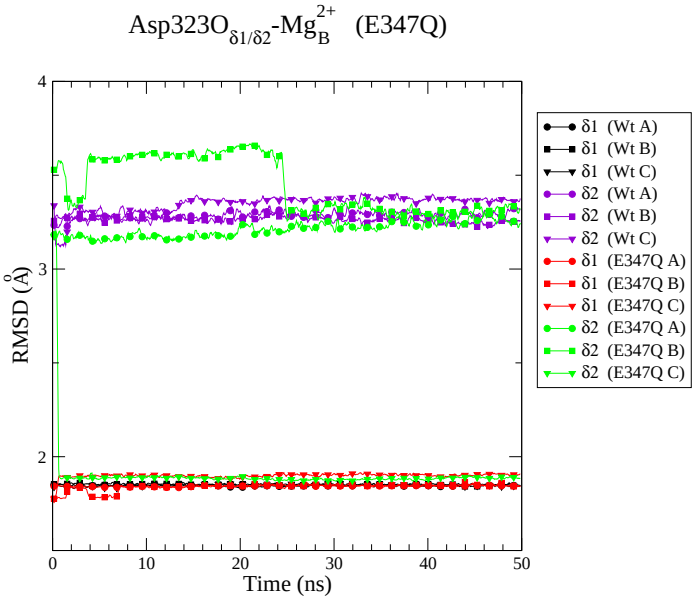

Figure A.25: Interaction between Asp 323 O and Mg_B^{2+} in *pf* Arg Glu 347 Gln compared to wild type. Both carboxyl oxygens ($\delta1/\delta2$) are included. Pairs of carboxyl O are indicated for chains A ($\circ$), B ($\square$) and C ($\triangledown$).

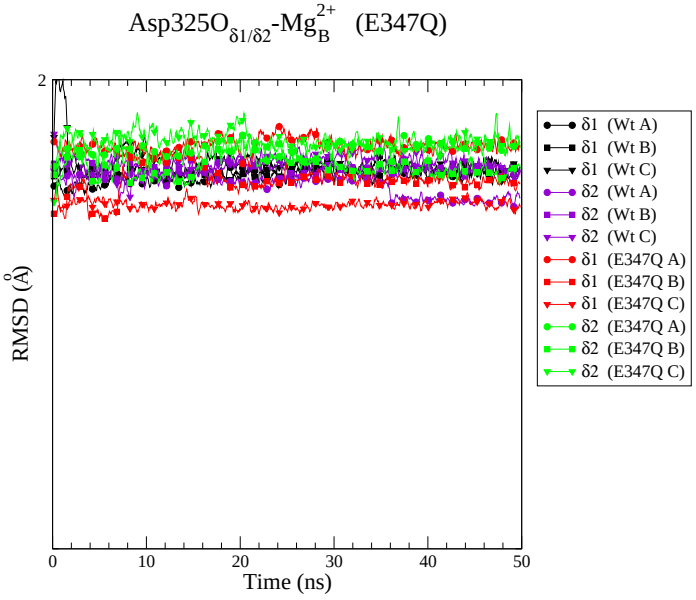

Figure A.26: Interaction between Asp 325 O and Mg_B^{2+} in *pf* Arg Glu 347 Gln compared to wild type. Both carboxyl oxygens ($\delta1/\delta2$) are included. Pairs of carboxyl O are indicated for chains A ($\circ$), B ($\square$) and C ($\triangledown$).

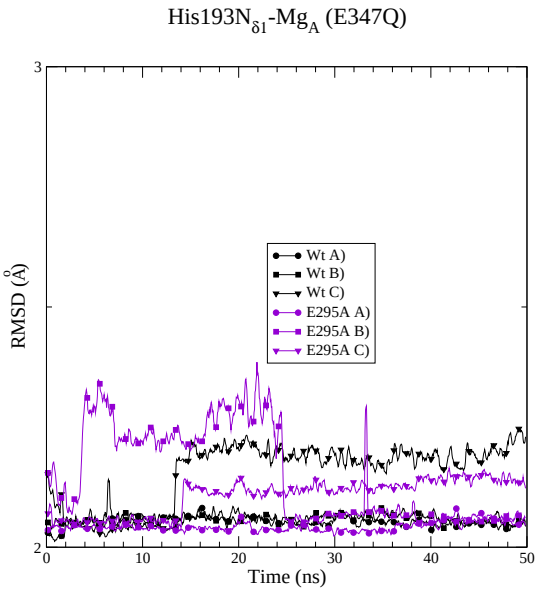

Figure A.27: Interaction between His 193 $N_{\delta1}$ and Mg_A^{2+} in *pf* Arg Glu 347 Gln compared to wild type. Both carboxyl oxygens ($\delta1/\delta2$) are included. Pairs of carboxyl O are indicated for chains A ($\circ$), B ($\square$) and C ($\triangledown$).

A.2.5 Arg 404 Ala

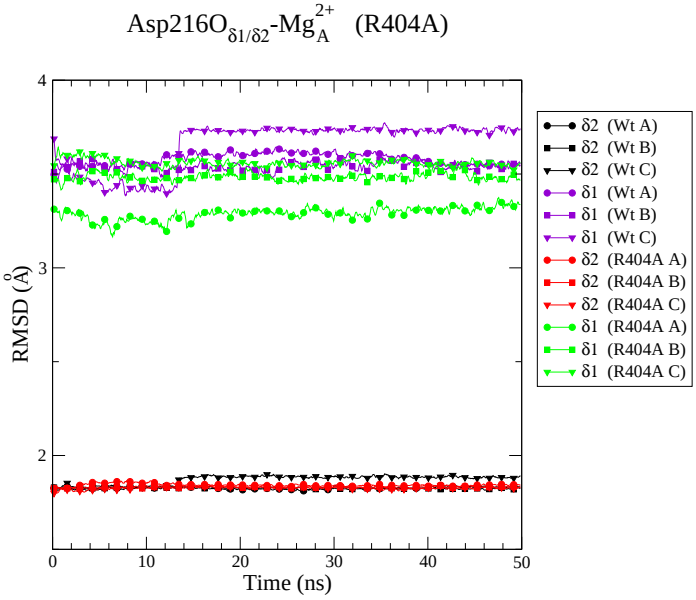

Figure A.28: Interaction between Asp 216 O and Mg^{2+}_{A} in *pf* Arg Arg 404 Ala compared to wild type. Both carboxyl oxygens ($\delta1/\delta2$) are included. Pairs of carboxyl O are indicated for chains A ($\circ$), B ($\square$) and C ($\triangledown$).

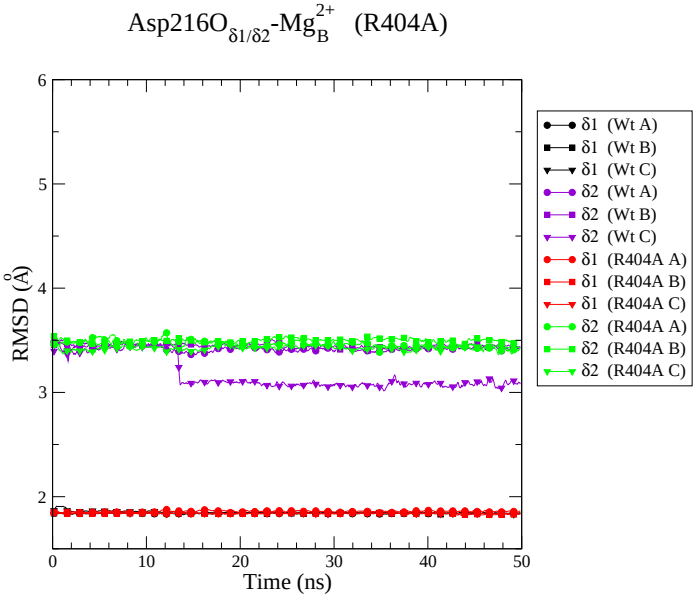

Figure A.29: Interaction between Asp 216 O and Mg^{2+}_{B} in *pf* Arg Arg,404 Ala compared to wild type. Both carboxyl oxygens ($\delta1/\delta2$) are included. Pairs of carboxyl O are indicated for chains A ($\circ$), B ($\square$) and C ($\triangledown$).

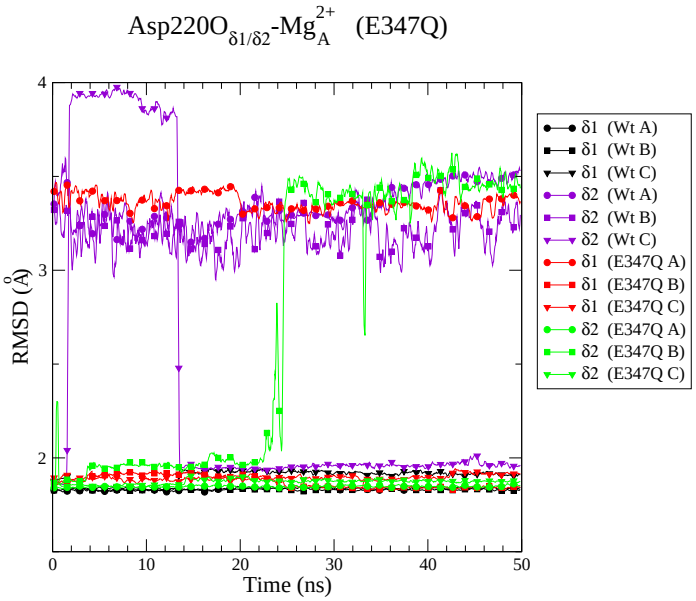

Figure A.30: Interaction between Asp 220 O and Mg^{2+}_{A} in *pf* Arg Arg,404 Ala compared to wild type. Both carboxyl oxygens ($\delta1/\delta2$) are included. Pairs of carboxyl O are indicated for chains A ($\circ$), B ($\square$) and C ($\triangledown$).

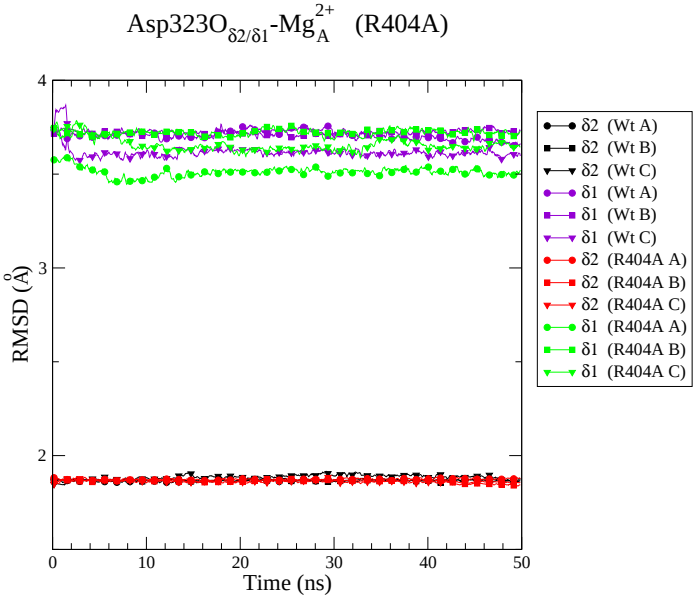

Figure A.31: Interaction between Asp 323 O and Mg^{2+}_{A} in *pf* Arg Arg 404 Ala compared to wild type. Both carboxyl oxygens ($\delta1/\delta2$) are included. Pairs of carboxyl O are indicated for chains A ($\circ$), B ($\square$) and C ($\triangledown$).

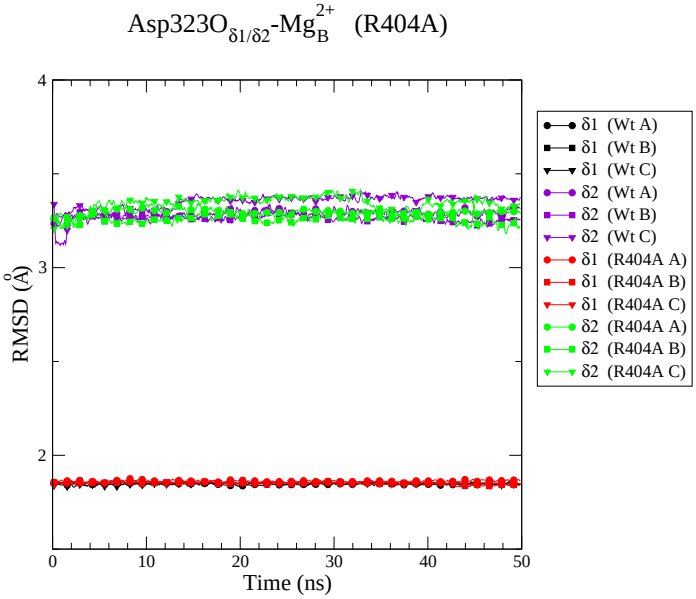

Figure A.32: Interaction between Asp 323 O and Mg^{2+}_{B} in *pf* Arg Arg 404 Ala compared to wild type. Both carboxyl oxygens ($\delta1/\delta2$) are included. Pairs of carboxyl O are indicated for chains A ($\circ$), B ($\square$) and C ($\triangledown$).

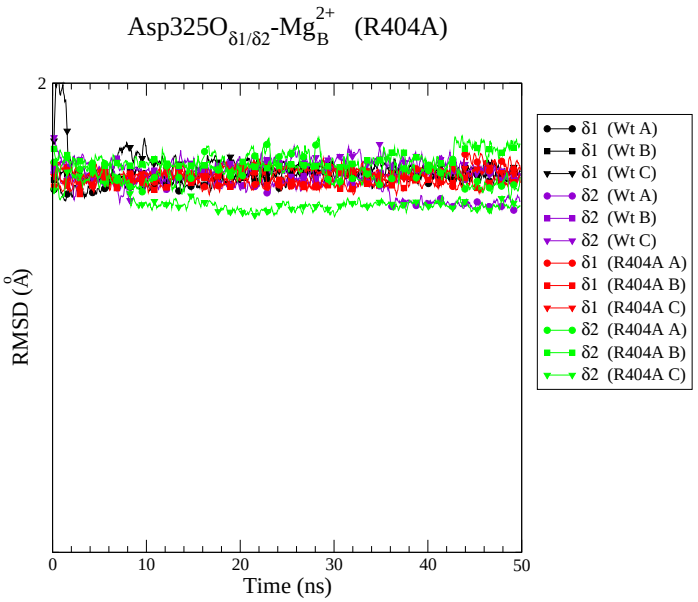

Figure A.33: Interaction between Asp 325 O and Mg_B^{2+} in *pf*Arg Arg 404 Ala compared to wild type. Both carboxyl oxygens ($\delta1/\delta2$) are included. Pairs of carboxyl O are indicated for chains A ($\circ$), B ($\square$) and C ($\triangledown$).

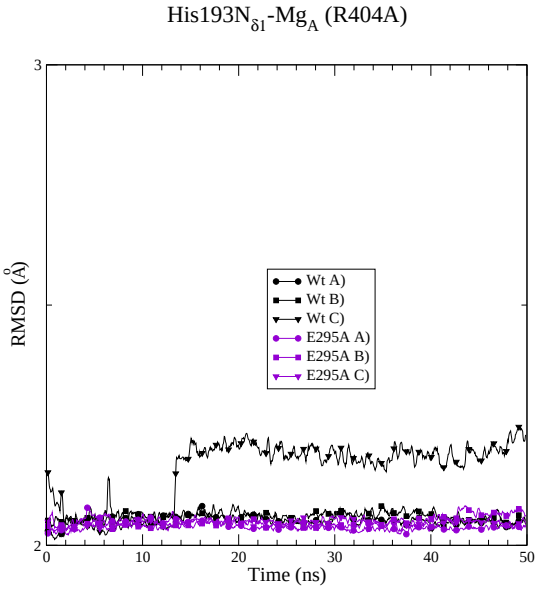

Figure A.34: Interaction between His 193 $N_{\delta1}$ and Mg_A^{2+} in *pf*Arg Arg 404 Ala compared to wild type. Both carboxyl oxygens ($\delta1/\delta2$) are included. Pairs of carboxyl O are indicated for chains A ($\circ$), B ($\square$) and C ($\triangledown$).

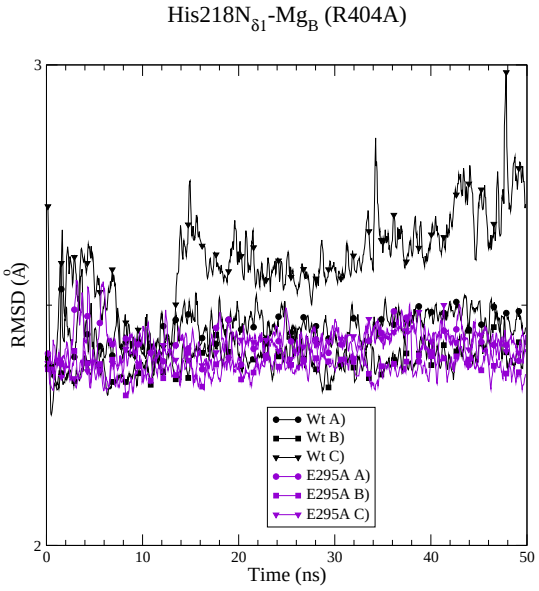

Figure A.35: Interaction between His 218 $N_{\delta1}$ and Mg_B^{2+} in *pf*Arg Arg 404 Ala compared to wild type. Both carboxyl oxygens ($\delta1/\delta2$) are included. Pairs of carboxyl O are indicated for chains A ($\circ$), B ($\square$) and C ($\triangledown$).

Appendix B

Supplementary data for Chapter 3

B.1 Model quality

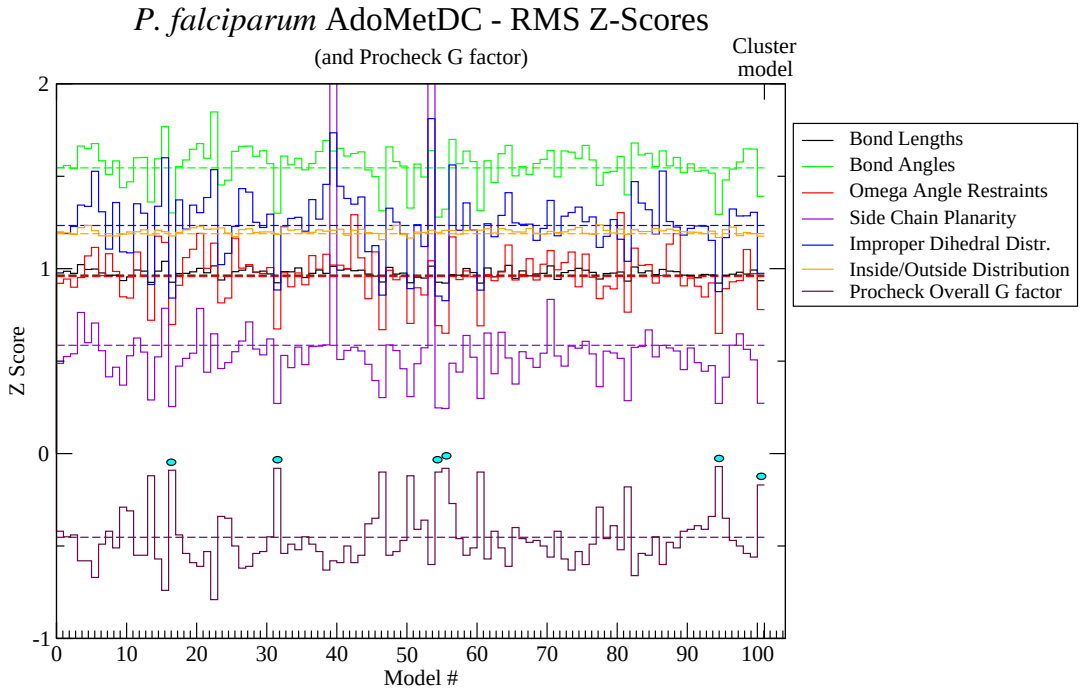

Figure B.1: WHATIF RMS Z-scores and PROCHECK G-factor for modeling of *P. falciparum* AdoMetDC. The models chosen for docking are indicated by the cyan dots.

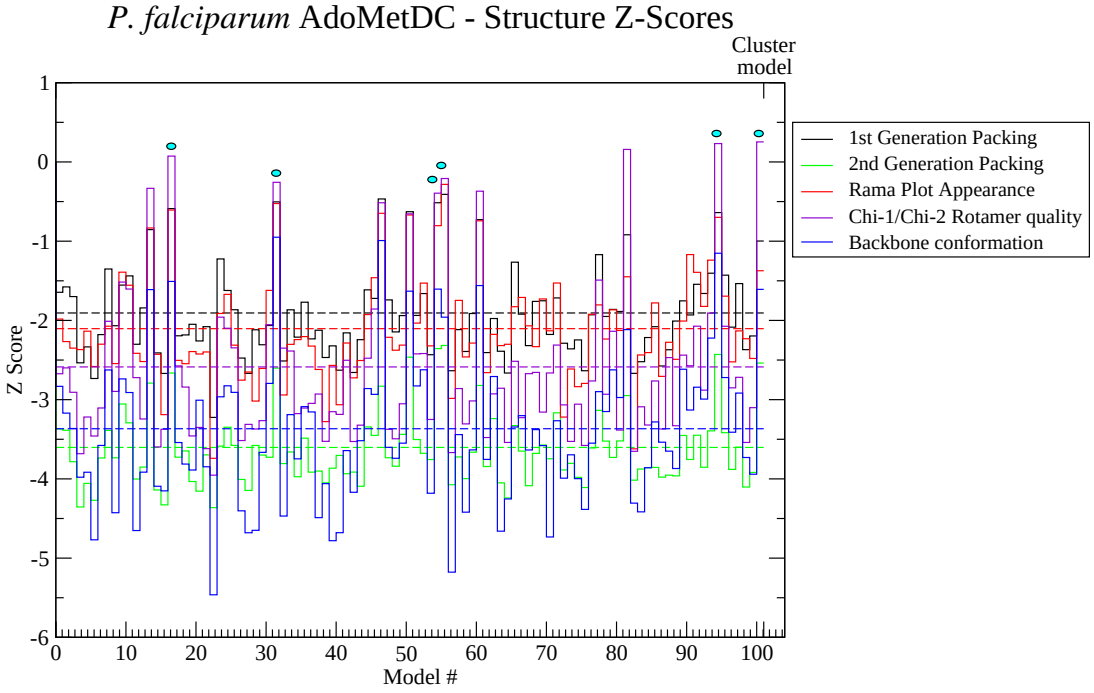

Figure B.2: WHATIF Structure Z-scores for modeling of *P. falciparum* AdoMetDC. The models chosen for docking are indicated by the cyan dots.

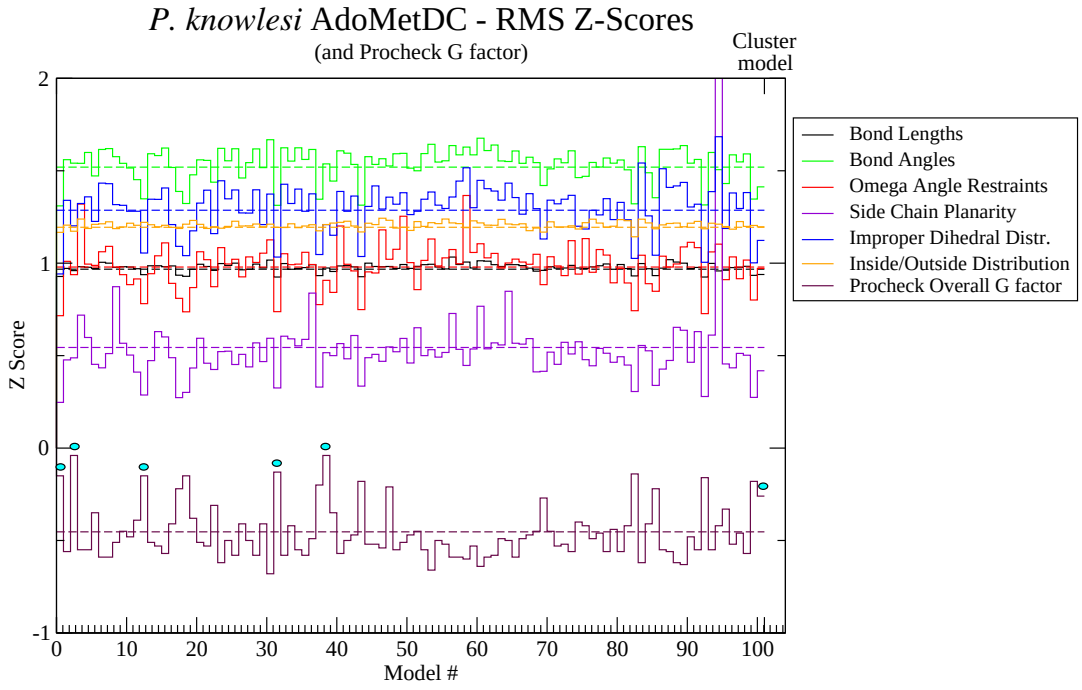

Figure B.3: WHATIF RMS Z-scores and PROCHECK G-factor for modeling of *P. knowlesi* AdoMetDC. The models chosen for docking are indicated by the cyan dots.

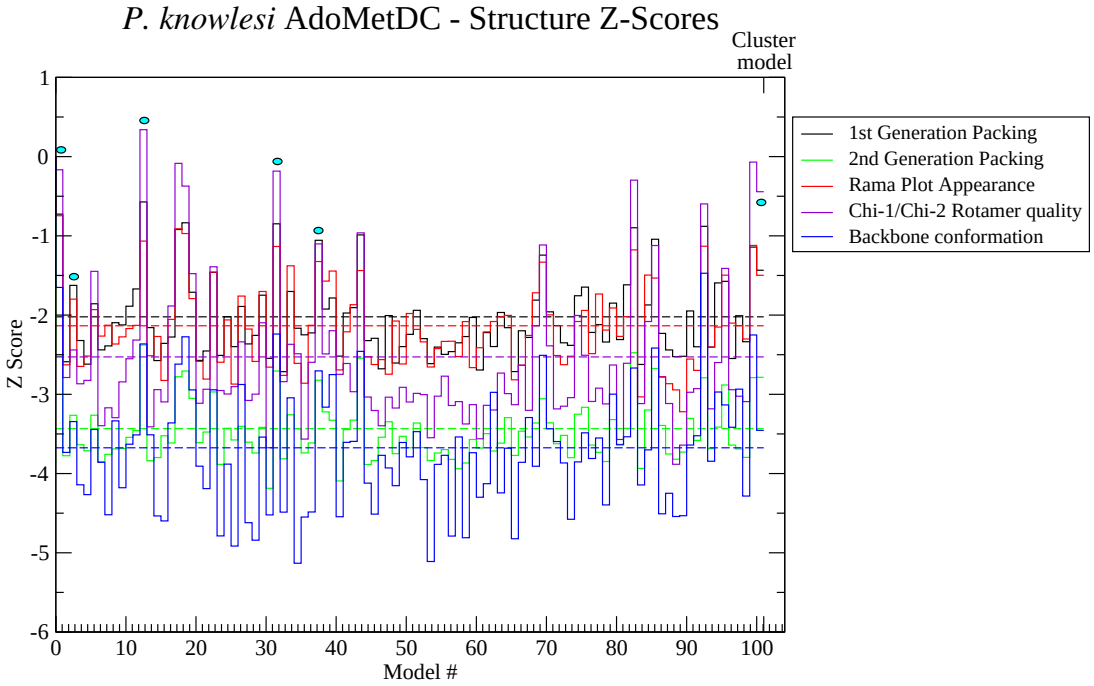

Figure B.4: WHATIF Structure Z-scores for modeling of *P. knowlesi* AdoMetDC. The models chosen for docking are indicated by the cyan dots.

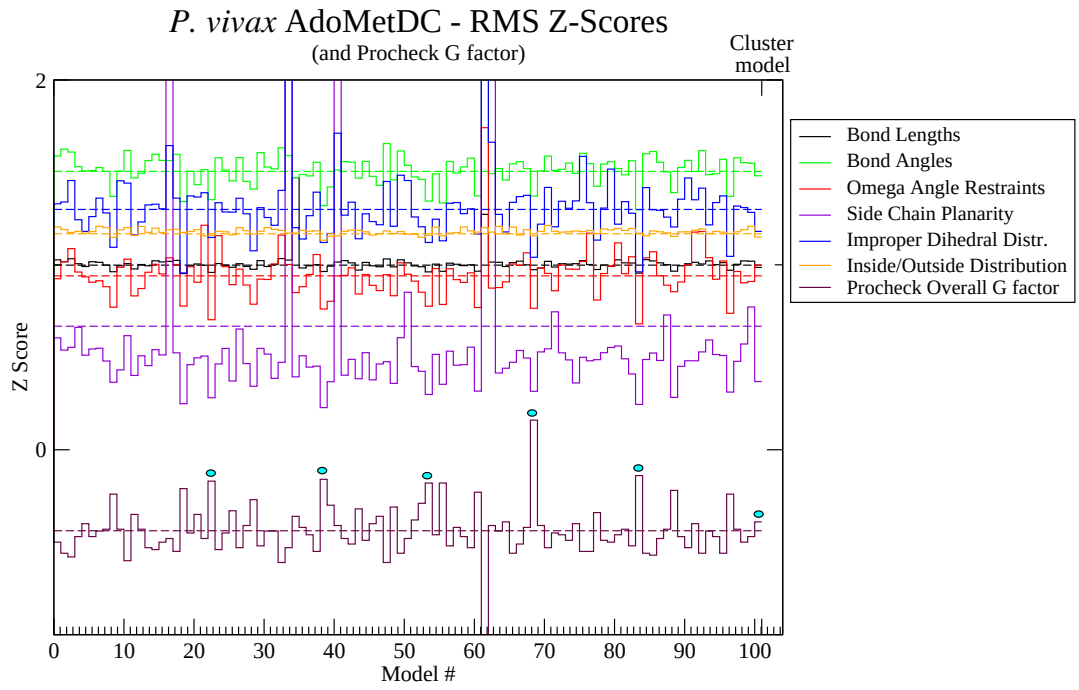

Figure B.5: WHATIF RMS Z-scores and PROCHECK G-factor for modeling of *P. vivax* AdoMetDC. The models chosen for docking are indicated by the cyan dots.

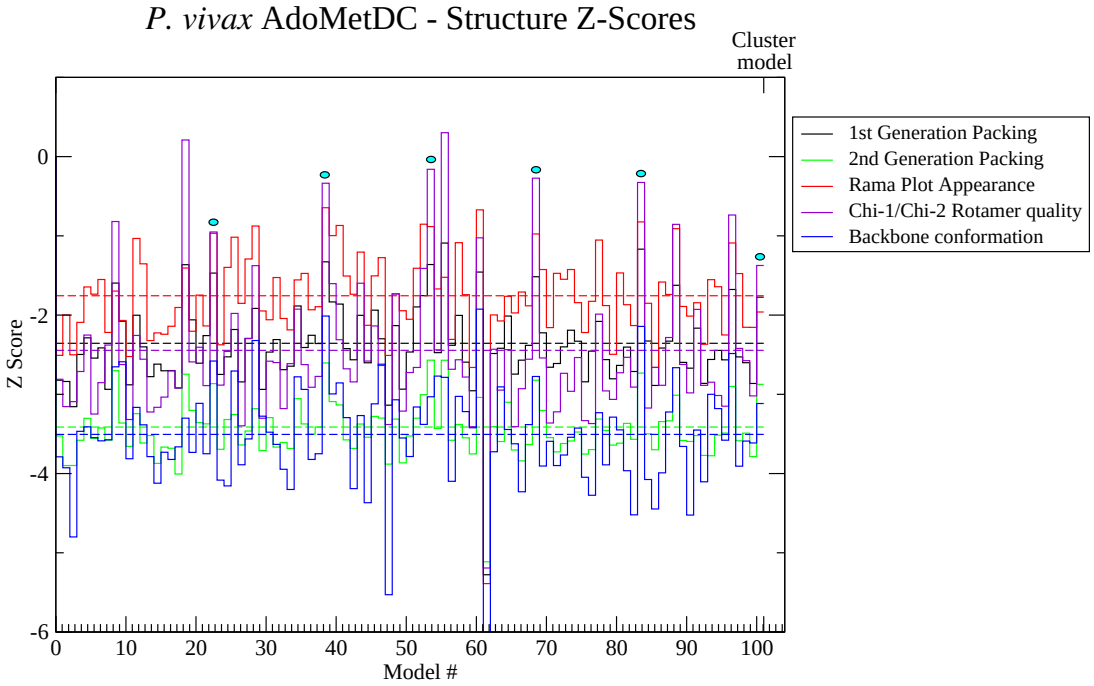

Figure B.6: WHATIF Structure Z-scores for modeling of *P. vivax* AdoMetDC. The models chosen for docking are indicated by the cyan dots.

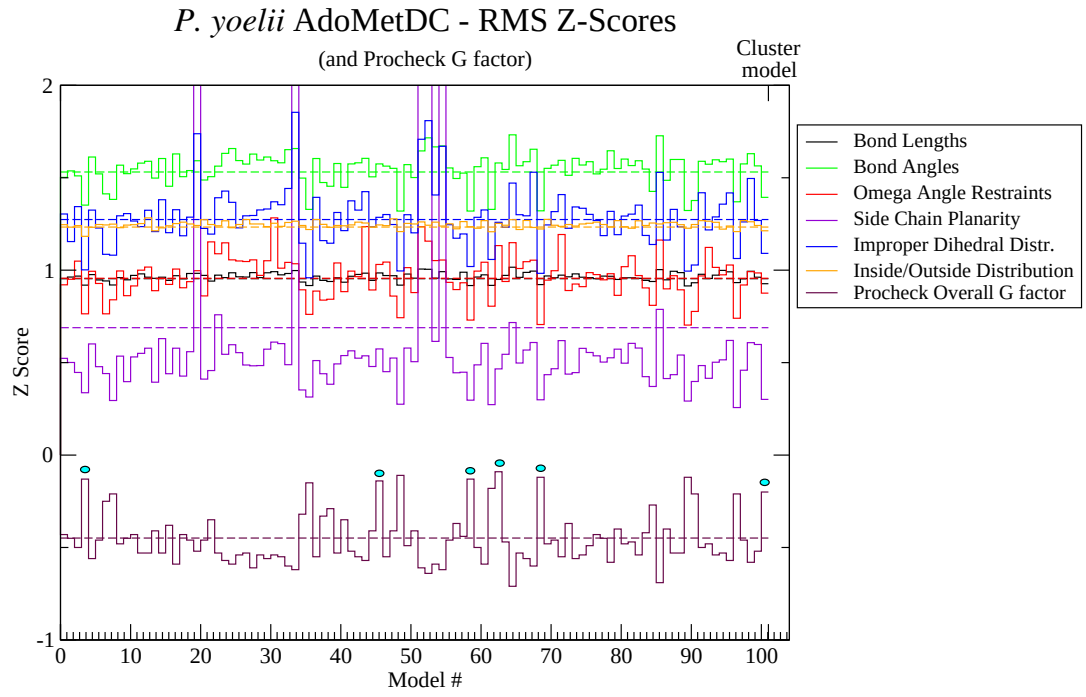

Figure B.7: WHATIF RMS Z-scores and PROCHECK G-factor for modeling of *P. yoelii* AdoMetDC. The models chosen for docking are indicated by the cyan dots.

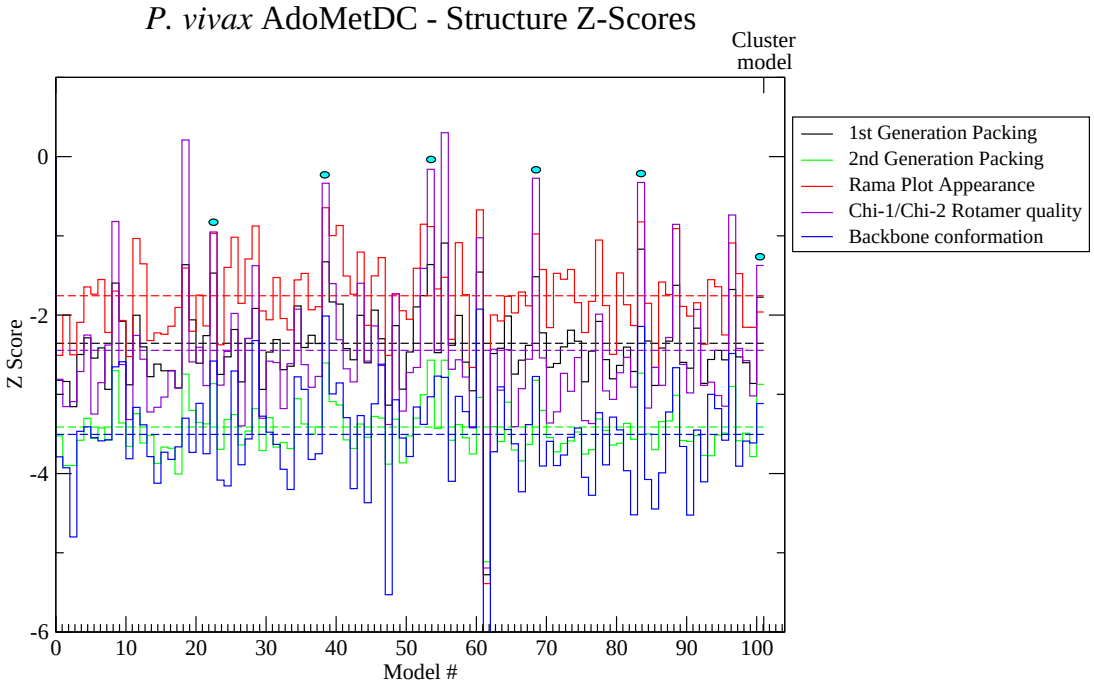

Figure B.8: WHATIF Structure Z-scores for modeling of *P. yoelii* AdoMetDC. The models chosen for docking are indicated by the cyan dots.

B.2 Surface distribution of divergence

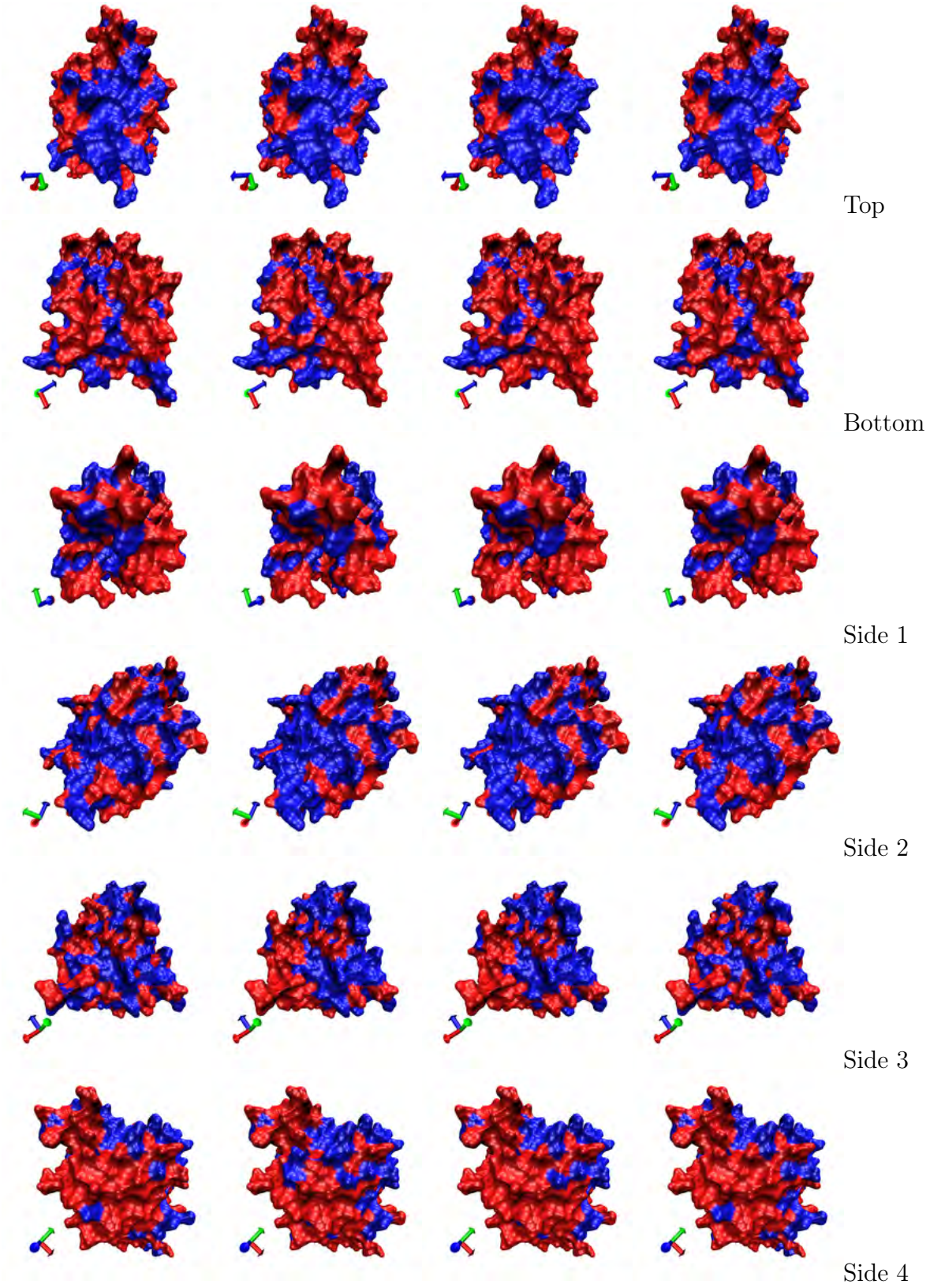

Figure B.9: Pairwise conservation of *P. falciparum* AdoMetDC surface residues. *P. falciparum* is compared to *P. berghei*, *P. knowlesi*, *P. vivax* and *P. yoelii* in columns 1-4, respectively. Rows 1 -6 correspond to the arbitrary top, bottom, side 1, side 2, side 3 and side 4 poses, respectively. Blue: identical residues, red: not conserved.

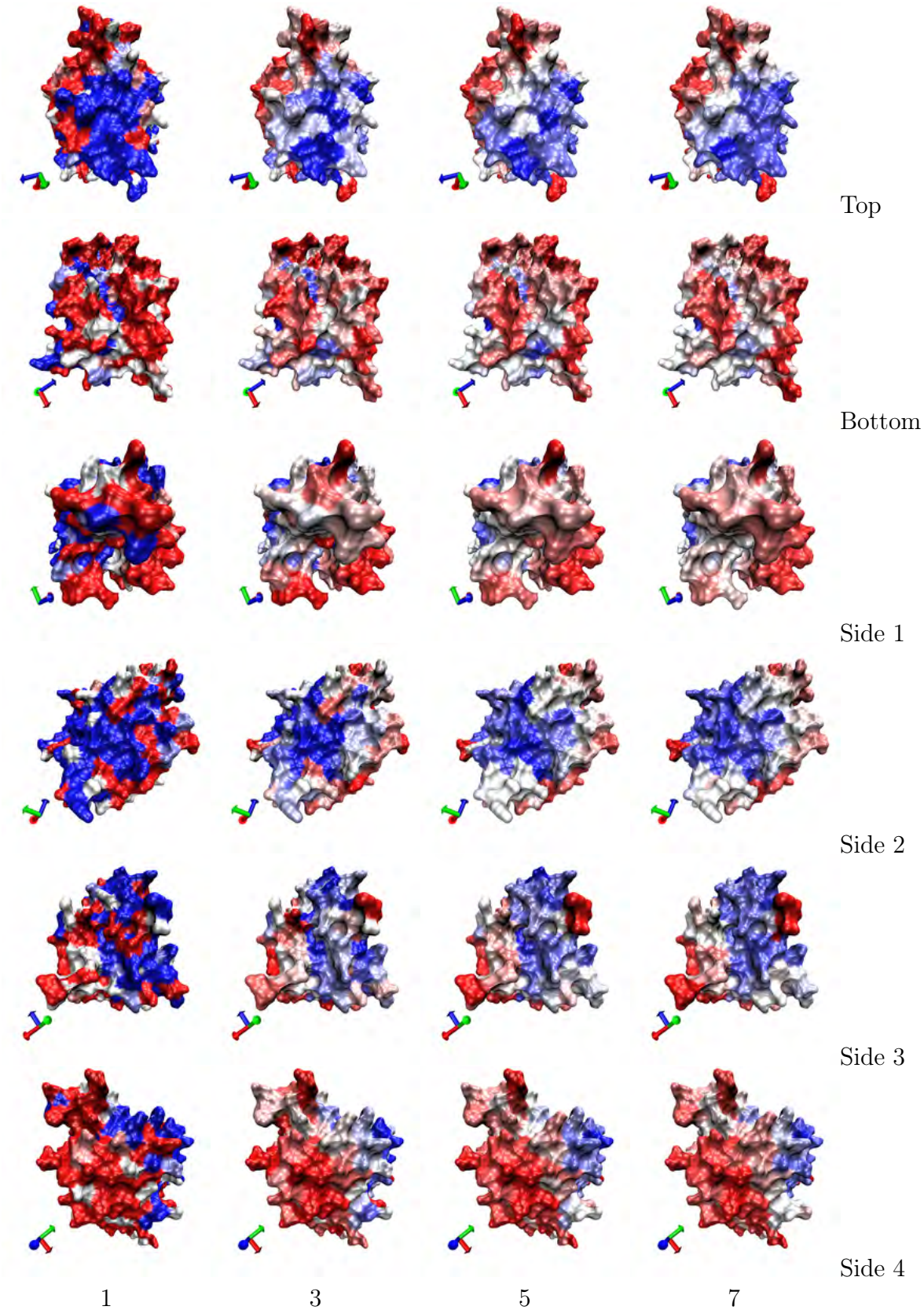

Figure B.10: Conservation of *P. falciparum* AdoMetDC surface residues. *P. falciparum* is compared simultaneously to all other *Plasmodium sp.* with sliding windows of 1, 3, 5 and 7 residues in columns 1-4, respectively. Rows 1 -6 correspond to the arbitrary top, bottom, side 1, side 2, side 3 and side 4 poses, respectively. Blue: identical residues, red: not conserved.

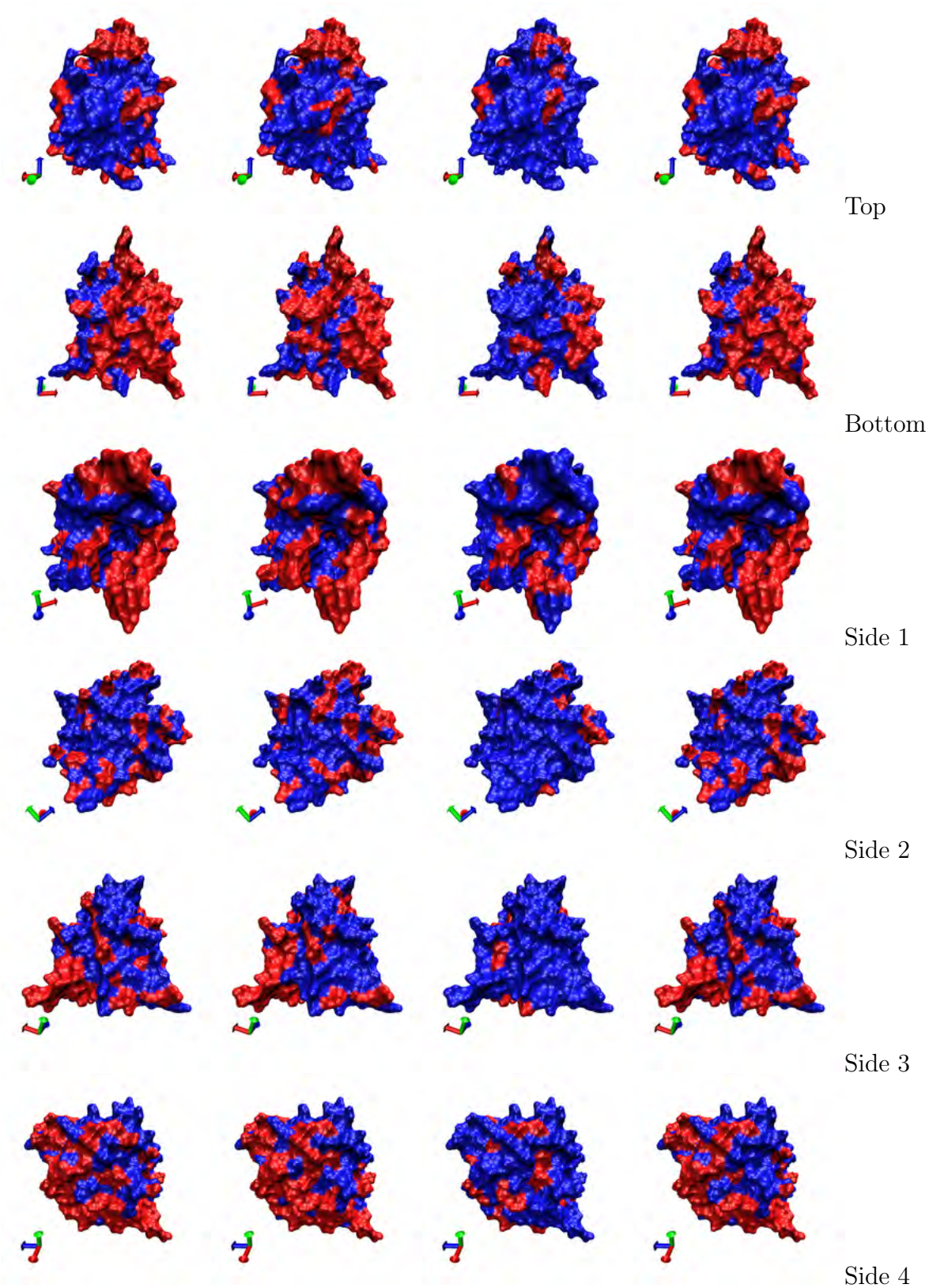

Figure B.11: Pairwise conservation of *P. knowlesi* AdoMetDC surface residues. *P. knowlesi* is compared to *P. berghei, P. falciparum*, *P. vivax* and *P. yoelii* in columns 1-4, respectively. Rows 1 -6 correspond to the arbitrary top, bottom, side 1, side 2, side 3 and side 4 poses, respectively. Blue: identical residues, red: not conserved.

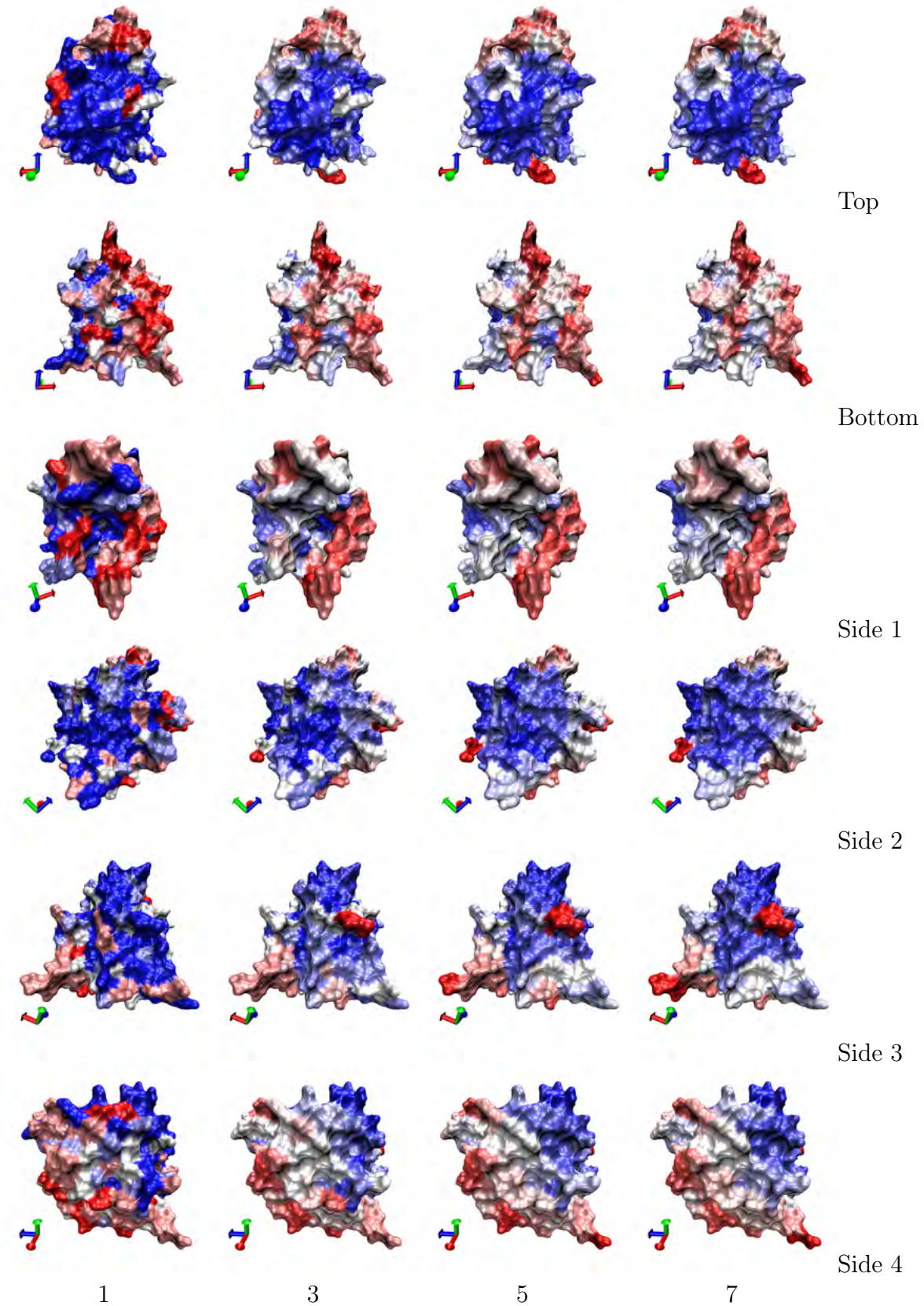

Figure B.12: Conservation of *P. knowlesi* AdoMetDC surface residues. *P. knowlesi* is compared simultaneously to all other *Plasmodium sp.* with sliding windows of 1, 3, 5 and 7 residues in columns 1-4, respectively. Rows 1 -6 correspond to the arbitrary top, bottom, side 1, side 2, side 3 and side 4 poses, respectively. Blue: identical residues, red: not conserved.

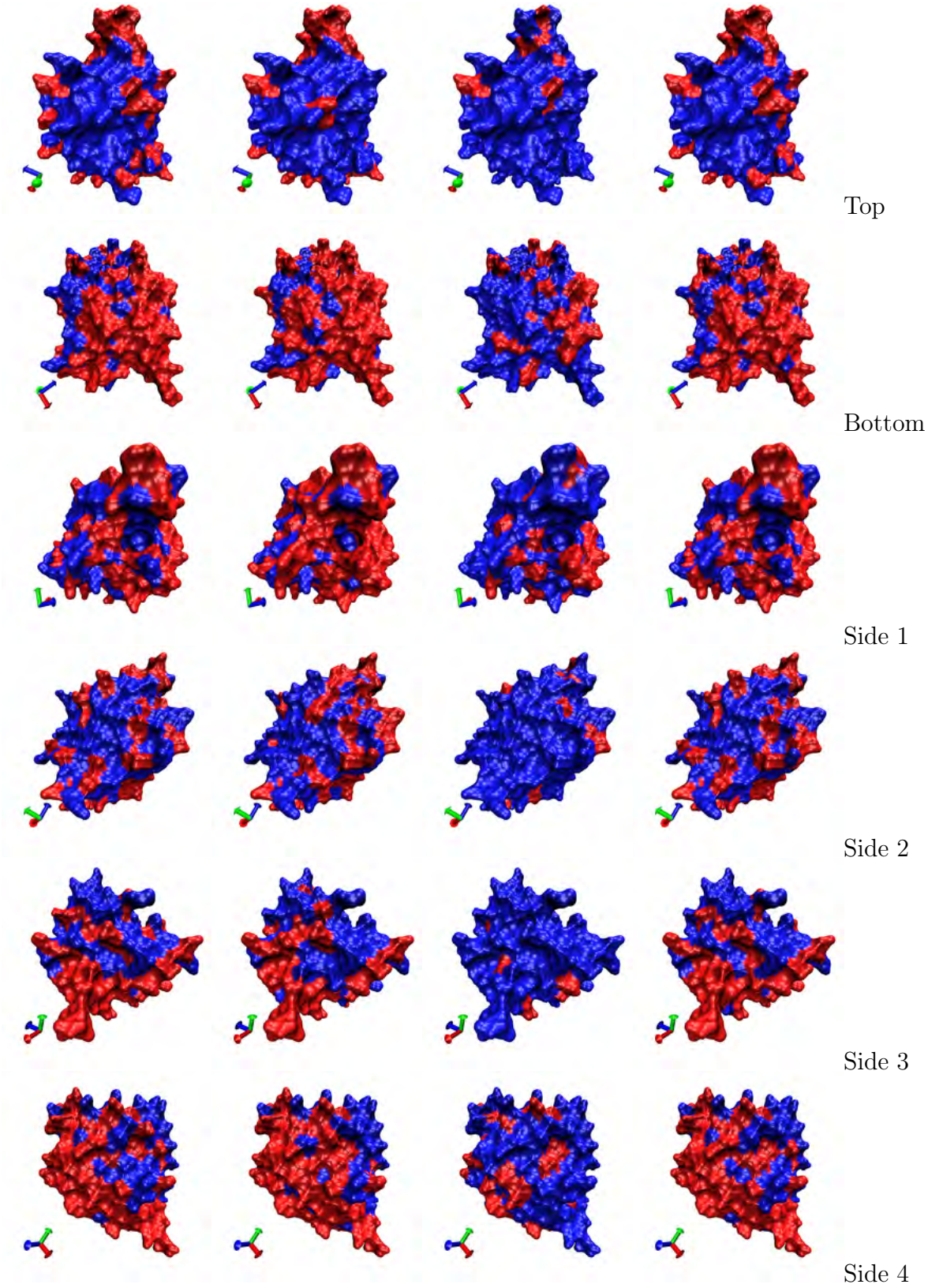

Figure B.13: Pairwise conservation of *P. vivax* AdoMetDC surface residues. *P. vivax* is compared to *P. berghei, P. falciparum*, *P. knowlesi* and *P. yoelii* in columns 1-4, respectively. Rows 1 -6 correspond to the arbitrary top, bottom, side 1, side 2, side 3 and side 4 poses, respectively. Blue: identical residues, red: not conserved.

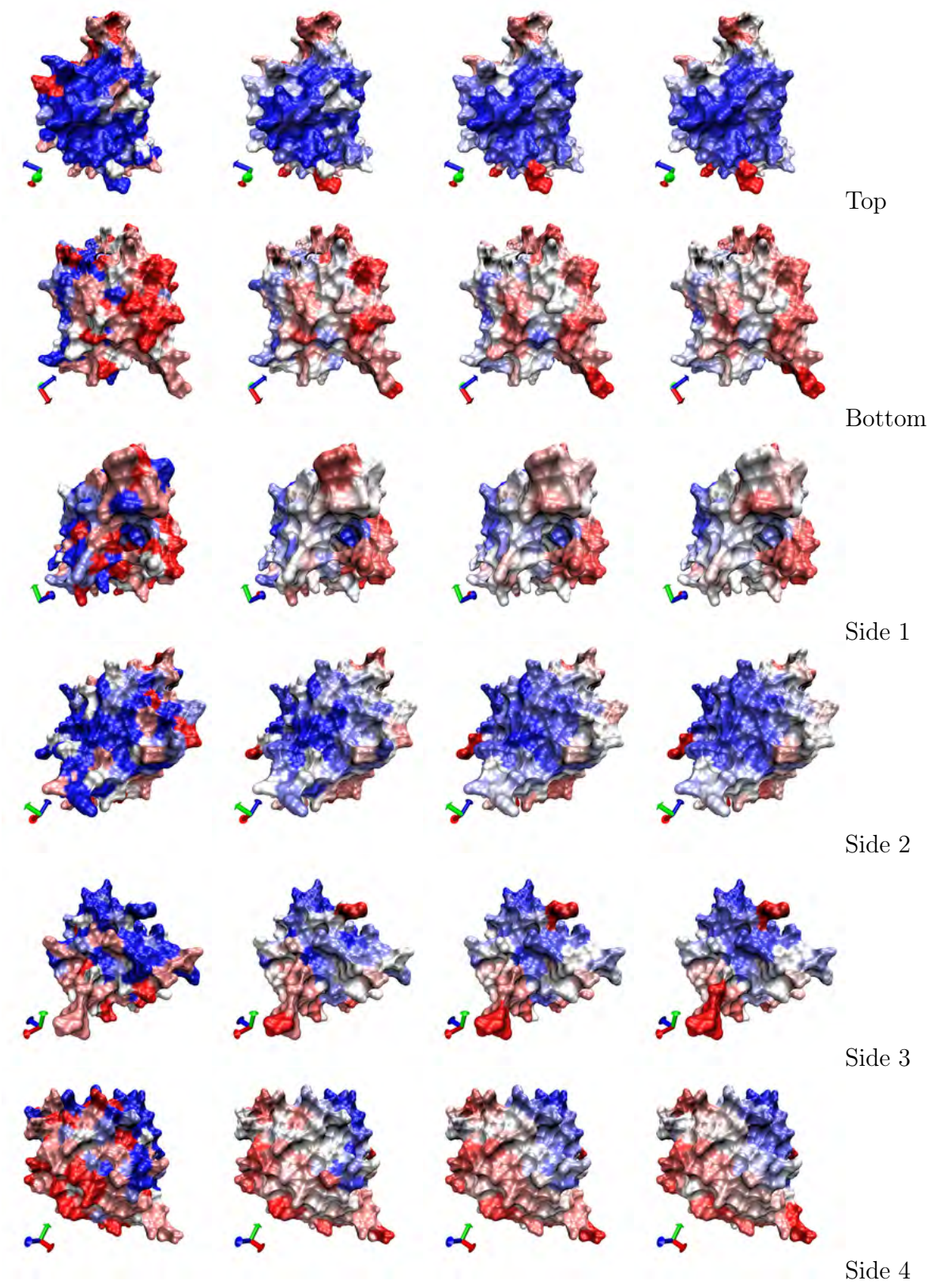

Figure B.14: Conservation of *P. vivax* AdoMetDC surface residues. *P. vivax* is compared simultaneously to all other *Plasmodium sp.* with sliding windows of 1, 3, 5 and 7 residues in columns 1-4, respectively. Rows 1 -6 correspond to the arbitrary top, bottom, side 1, side 2, side 3 and side 4 poses, respectively. Blue: identical residues, red: not conserved.

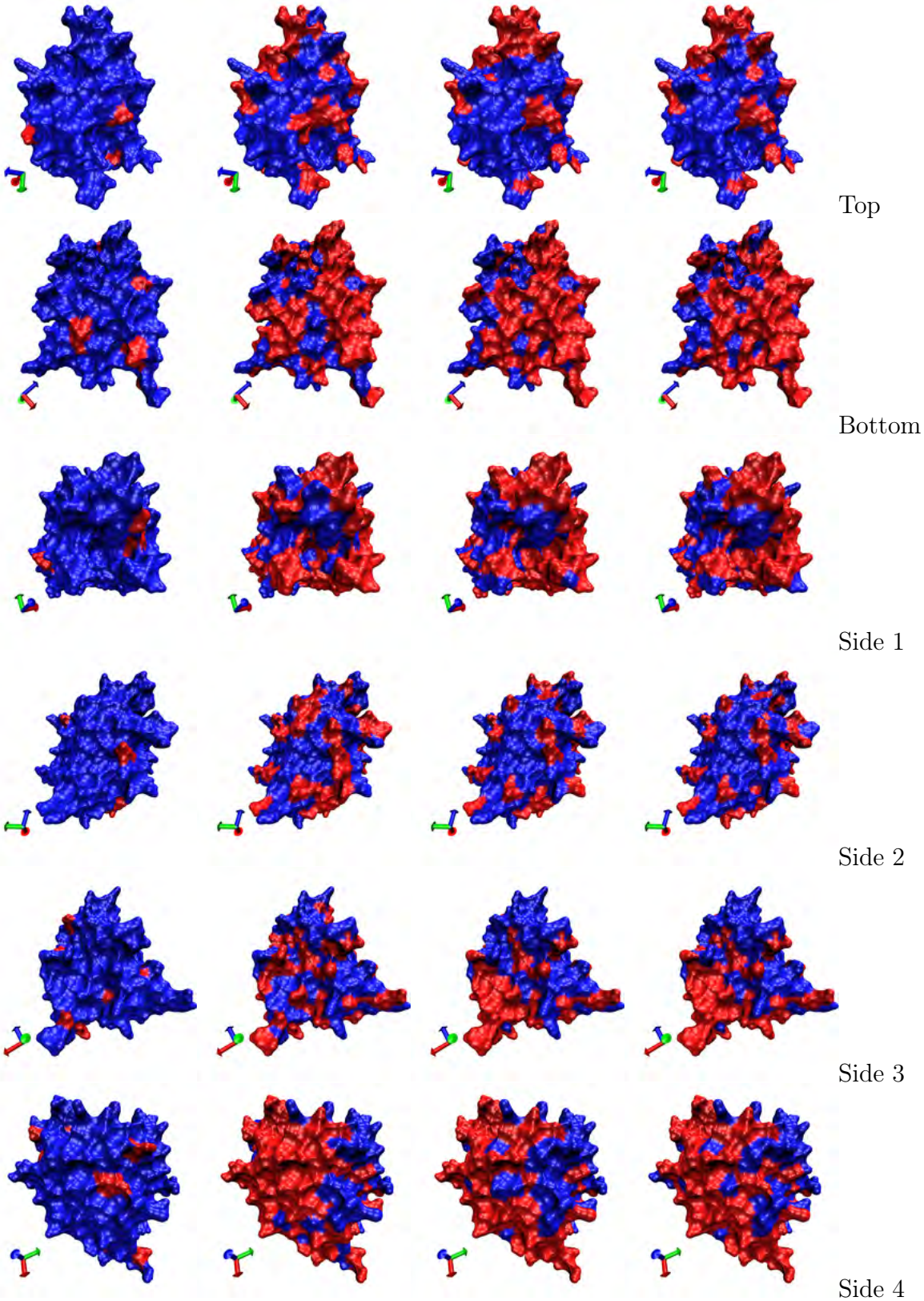

Figure B.15: Pairwise conservation of *P. yoelii* AdoMetDC surface residues. *P. yoelii* is compared to *P. berghei, P. falciparum*, *P. knowlesi* and *P. vivax* in columns 1-4, respectively. Rows 1 -6 correspond to the arbitrary top, bottom, side 1, side 2, side 3 and side 4 poses, respectively. Blue: identical residues, red: not conserved.

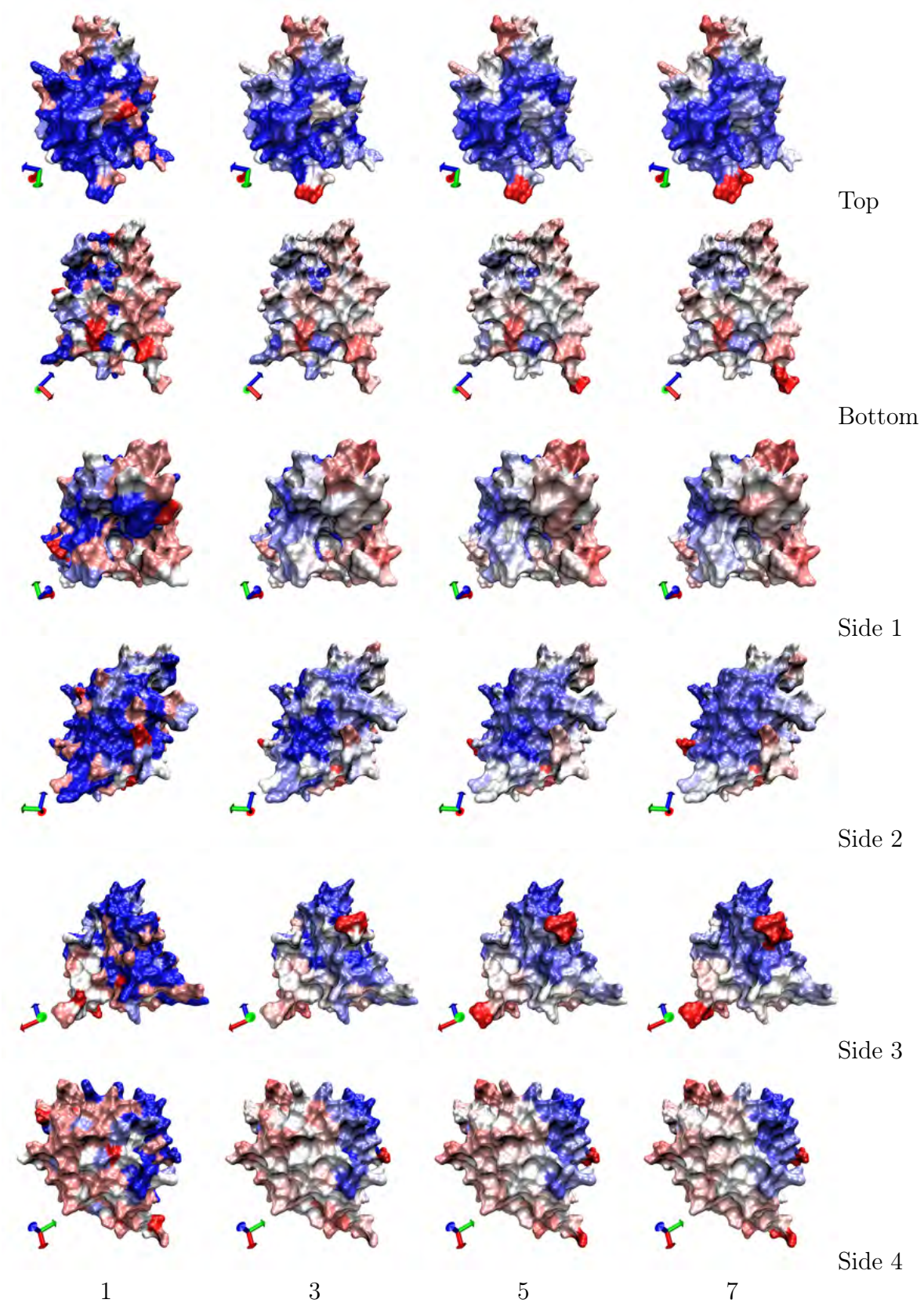

Figure B.16: Conservation of *P. yoelii* AdoMetDC surface residues. *P. yoelii* is compared simultaneously o all other *Plasmodium sp.* with sliding windows of 1, 3, 5 and 7 residues in columns 1-4, respectively. Rows 1 -6 correspond to the arbitrary top, bottom, side 1, side 2, side 3 and side 4 poses, respectively. Blue: identical residues, red: not conserved.

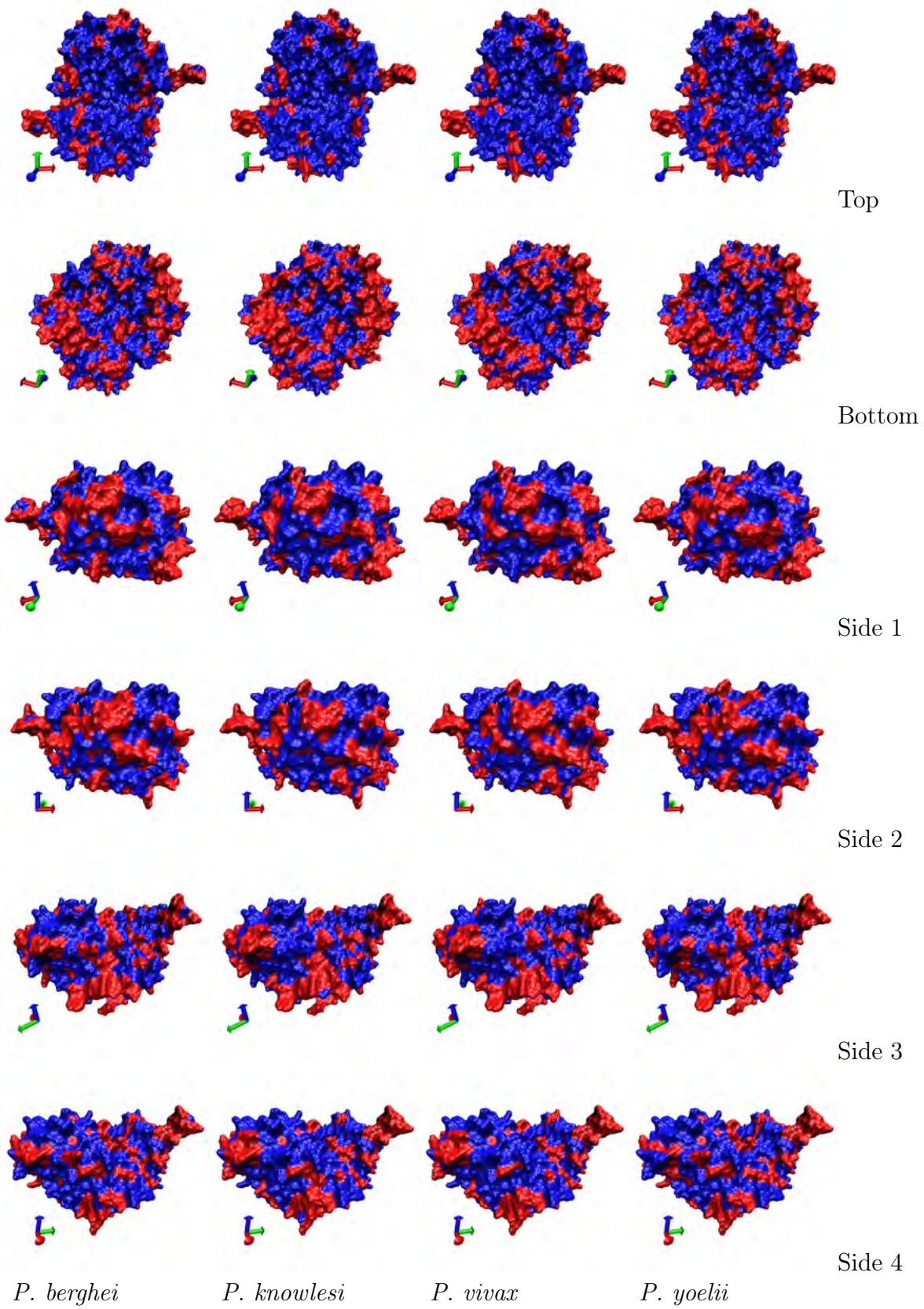

Figure B.17: Pairwise conservation of *P. falciparum* ODC surface residues. *P. falciparum* is compared to *P. berghei, P. knowlesi*, *P. vivax* and *P. yoelii* in columns 1-4, respectively. Rows 1 -6 correspond to the arbitrary top, bottom, side 1, side 2, side 3 and side 4 poses, respectively. Blue: identical residues, red: not conserved.

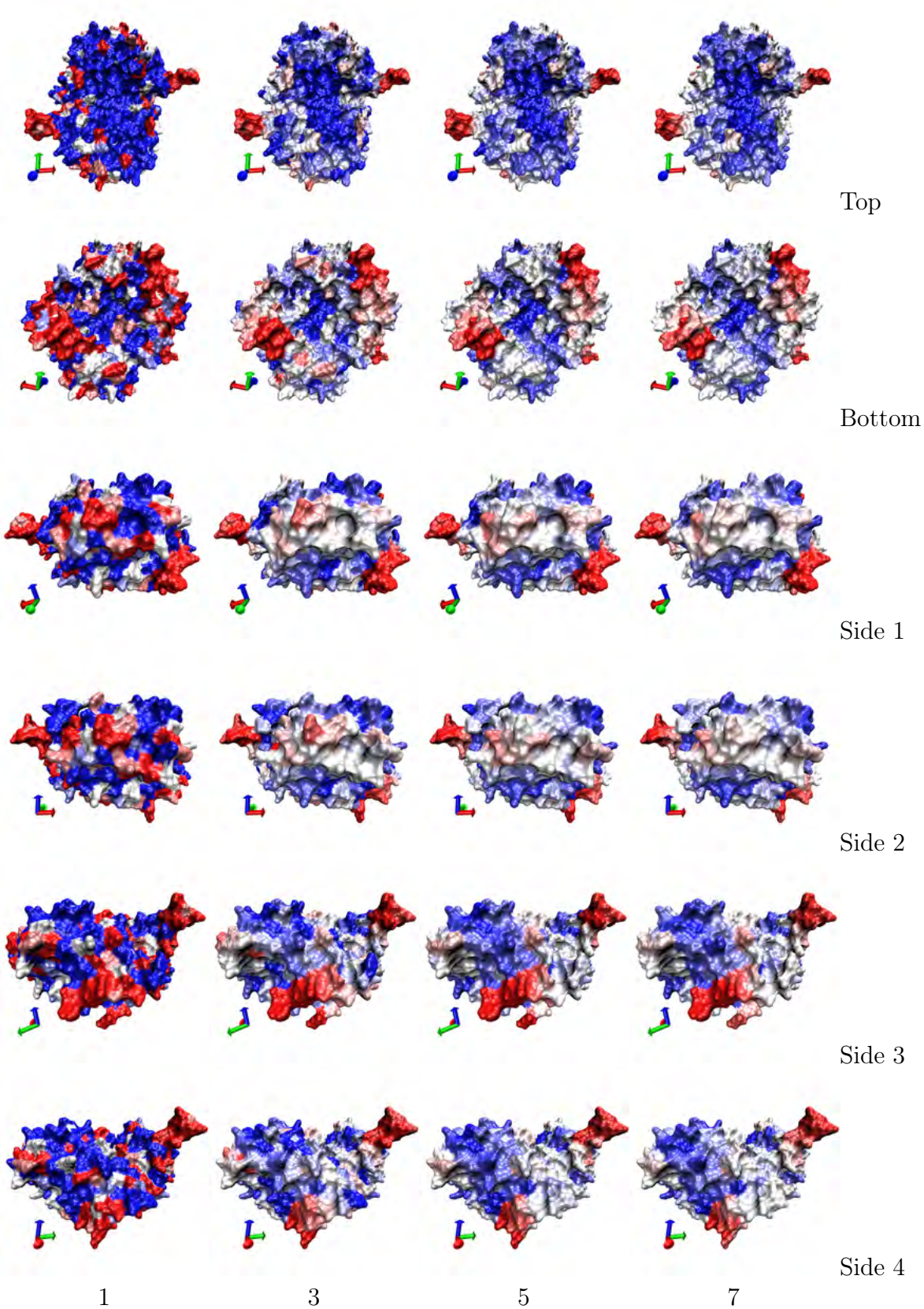

Figure B.18: Conservation of *P. falciparum* ODC surface residues. *P. falciparum* is compared simultaneously to all other *Plasmodium sp.* with sliding windows of 1, 3, 5 and 7 residues in columns 1-4, respectively. Rows 1 -6 correspond to the arbitrary top, bottom, side 1, side 2, side 3 and side 4 poses, respectively. Blue: identical residues, red: not conserved.

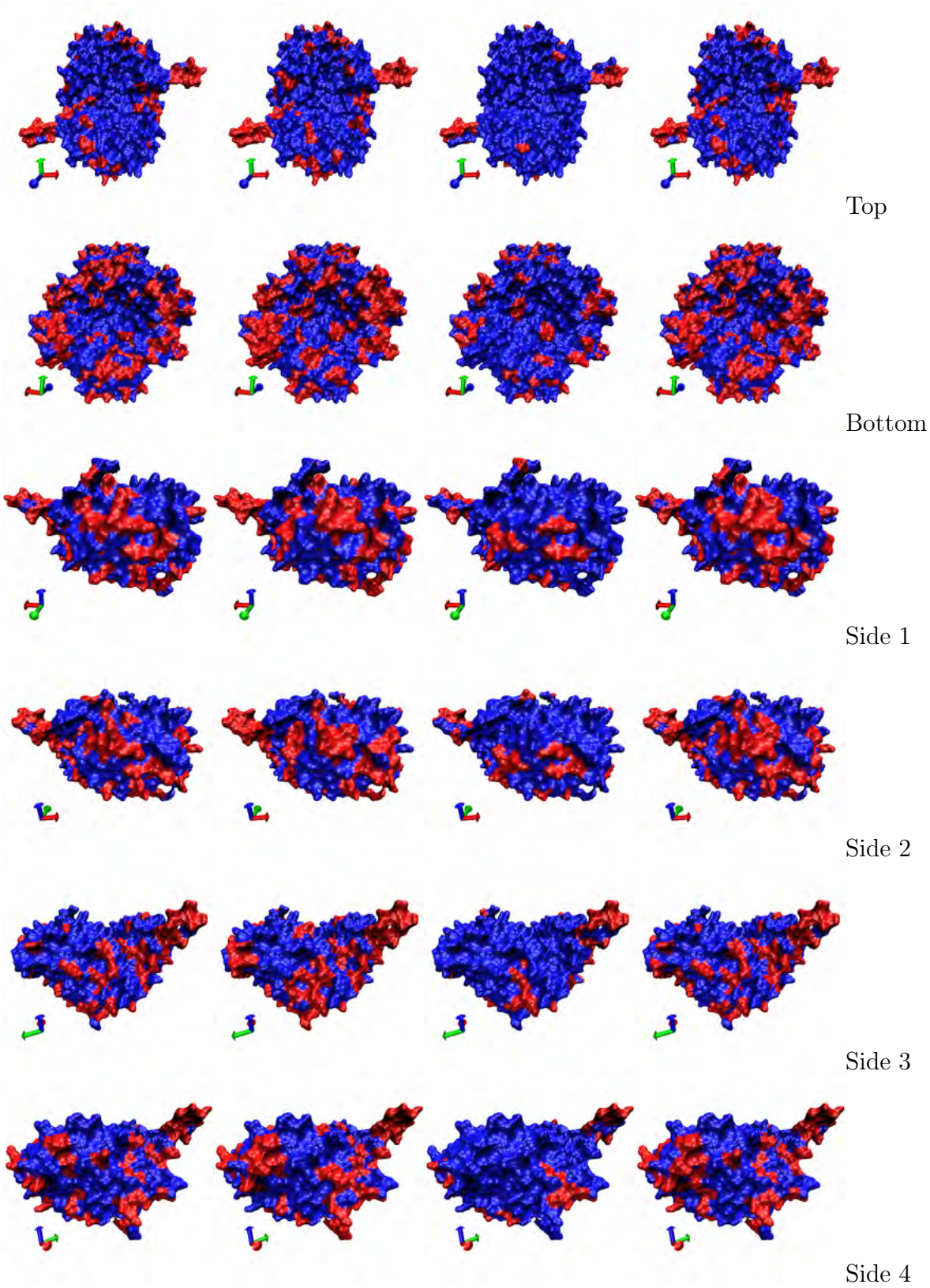

Figure B.19: Pairwise conservation of *P. knowlesi* ODC surface residues. *P. knowlesi* is compared to *P. berghei, P. falciparum*, *P. vivax* and *P. yoelii* in columns 1-4, respectively. Rows 1 -6 correspond to the arbitrary top, bottom, side 1, side 2, side 3 and side 4 poses, respectively. Blue: identical residues, red: not conserved.

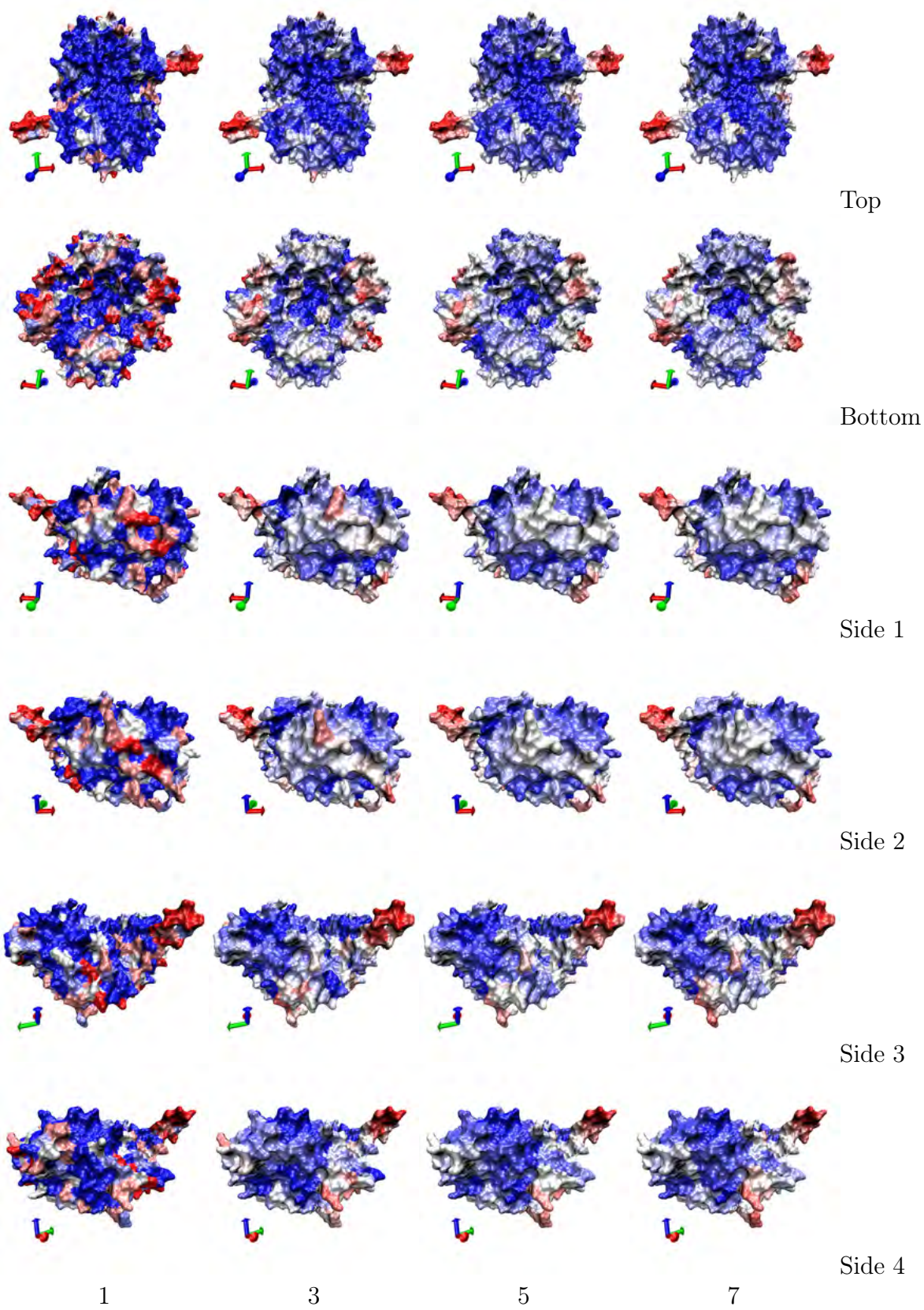

Figure B.20: Conservation of *P. knowlesi* ODC surface residues. *P. knowlesi* is compared simultaneously to all other *Plasmodium sp.* with sliding windows of 1, 3, 5 and 7 residues in columns 1-4, respectively. Rows 1 -6 correspond to the arbitrary top, bottom, side 1, side 2, side 3 and side 4 poses, respectively. Blue: identical residues, red: not conserved.

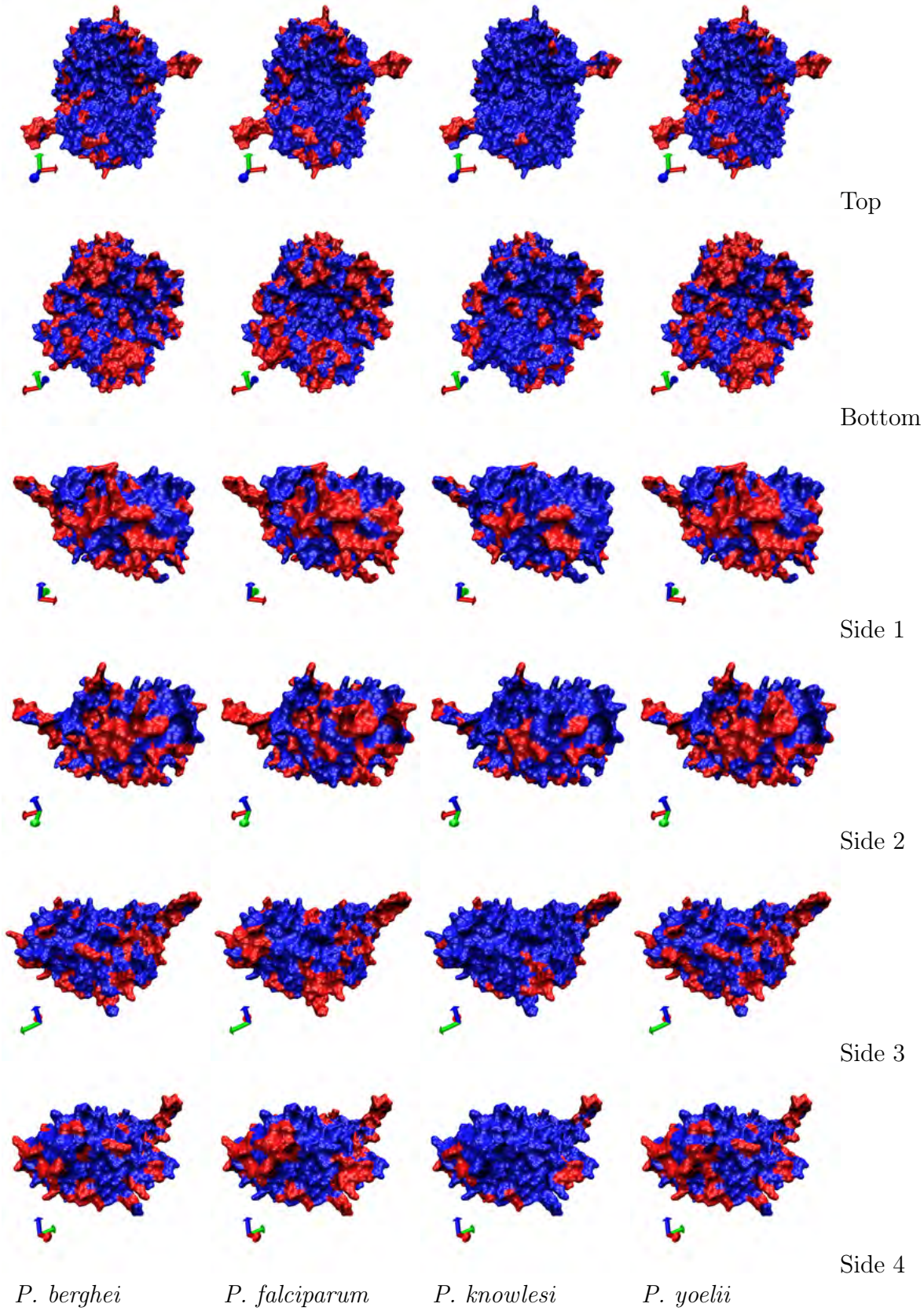

Figure B.21: Pairwise conservation of *P. vivax* ODC surface residues. *P. vivax* is compared to *P. berghei, P. falciparum*, *P. knowlesi* and *P. yoelii* in columns 1-4, respectively. Rows 1 -6 correspond to the arbitrary top, bottom, side 1, side 2, side 3 and side 4 poses, respectively. Blue: identical residues, red: not conserved.

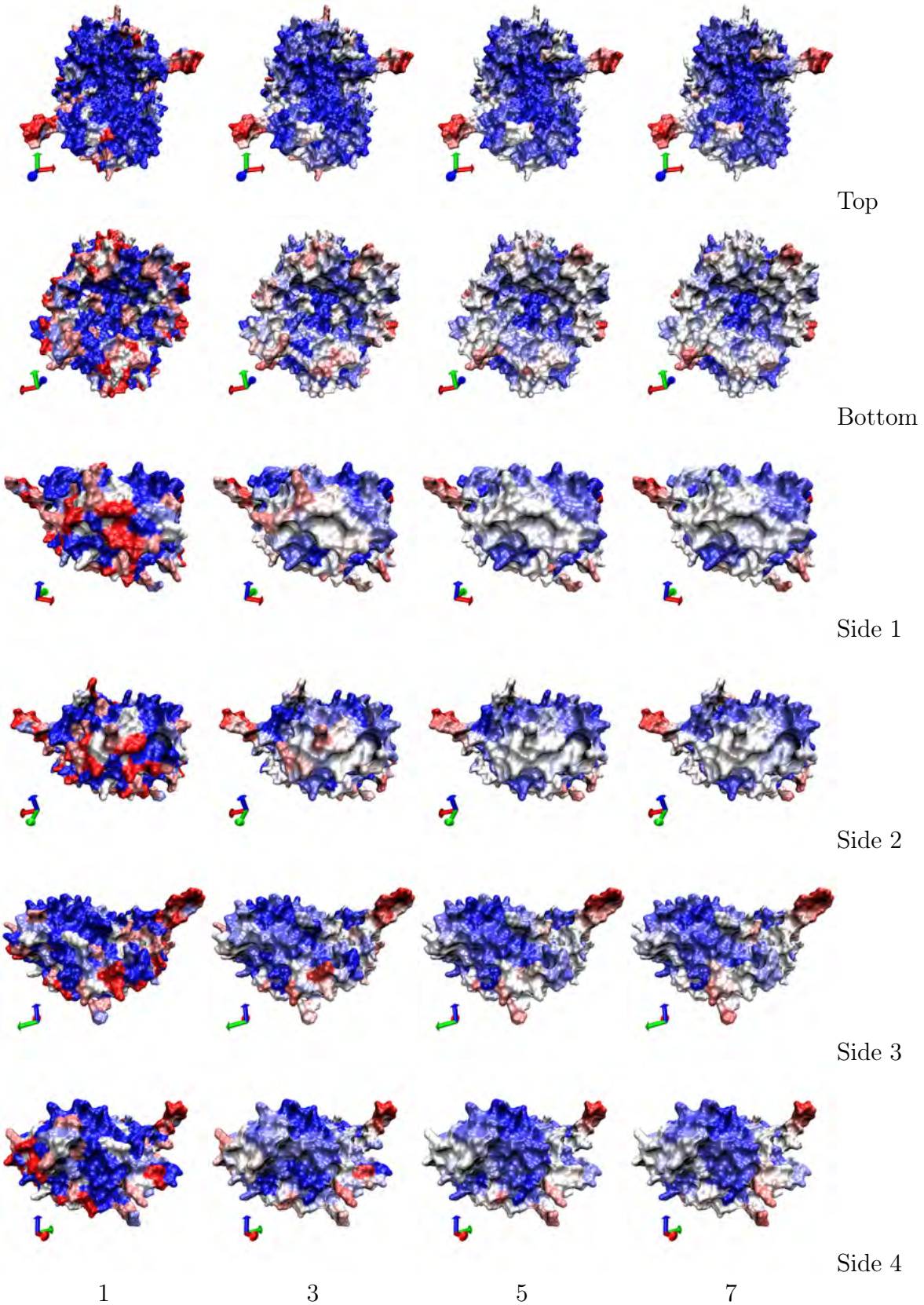

Figure B.22: Conservation of *P. vivax* ODC surface residues. *P. vivax* is compared simultaneously to all other *Plasmodium sp.* with sliding windows of 1, 3, 5 and 7 residues in columns 1-4, respectively. Rows 1 -6 correspond to the arbitrary top, bottom, side 1, side 2, side 3 and side 4 poses, respectively. Blue: identical residues, red: not conserved.

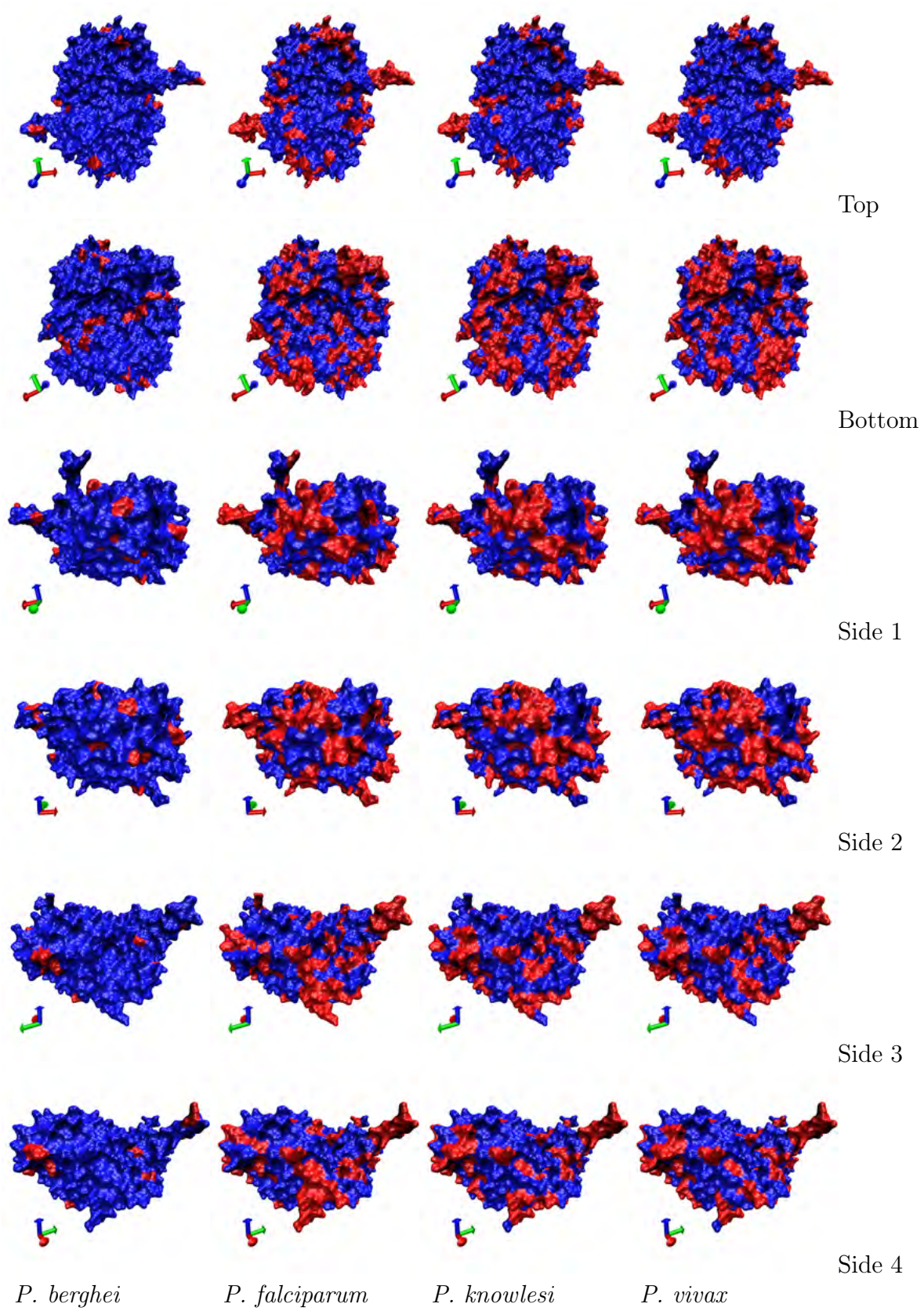

Figure B.23: Pairwise conservation of *P. yoelii* ODC surface residues. *P. yoelii* is compared to *P. berghei, P. falciparum*, *P. vivax* and *P. yoelii* in columns 1-4, respectively. Rows 1 -6 correspond to the arbitrary top, bottom, side 1, side 2, side 3 and side 4 poses, respectively. Blue: identical residues, red: not conserved.

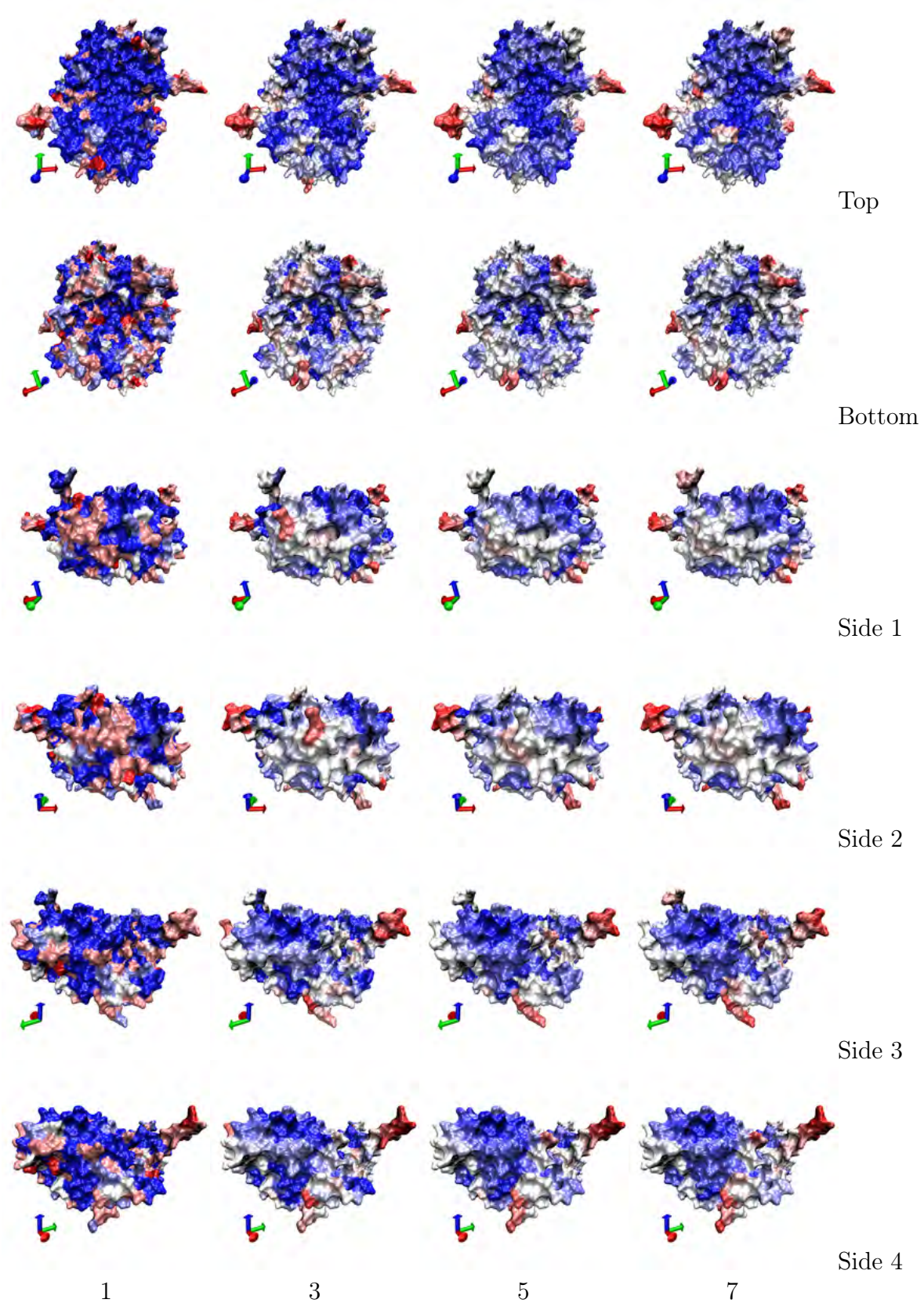

Figure B.24: Conservation of *P. yoelii* ODC surface residues. *P. yoelii* is compared simultaneously to all other *Plasmodium sp.* with sliding windows of 1, 3, 5 and 7 residues in columns 1-4, respectively. Rows 1 -6 correspond to the arbitrary top, bottom, side 1, side 2, side 3 and side 4 poses, respectively. Blue: identical residues, red: not conserved.

B.3 Distribution of RP scores

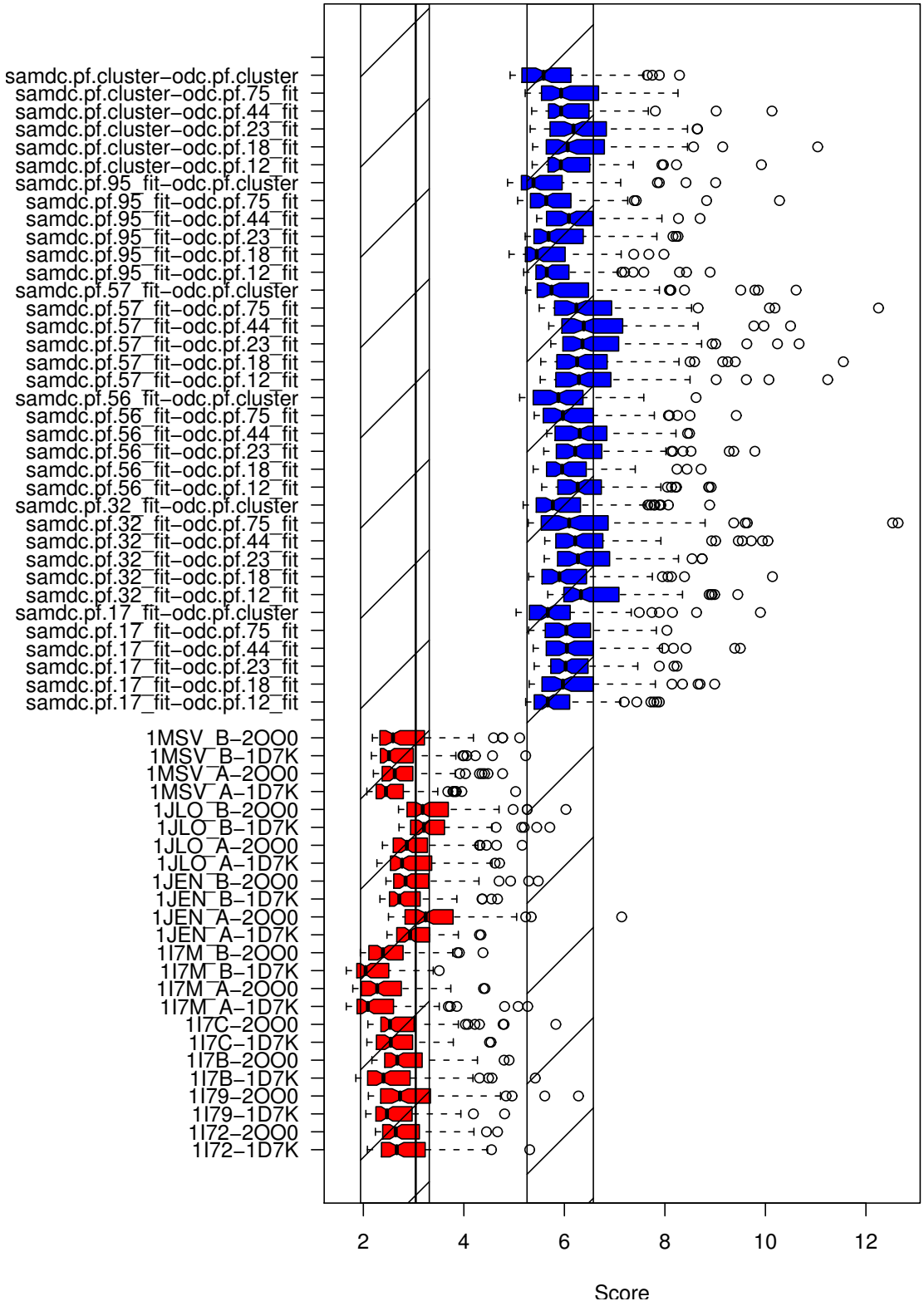

Figure B.25: Distribution of top 100 RP scores for docking of human (red) and *P. falciparum* (blue) AdoMetDC/ODC. The notch overlaps are indicated by the hatched bars. Two overlaps can be observed for human and one for *P. falciparum* (The gap is too small to be visible on this scale). The RP score is plotted on the x-axis against the AdoMetDC/ODC model (blue) or structure (red) combinations.

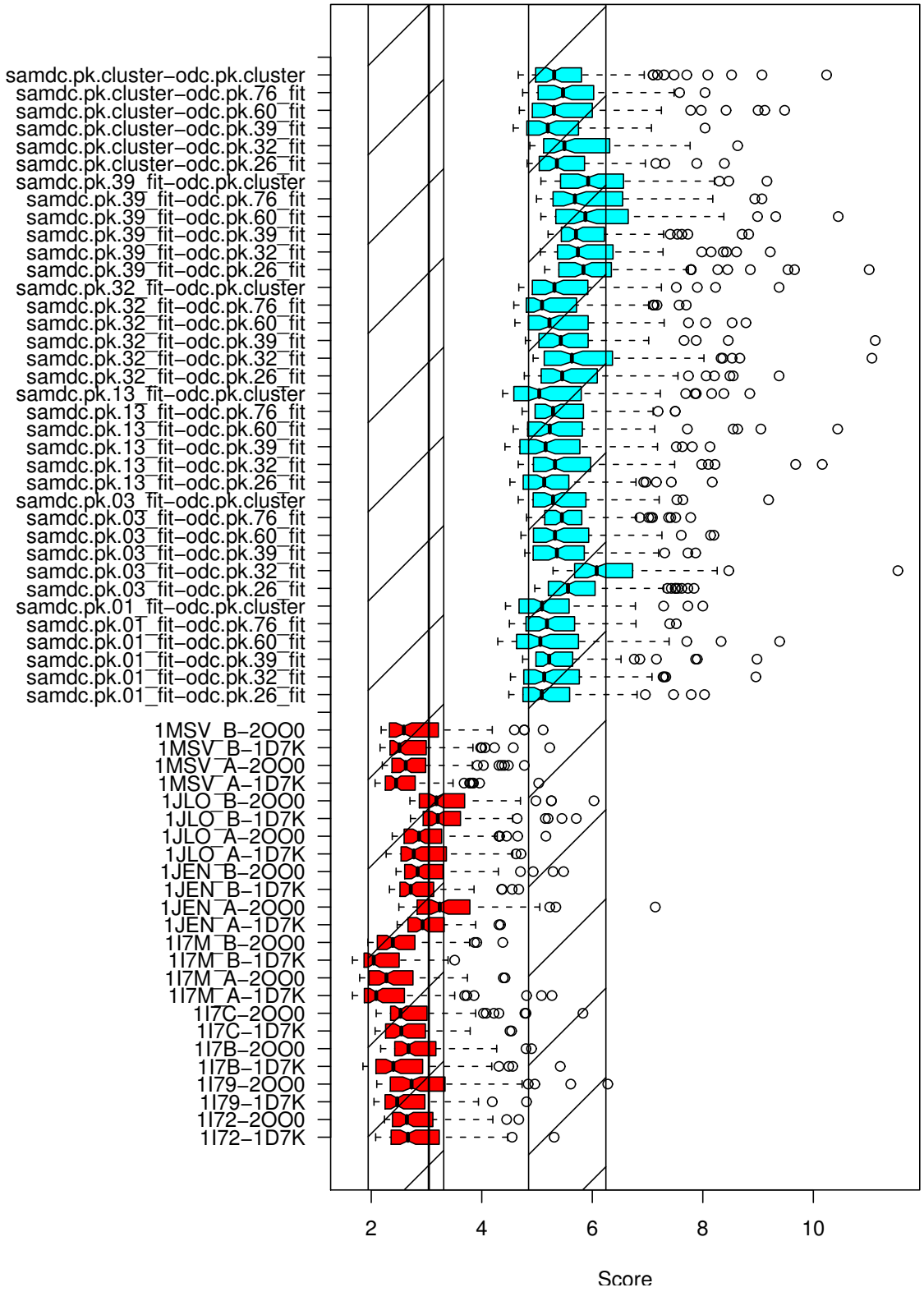

Figure B.26: Distribution of top 100 RP scores for docking of human (red) and *P. knowlesi* (cyan) AdoMetDC/ODC. The notch overlaps are indicated by the hatched bars. Two overlaps can be observed for human and one for *P. knowlesi* (The gap is too small to be visible on this scale). The RP score is plotted on the x-axis against the AdoMetDC/ODC model (cyan) or structure (red) combinations.

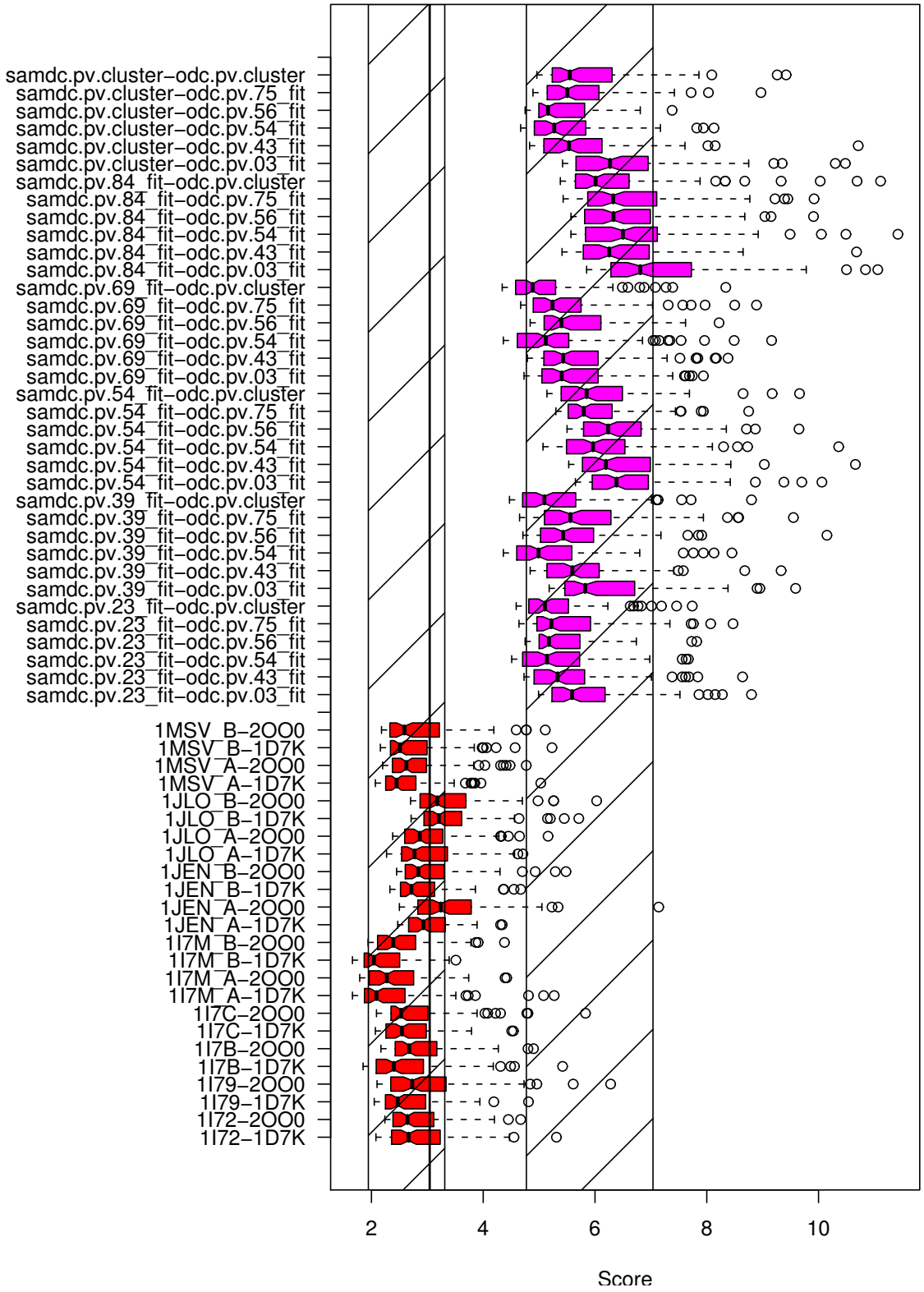

Figure B.27: Distribution of top 100 RP scores for docking of human (red) and *P. vivax* (magenta) AdoMetDC/ODC. The notch overlaps are indicated by the hatched bars. Two overlaps can be observed for human and one for *P. vivax* (The gap is too small to be visible on this scale). The RP score is plotted on the x-axis against the AdoMetDC/ODC model (pink) or structure (red) combinations.

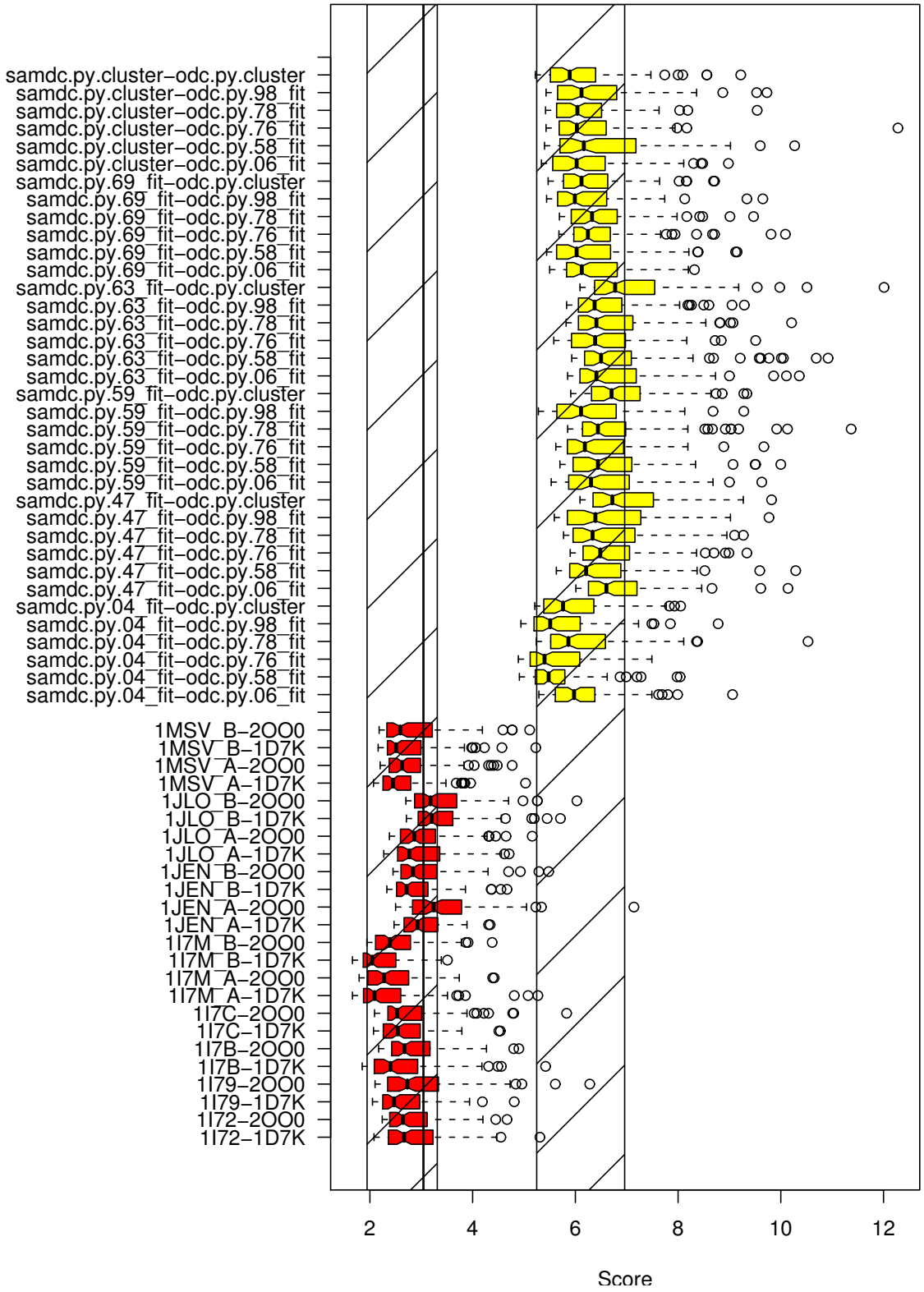

Figure B.28: Distribution of top 100 RP scores for docking of human (red) and *P. yoelii* (yellow) AdoMetDC/ODC. The notch overlaps are indicated by the hatched bars. Two overlaps can be observed for human and one for *P. yoelii* (The gap is too small to be visible on this scale). The RP score is plotted on the x-axis against the AdoMetDC/ODC model (yellow) or structure (red) combinations.

B.4 Distribution of centres of mass

B.4.1 AdoMetDC relative to ODC

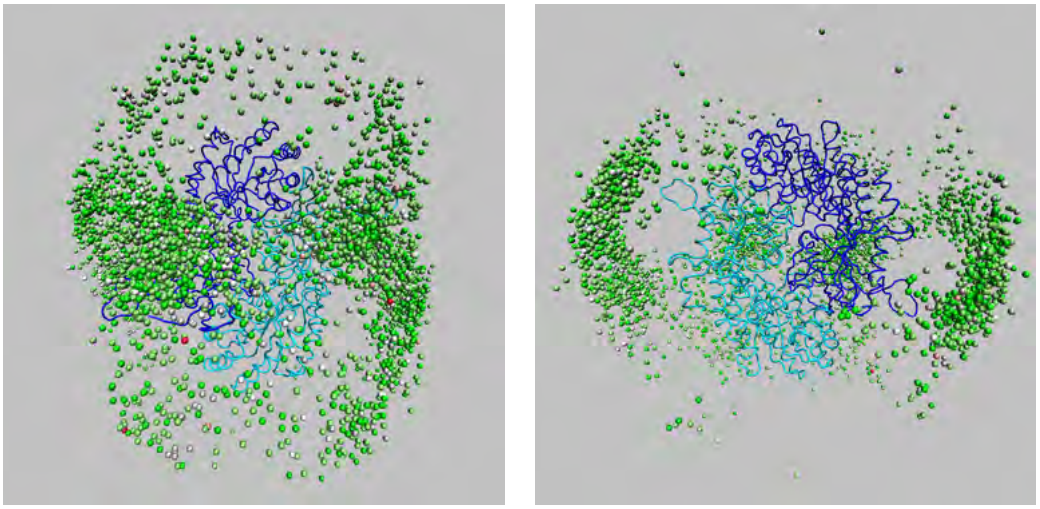

(a) Top

(b) Bottom

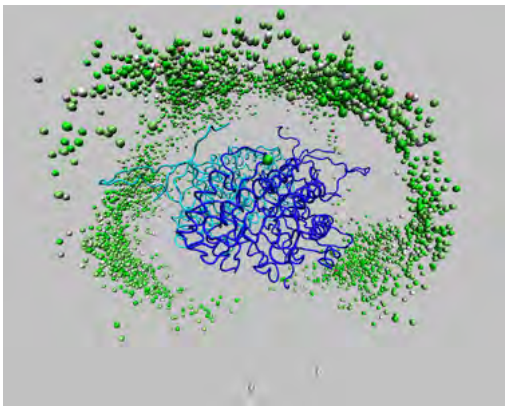

(c) Side 1

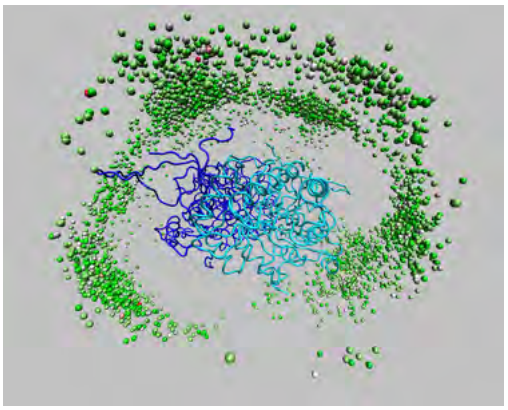

(d) Side 2

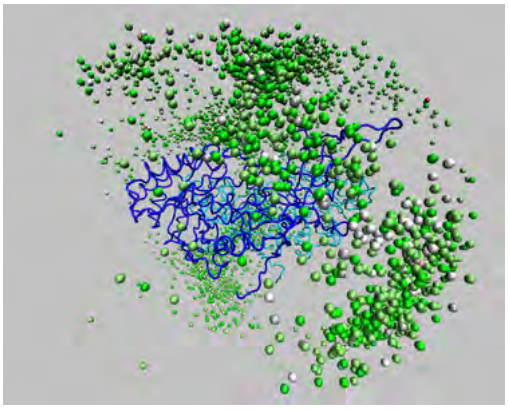

(e) Side 3

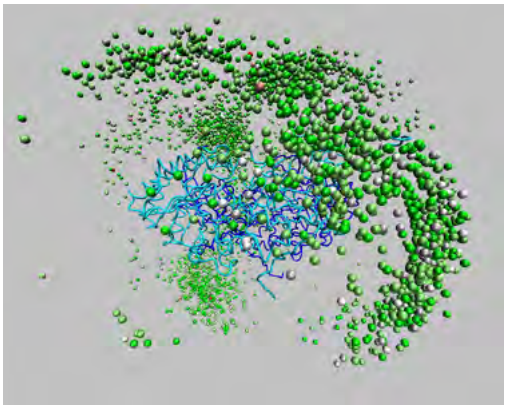

(f) Side 4

Figure B.29: Centre of mass (COM) distributions of *P. knowlesi* AdoMetDC relative to ODC. ODC chains A (blue) and (cyan) B are represented by C_α trace. The COMs of all top 100 (by RP score) from all dockings are represented as spheres (total 3600 positions). COM colour scaling is based on the RP score (4.29: green → 11.53: red).

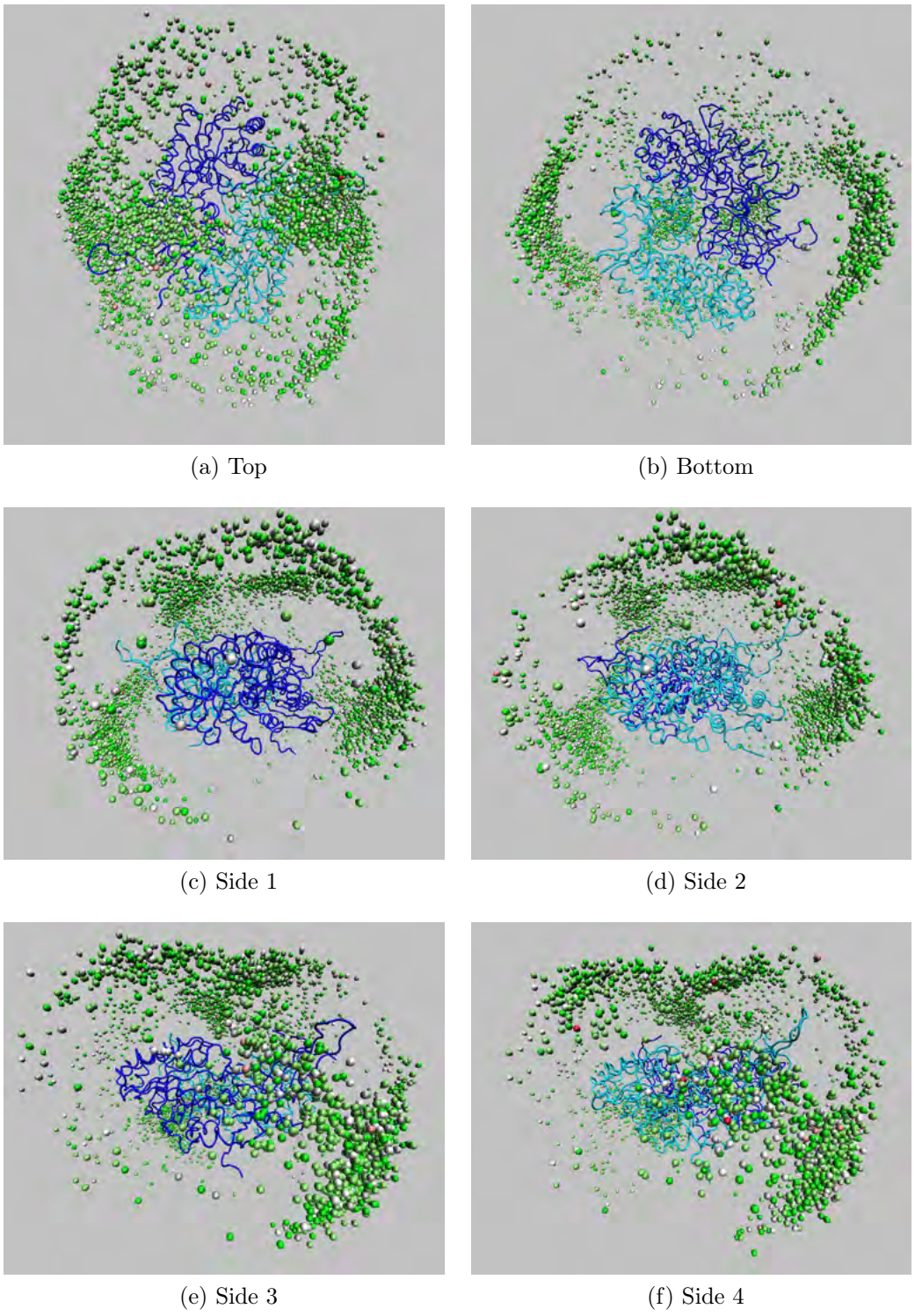

(a) Top (b) Bottom

(c) Side 1 (d) Side 2

(e) Side 3 (f) Side 4

Figure B.30: Centre of mass (COM) distributions of *P. vivax* AdoMetDC relative to ODC. ODC chains A (blue) and (cyan) B are represented by C_α trace. The COMs of all top 100 (by RP score) from all dockings are represented as spheres (total 3600 positions). COM colour scaling is based on the RP score (4.34: green → 11.42: red).

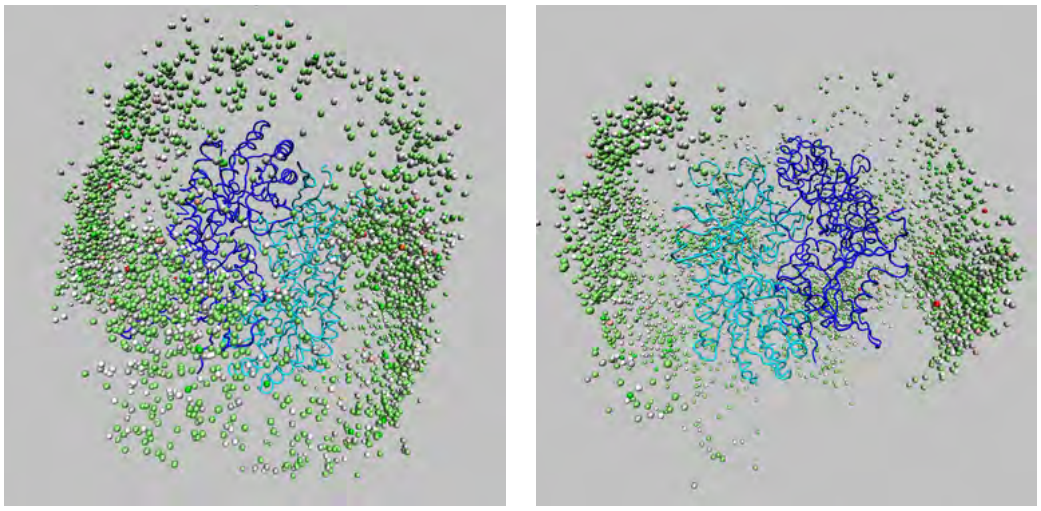

(a) Top

(b) Bottom

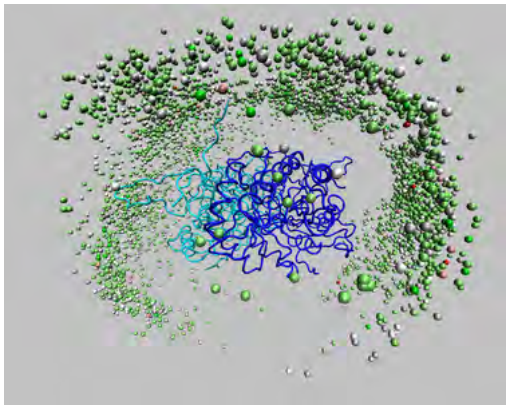

(c) Side 1

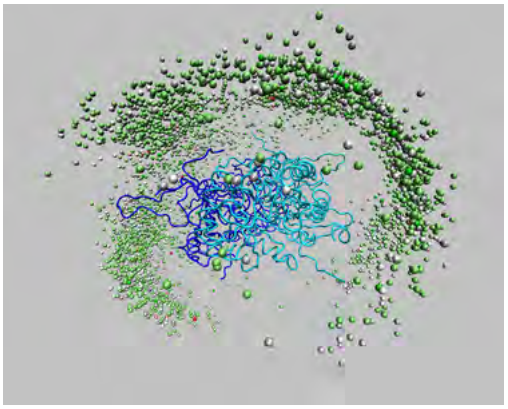

(d) Side 2

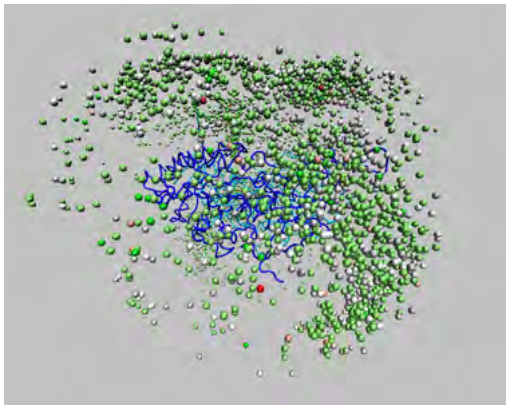

(e) Side 3

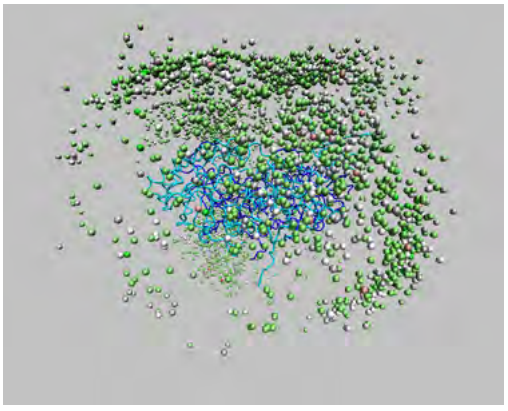

(f) Side 4

Figure B.31: Centre of mass (COM) distributions of *P. yoelii* AdoMetDC relative to ODC. ODC chains A (blue) and (cyan) B are represented by C_α trace. The COMs of all top 100 (by RP score) from all dockings are represented as spheres (total 3600 positions). COM colour scaling is based on the RP score (7.49: green → 12.28: red).

B.4.2 ODC relative to AdoMetDC

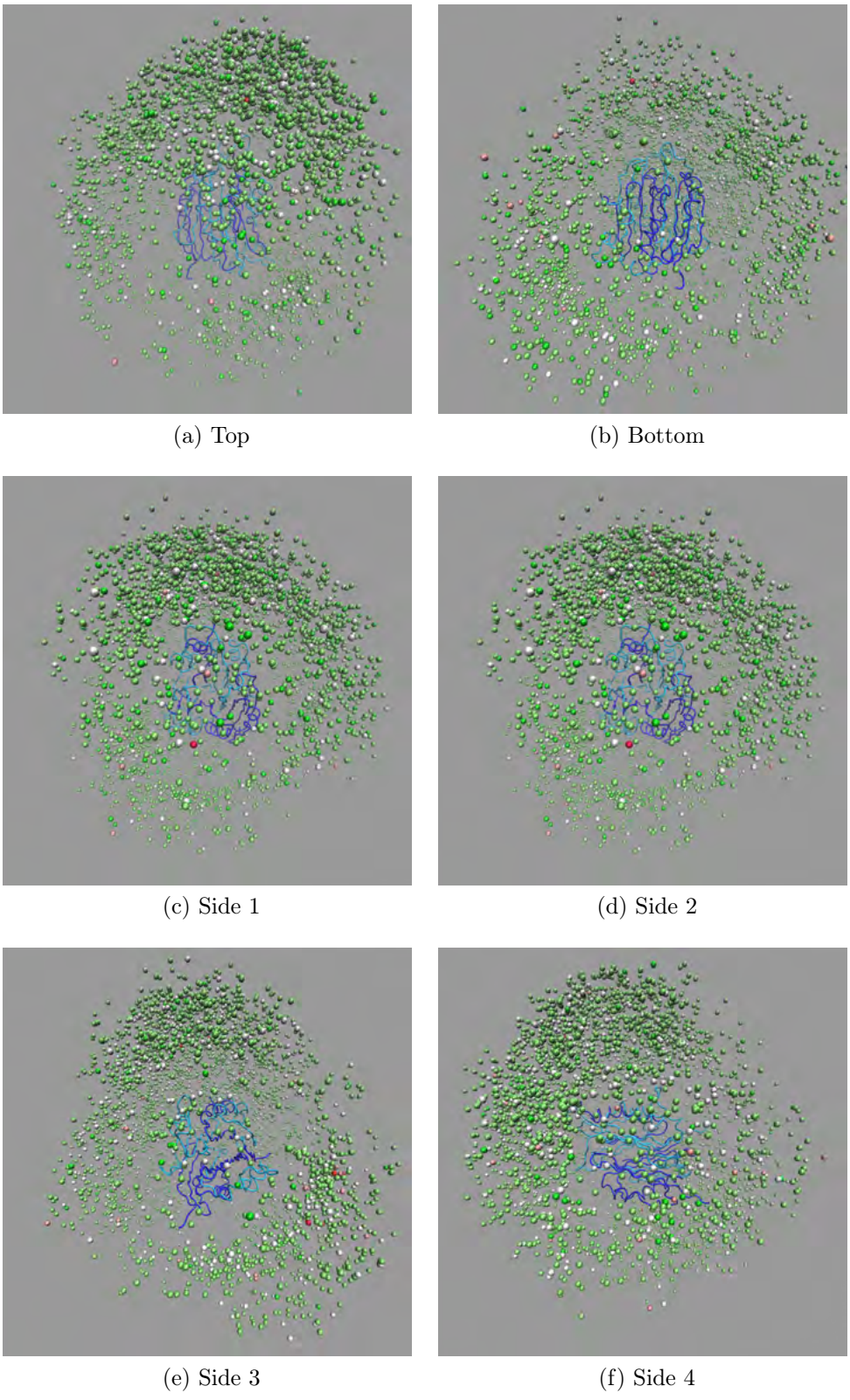

(a) Top (b) Bottom

(c) Side 1 (d) Side 2

(e) Side 3 (f) Side 4

Figure B.32: Centre of mass (COM) distributions of *P. falciparum* ODC relative to AdoMetDC. AdoMetDC chains A & C (blue) and (cyan) B & D are represented by C_α trace. The COMs of all top 100 (by RP score) from all dockings are represented as spheres (total 3600 positions). COM colour scaling is based on the RP score (4.87: green → 12.64: red).

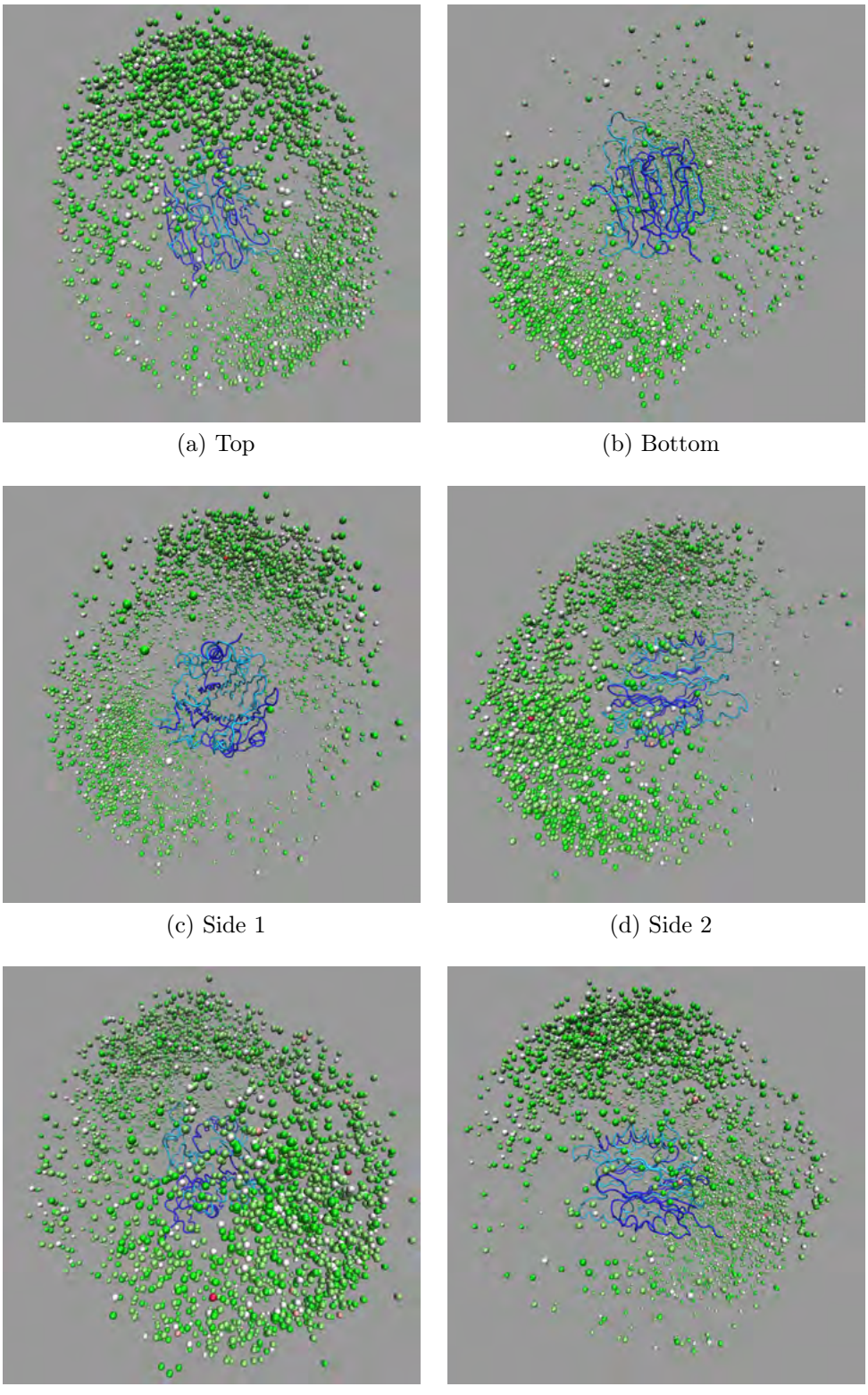

(a) Top (b) Bottom

(c) Side 1 (d) Side 2

(e) Side 3 (f) Side 4

Figure B.33: Centre of mass (COM) distributions of *P. knowlesi* ODC relative to AdoMetDC. AdoMetDC chains A & C (blue) and (cyan) B & D are represented by C_α trace. The COMs of all top 100 (by RP score) from all dockings are represented as spheres (total 3600 positions). COM colour scaling is based on the RP score (4.29: green → 11.53: red).

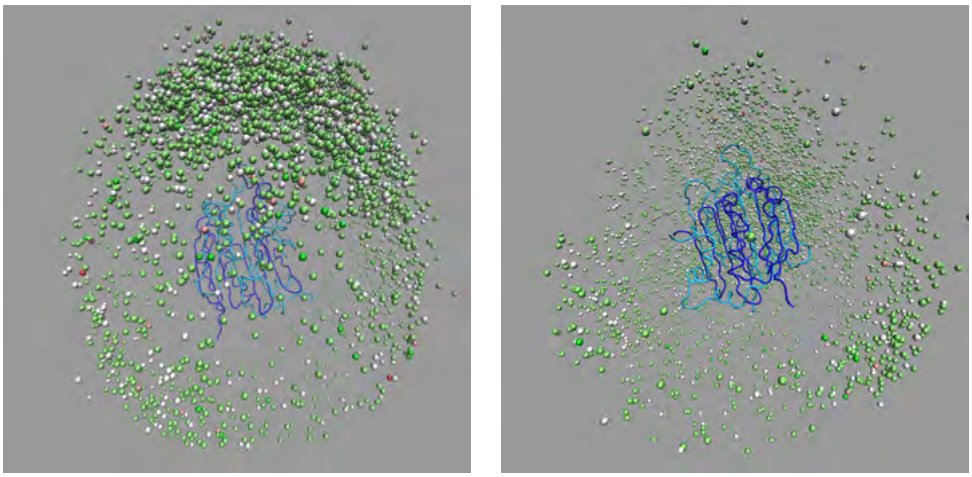

(a) Top (b) Bottom

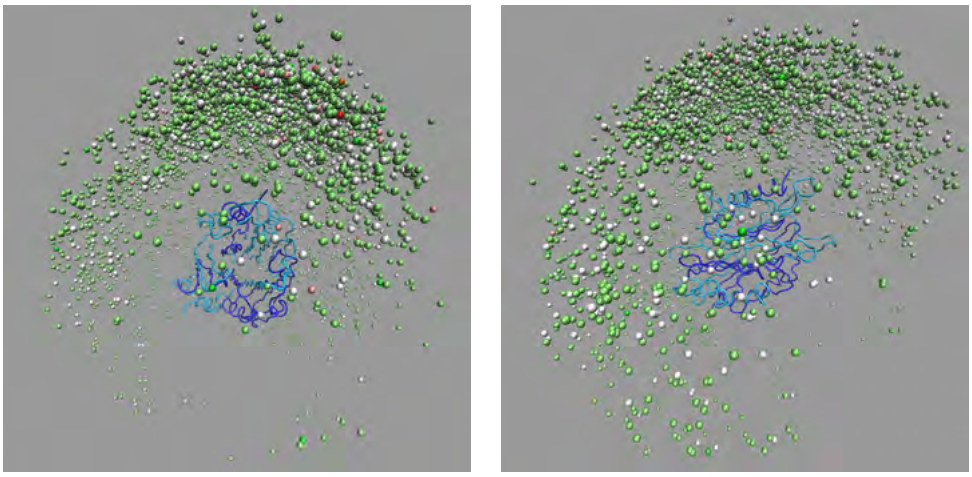

(c) Side 1 (d) Side 2

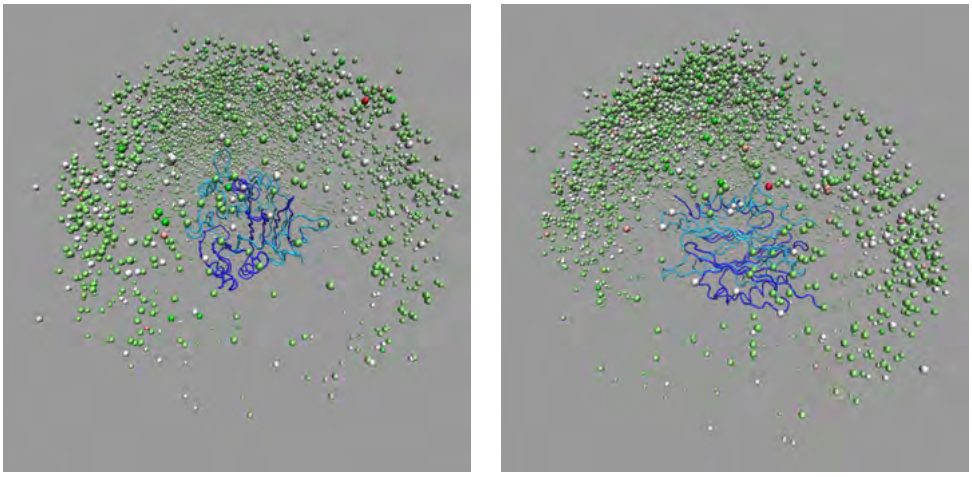

(e) Side 3 (f) Side 4

Figure B.34: Centre of mass (COM) distributions of *P. yoelii* ODC relative to AdoMetDC. AdoMetDC chains A & C (blue) and (cyan) B & D are represented by C_α trace. The COMs of all top 100 (by RP score) from all dockings are represented as spheres (total 3600 positions). COM colour scaling is based on the RP score (4.89: green → 12.28: red).

B.5 Conserved interactions between AdoMetDC and ODC

B.5.0.1 All pairs

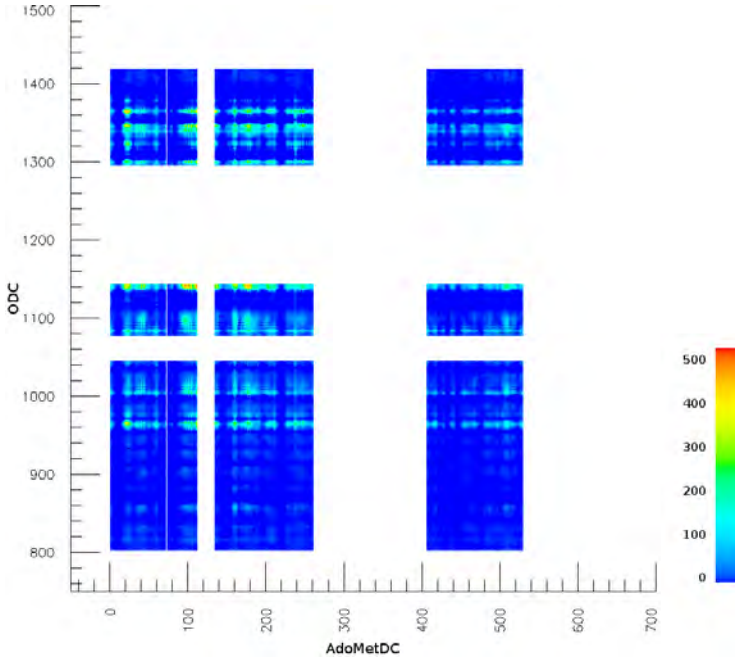

Figure B.35: Contact count heat-map for *P. falciparum*. AdoMetDC and ODC residue numbers are indicated on the x and y axes, respectively. The colour gradient (blue→green→red) corresponds to the number of times a residue pair makes contact (C_{α}^{ADC}-C_{α}^{ODC}<15 Å). The typical range is between 0-500, out of a possible 3600.

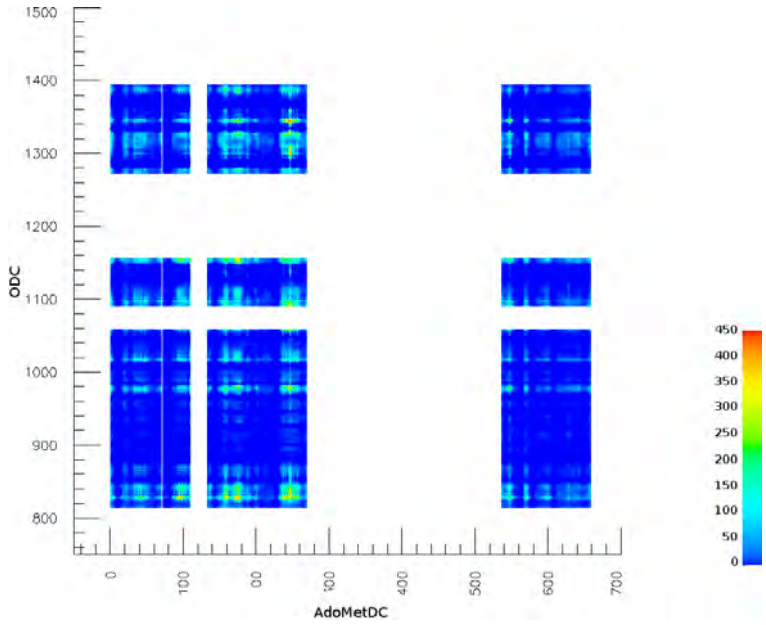

Figure B.36: Contact count heat-map for *P. knowlesi*. AdoMetDC and ODC residue numbers are indicated on the x and y axes, respectively. The colour gradient (blue→green→red) corresponds to the number of times a residue pair makes contact (C_α^{ADC}-C_α^{ODC}<15 Å). The typical range is between 0-500, out of a possible 3600.

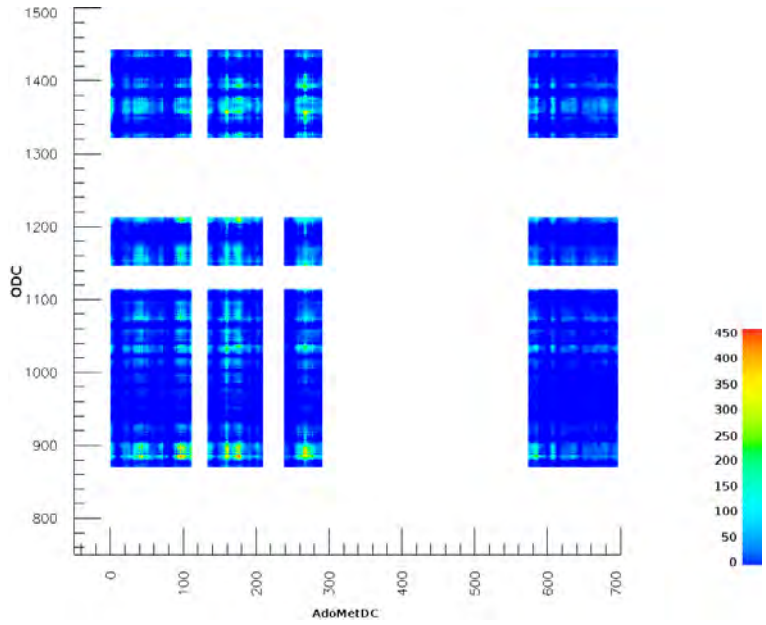

Figure B.37: Contact count heat-map for *P. vivax*. AdoMetDC and ODC residue numbers are indicated on the x and y axes, respectively. The colour gradient (blue→green→red) corresponds to the number of times a residue pair makes contact (C_α^{ADC}-C_α^{ODC}<15 Å). The typical range is between 0-500, out of a possible 3600.

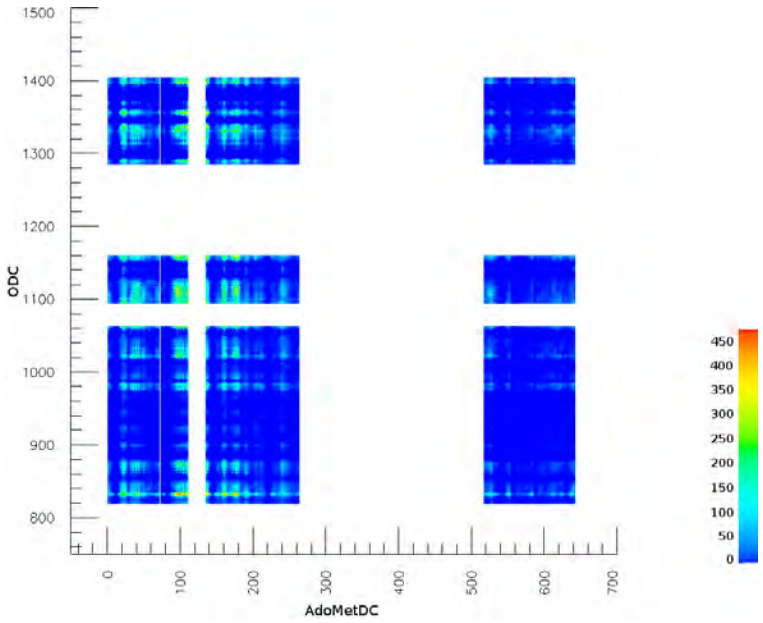

Figure B.38: Contact count heat-map for *P. yoelii*. AdoMetDC and ODC residue numbers are indicated on the x and y axes, respectively. The colour gradient (blue→green→red) corresponds to the number of times a residue pair makes contact (C_{α}^{ADC}-C_{α}^{ODC}<15 Å). The typical range is between 0-500, out of a possible 3600.

B.5.1 Conserved pairs

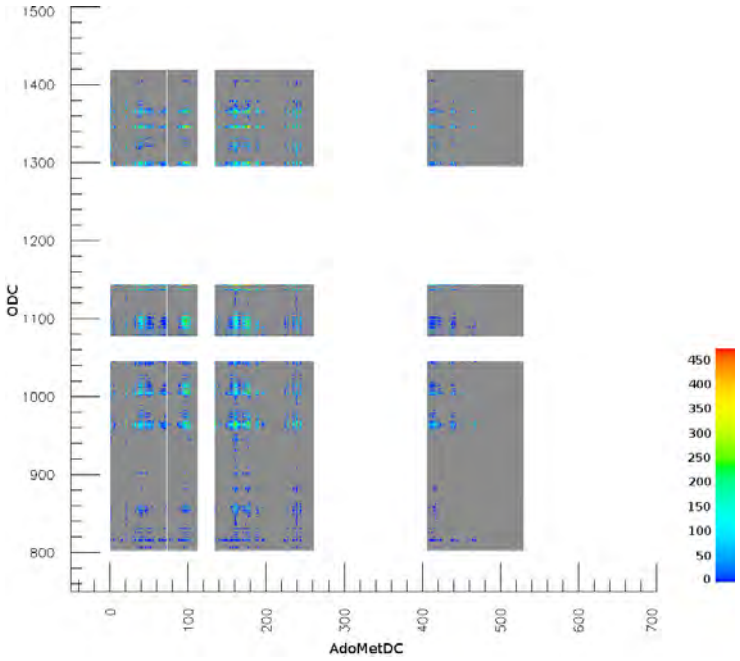

Figure B.39: *P. falciparum* contact count heat-map, restricted to pairs of identical residues across all *Plasmodium* species. AdoMetDC and ODC residue numbers are indicated on the x and y axes, respectively. The colour gradient corresponds (blue→green→red) to the number of times a residue pair makes contact (C_{α}^{ADC}-C_{α}^{ODC}<15 Å). Counts of zero are indicated in light-grey. The typical range is between 0-450, out of a possible 3600.

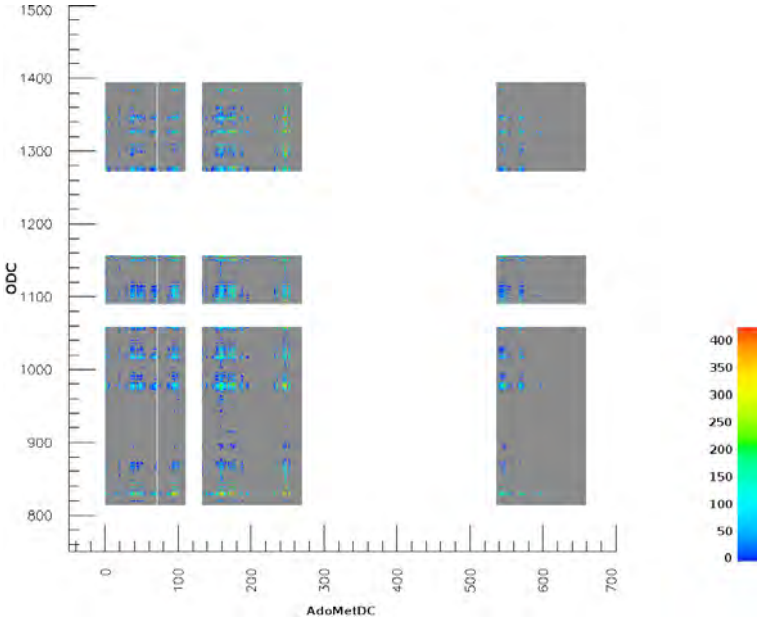

Figure B.40: *P. knowlesi* contact count heat-map, restricted to pairs of identical residues across all *Plasmodium* species. AdoMetDC and ODC residue numbers are indicated on the x and y axes, respectively. The colour gradient corresponds (blue→green→red) to the number of times a residue pair makes contact (C_{α}^{ADC}-C_{α}^{ODC}<15 Å). Counts of zero are indicated in light-grey. The typical range is between 0-450, out of a possible 3600.

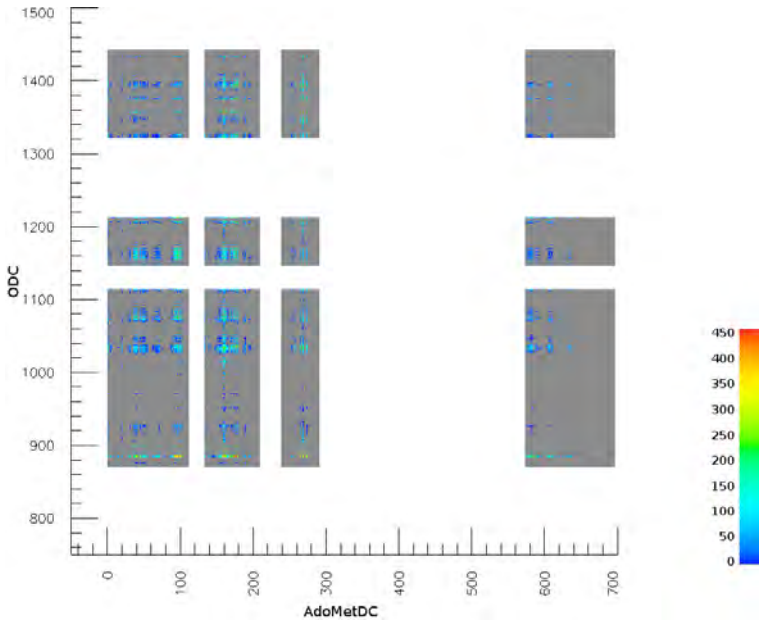

Figure B.41: *P. vivax* contact count heat-map, restricted to pairs of identical residues across all *Plasmodium* species. AdoMetDC and ODC residue numbers are indicated on the x and y axes, respectively. The colour gradient corresponds (blue→green→red) to the number of times a residue pair makes contact (C_α^{ADC}-C_α^{ODC}<15 Å). Counts of zero are indicated in light-grey. The typical range is between 0-450, out of a possible 3600.

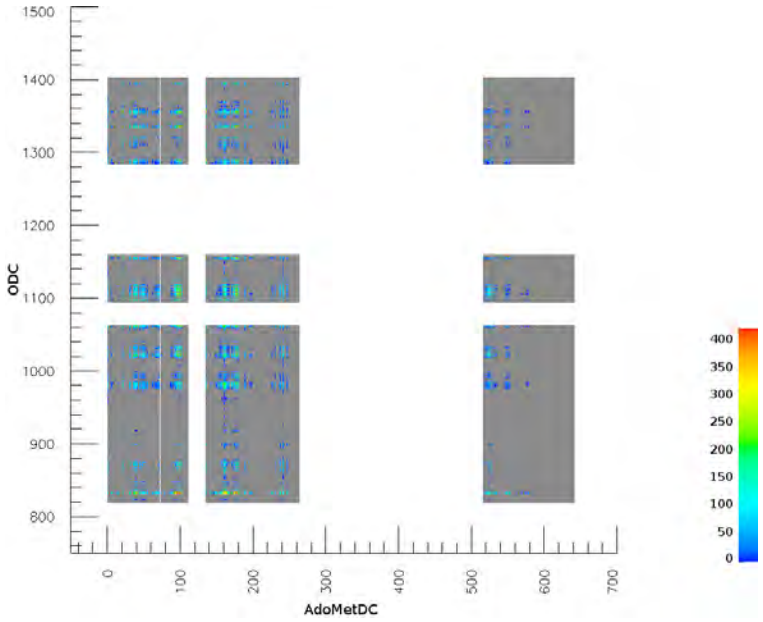

Figure B.42: *P. yoelii* contact count heat-map, restricted to pairs of identical residues across all *Plasmodium* species. AdoMetDC and ODC residue numbers are indicated on the x and y axes, respectively. The colour gradient corresponds (blue→green→red) to the number of times a residue pair makes contact (C_α^{ADC}-C_α^{ODC}<15 Å). Counts of zero are indicated in light-grey. The typical range is between 0-450, out of a possible 3600.